

# Review of the status and mass changes of Himalayan-Karakoram glaciers

MOHD FAROOQ AZAM,<sup>1,2</sup> PATRICK WAGNON,<sup>3,4</sup> ETIENNE BERTHIER,<sup>5</sup>  
CHRISTIAN VINCENT,<sup>3</sup> KOJI FUJITA,<sup>6</sup> JEFFREY S. KARGEL<sup>7</sup>

<sup>1</sup>National Institute of Hydrology, Roorkee, Uttarakhand, India

<sup>2</sup>Discipline of Civil Engineering, School of Engineering, Indian Institute of Technology Indore, Simrol 453552, India

<sup>3</sup>Univ. Grenoble Alpes, CNRS, IRD, IGE, F-38000 Grenoble, France

<sup>4</sup>International Centre for Integrated Mountain Development, Kathmandu, Nepal

<sup>5</sup>LEGOS, CNRS, Université de Toulouse, Toulouse, France

<sup>6</sup>Graduate School of Environmental Studies, Nagoya University, Nagoya, Japan

<sup>7</sup>Department of Hydrology and Atmospheric Sciences, University of Arizona, Tucson, AZ, USA

Correspondence: Mohd Farooq Azam <[farooqaman@yahoo.co.in](mailto:farooqaman@yahoo.co.in)>

**ABSTRACT.** We present a comprehensive review of the status and changes in glacier length (since the 1850s), area and mass (since the 1960s) along the Himalayan-Karakoram (HK) region and their climate-change context. A quantitative reliability classification of the field-based mass-balance series is developed. Glaciological mass balances agree better with remotely sensed balances when we make an objective, systematic exclusion of likely flawed mass-balance series. The Himalayan mean glaciological mass budget was similar to the global average until 2000, and likely less negative after 2000. Mass wastage in the Himalaya resulted in increasing debris cover, the growth of glacial lakes and possibly decreasing ice velocities. Geodetic measurements indicate nearly balanced mass budgets for Karakoram glaciers since the 1970s, consistent with the unchanged extent of supraglacial debris-cover. Himalayan glaciers seem to be sensitive to precipitation partly through the albedo feedback on the short-wave radiation balance. Melt contributions from HK glaciers should increase until 2050 and then decrease, though a wide range of present-day area and volume estimates propagates large uncertainties in the future runoff. This review reflects an increasing understanding of HK glaciers and highlights the remaining challenges.

**KEYWORDS:** climate change, glacier fluctuations, glacier hydrology, glacier monitoring, mountain glaciers

## 1. INTRODUCTION

The 2500 km long Himalaya-Karakoram (HK) region – extending westward from Yunnan Province (China) in the east, across Bhutan, Nepal, southern Tibet, northern India, and into Pakistan – is one of the most glacierized regions on Earth. A large fraction of the subcontinent's fresh water is locked in this dynamic storage (Frey and others, 2014). HK glaciers influence the runoff regime of major regional river systems (Immerzeel and others, 2010; Kaser and others, 2010), for example the Indus, Ganges and Brahmaputra, by releasing water mainly in warm summer months in the Karakoram and western Himalaya, and in the dry-season spring and autumn months in most of the central and eastern Himalaya. This meltwater helps to sustain more than 750 million people and the economy of the surrounding countries by providing water for irrigation, hydropower, drinking, sanitation and manufacturing (Immerzeel and others, 2010; Pritchard, 2017).

Recent estimates of the glacierized area in the HK region varies from 36 845 to 50 750 km<sup>2</sup> (Supplementary Table S1), with roughly half of the area in the Karakoram Range. The ice volume estimates depend on the inventory and method; consequently, available volume estimates, varying from 2 955 to 4 737 km<sup>3</sup>, also indicate large uncertainties (Frey and others, 2014). The estimated impacts of these glacierized areas on river hydrology are influenced by each study's region of analysis and the area and volume

of ice estimated from different sources. This review inherits such heterogeneities, gaps and uncertainties of the published record, but gradually the problems are being remedied. The relative percentage of glacier meltwater to the total runoff is an indicator of the vulnerability of river systems to climate. Therefore, future climate changes are expected to alter the melt characteristics of the HK rivers, for instance, seasonal shifts in stream flow (Mölg and others, 2014). Further, the potentially important contributions of sub-surface ice contained in the active layer and of massive segregation ice of permafrost in HK river hydrology remains unknown.

The HK glaciers gained attention after the typographic error in the Intergovernmental Panel on Climate Change (IPCC) Fourth Assessment Report that suggested a catastrophic loss of HK glaciers by 2035 (Cogley and others, 2010). Moreover, while glaciers worldwide are in a recession (Zemp and others, 2015), stable or advancing glaciers dominate in the Karakoram (the 'Karakoram Anomaly') (Hewitt, 2005; Gardelle and others, 2012; Kääb and others, 2012), an anomaly which seems to be centered in the western Kunlun Shan (Kääb and others, 2015). The way-off IPCC typographic mistake (which was later retracted and then corrected (Vaughan and others, 2013)) and various conflicting and confusing publications led to a review (Bolch and others, 2012) 5 years ago that summarized the existing knowledge about HK glaciers and highlighted the gaps in the HK glaciology. Since then, as a result of growing interest

in the international scientific community, great progress has been achieved. Some key advancements are recent glacier trends (Brun and others, 2017), their climatology (Azam and others, 2014a, b; Maussion and others, 2014; Sakai and others, 2015), contributions to local (Nepal and others, 2014) or regional (Racoviteanu and others, 2013; Lutz and others, 2014; Mukhopadhyay and Khan, 2014a) water supply and sea-level rise (Jacob and others, 2012; Gardner and others, 2013; Huss and Hock, 2015) and natural hazards (Khanal and others, 2015). This rapid recent expansion of knowledge about HK glaciers has motivated this up-to-date review. We present: (i) the most complete compilation of in situ-, model- and remote-sensing-based glaciological studies from the HK region, (ii) analysis to check the reliability of available data (length/area changes and mass changes from different methods) with a focus on glaciological mass balances, (iii) discussion of glacier behaviors under regional climatic settings and (iv) future research strategies to strengthen the cryospheric knowledge in the HK region.

## 2. CLIMATE DYNAMICS AND GLACIER CHARACTERISTICS

The hydrological cycle of the HK region is complex because of the impact of two circulation systems, the Asian Monsoon (AM) and Western Disturbances (WD) (Bookhagen and Burbank, 2010). Most glaciers in the eastern and central Himalaya experience maximum accumulation in the summer due to high monsoonal precipitation and high elevations, where periods of summertime ablation punctuate overall summer-long snow accumulation (Ageta and Higuchi, 1984). The summer accumulation in the western Himalaya is weak while the AM barely reaches to the Karakoram Range (Bookhagen and Burbank, 2010). In the Karakoram, WD is the important source of moisture providing maximum precipitation during winter due to strong storms (Lang and Barros, 2004) with generally short life spans of 2–4 days (Dimri and Mohanty, 2009). The western Himalaya is a transition region receiving precipitation from both the AM and WD (Azam and others, 2016). Further, there are strong orographic differences in precipitation from south to north across the HK (Shrestha and others, 1999). The HK is a barrier to monsoon winds, causing maximum precipitation on southern slopes with a regional east to west decrease in the monsoon intensity (Shrestha and others, 1999) and large local orographic controls on climate. For instance, AM provided low precipitation (21% of the annual sum) on the leeward side of the orographic barrier at Chhota Shigri Glacier (western Himalaya) and high precipitation (51% of annual total) on the windward side at Bhuntar city (~50 km south from Chhota Shigri) (Azam and others, 2014b). Therefore, depending on their geographical position and regional orography, the glaciers in the HK region are subjected to different climates. This variability of precipitation regimes along the HK region begets varying types and behaviors of glaciers over short distances (Maussion and others, 2014). Five classes of glaciers were defined (Maussion and others, 2014): two dominant classes with winter (DJF) and summer (JJA) accumulation type, a class with maximum precipitation in pre-monsoon (MAM) months and two intermediate classes which tend to receive either winter (DJF/MAM) or summer (MAM/JJA) precipitation but with less pronounced centers (precipitation amounts) in winter or summer seasons, respectively.

## 3. GLACIER FLUCTUATIONS AND AREA CHANGE RECORDS

We present the maximum possible compilation of glaciological studies including many Geological Survey of India reports, which are not available easily, but scanned for this study. Compared with snout fluctuation records for almost 100 glaciers/basins in a previous review (Bolch and others, 2012), our compilation includes historical records of 154 glaciers/basins, some available since the 1840s (Fig. 1a). We carefully assess the quality of satellite imageries or topographic maps used to estimate the length changes and assign the caution flags to each length change record (Supplementary Table S2). The longest historical records are for Milam, Gangotri, Pindari, Siachen and Biafo glaciers. Between the mid-19th and mid-20th century, glacier fluctuation records (Fig. 2a) are at multi-decadal scale, extracted from field photographs or maps. After that, the records are usually available at decadal scale, and for some glaciers like Chorabari, Pindari and Raikot records are available annually for recent years. There are 25 records available per year between the mid-19th and the mid-20th century (Fig. 2b). An abrupt increase of records occurred in the early 1960s, with a peak exceeding 125 records per year in the 1975–2000 period (Fig. 2b). This is because Survey of India maps, available since the 1960s, were combined with recent satellite images or field surveys to estimate the fluctuations (Supplementary material).

Since the mid-19th century, a majority of Himalayan glaciers retreated with rates varying regionally and from glacier to glacier, while in the Karakoram, the glaciers snouts have been retreating, stable or advancing (Fig. 2a; Supplementary Table S2). The interpretation of the length record in the Karakoram is complicated by the occurrence of surges. For example, in upper Shyok Valley in the Karakoram, 18 glaciers (1 004 km<sup>2</sup>) out of 2 123 glaciers (2 978 km<sup>2</sup>) showed surge-type behavior (Bhambri and others, 2013).

Glacier area change studies were performed generally at basin-wide scale with few individual glacier estimates (Fig. 1b; Supplementary Table S3). We assign the caution flags to each area change record based on the quality of satellite imageries and topographic maps used in the studies (Supplementary Table S3). Along the Himalayan Range shrinkage is common over the last 5–6 decades (Fig. 1b) with high variability in rates ranging from  $-0.07\% \text{ a}^{-1}$  for Kimoshung Glacier over 1974–2015 to  $-1.38\% \text{ a}^{-1}$  for Ganju La Glacier over 2004–14 (Fig. 2c). Conversely, glaciers in the Karakoram Range showed a slight shrinkage or stable area since the mid-19th century (Supplementary Table S3).

The example of the Khumbu Region (Everest) is striking to illustrate how difficult it can be to compare different area change estimates. A small fraction of the glaciers in this region (~92 km<sup>2</sup>) showed an area reduction of  $-0.12\% \text{ a}^{-1}$  over 1965–2005 (Bolch and others, 2008). Another study (Salerno and others, 2008), using historical maps (1 : 50 000 scale), reported similar reduction rate of  $-0.14\% \text{ a}^{-1}$  over a 404 km<sup>2</sup> glacierized area in the same region for 1956–90. A study covering 4000 km<sup>2</sup> over the Koshi Basin (including Khumbu Region) estimated the much more negative rate of area changes of  $-0.59 \pm 0.17\% \text{ a}^{-1}$  over 1976–2009 (Shangguan and others, 2014). The large discrepancies in those estimates can be attributed to the differing extents of



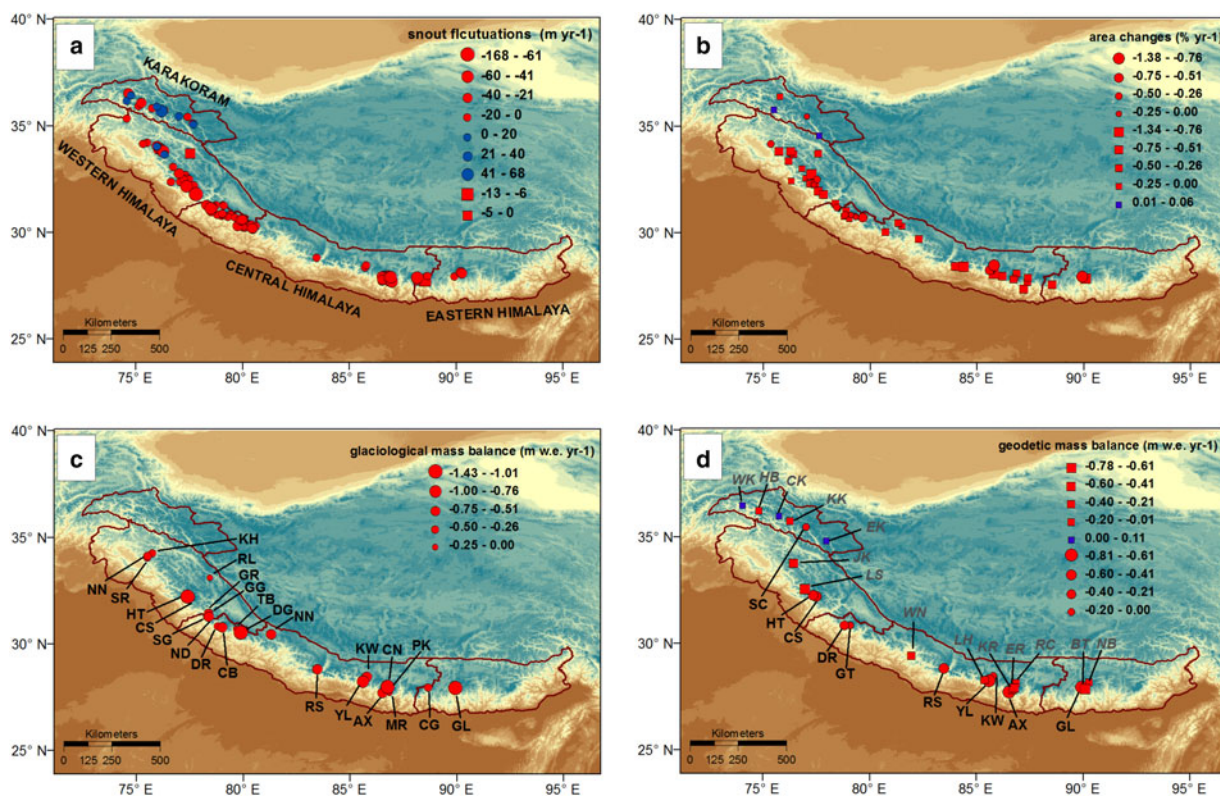


**Fig. 1.** Spatial glacier/basin behaviors over the HK region (Note: the observation time is different and given in corresponding supplementary tables). The regions are defined following (Bolch and others, 2012). Symbology: Circles represent the glacier scale observations while squares represent basin/regional scale observations. Red (or blue) color represents negative (or positive) changes in length, area or mass balance. The abbreviations are given in corresponding supplementary tables. (a) Glacier snout fluctuations for 152 glaciers and 2 basins (Supplementary Table S2). (b) Area changes for 24 glaciers and 47 basins (Supplementary Table S3). (c) Glaciological mass balances for 24 glaciers (Supplementary Table S4 and S6) and (d) geodetic mass balances for 10 glaciers and 24 basins/regions (Supplementary Table S8).

the glacierized area, difficulties in mapping debris-covered glaciers, different observation periods, methodologies, data used and related uncertainties.

The glacier area shrinkage causes fragmentation of large glaciers; consequently, the number of glaciers increased in the Himalaya over the past 5–6 decades (Kulkarni and others, 2007; Ojha and others, 2016). The area shrinkage of clean-ice areas, and perhaps reducing glacier flow speeds and possibly accelerating mass wasting from deglaciated surfaces also resulted in increasing supraglacial debris-covered area in the Himalaya (Scherler and others, 2011; Nuimura and others, 2012; Thakuri and others, 2014). Small and low elevation glaciers were found to be shrinking faster than larger ones (Thakuri and others, 2014; Ojha and others, 2016). Studies with multiple observation periods revealed specific trends of area shrinkage rates from different regions of the HK. Steady trends in the eastern Himalaya (Racoviteanu and others, 2015), accelerated shrinkage in the central Himalaya (Bolch and others, 2008; Thakuri and others, 2014) and decreasing shrinkage in Zaskar and Ravi basins of the western Himalaya (Schmidt and Nüsser, 2012; Chand and Sharma, 2015) were found over the last 5–6 decades.

The mean shrinkage rates were computed for the Himalayan glaciers using 60 data series (excluding highly uncertain data; Supplementary Table S3). The shrinkage rates were available since the 1950s to present, but a time window from 1960 to 2010 was selected to avoid the sparse data outside this window. Despite the regional variation in shrinkage rates, Himalayan glaciers showed a

continuous mean area shrinkage over the last 5 decades which is slightly higher (more negative) between 1980 and 2000 (Fig. 2c). The calculated unweighted mean area shrinkage for Himalayan glaciers is  $-0.36\% \text{ a}^{-1}$  for 1960–2010. This rate is less than the unweighted mean shrinkage rate ( $-0.57\% \text{ a}^{-1}$ ) and very close to the weighted mean shrinkage rates ( $-0.40\% \text{ a}^{-1}$ ) calculated for the whole of High Mountain Asia (HMA) (Cogley, 2016) for the same period. Only four area change studies are available from the Karakoram Range covering different regions (Supplementary Table S3). A time window of 1980–2010 was selected to get at least three estimates for the mean rate of area change. The unweighted mean rate of area change for the Karakoram glaciers varies from  $\sim -0.06\% \text{ a}^{-1}$  during the 1980s to almost  $0\% \text{ a}^{-1}$  in 2000s (Fig. 2c), but the temporal trend is hard to interpret and probably not significant given the scarcity of the measurements. Overall, these close to  $0\% \text{ a}^{-1}$  area changes rates are in line with the Karakoram Anomaly (Hewitt, 2005; Gardelle and others, 2012; Kääb and others, 2012). Importantly, due to the unweighted nature of these mean rates, and the fact that small glaciers tend to lose area faster than big ones when expressed in % change, these means are different than the mean rate of change of total glacierized area.

#### 4. GLACIER MASS CHANGES

Although the databases of the glacier changes in the HK have greatly improved recently, field observations about mass balance are still scarce. In this review, we include results of

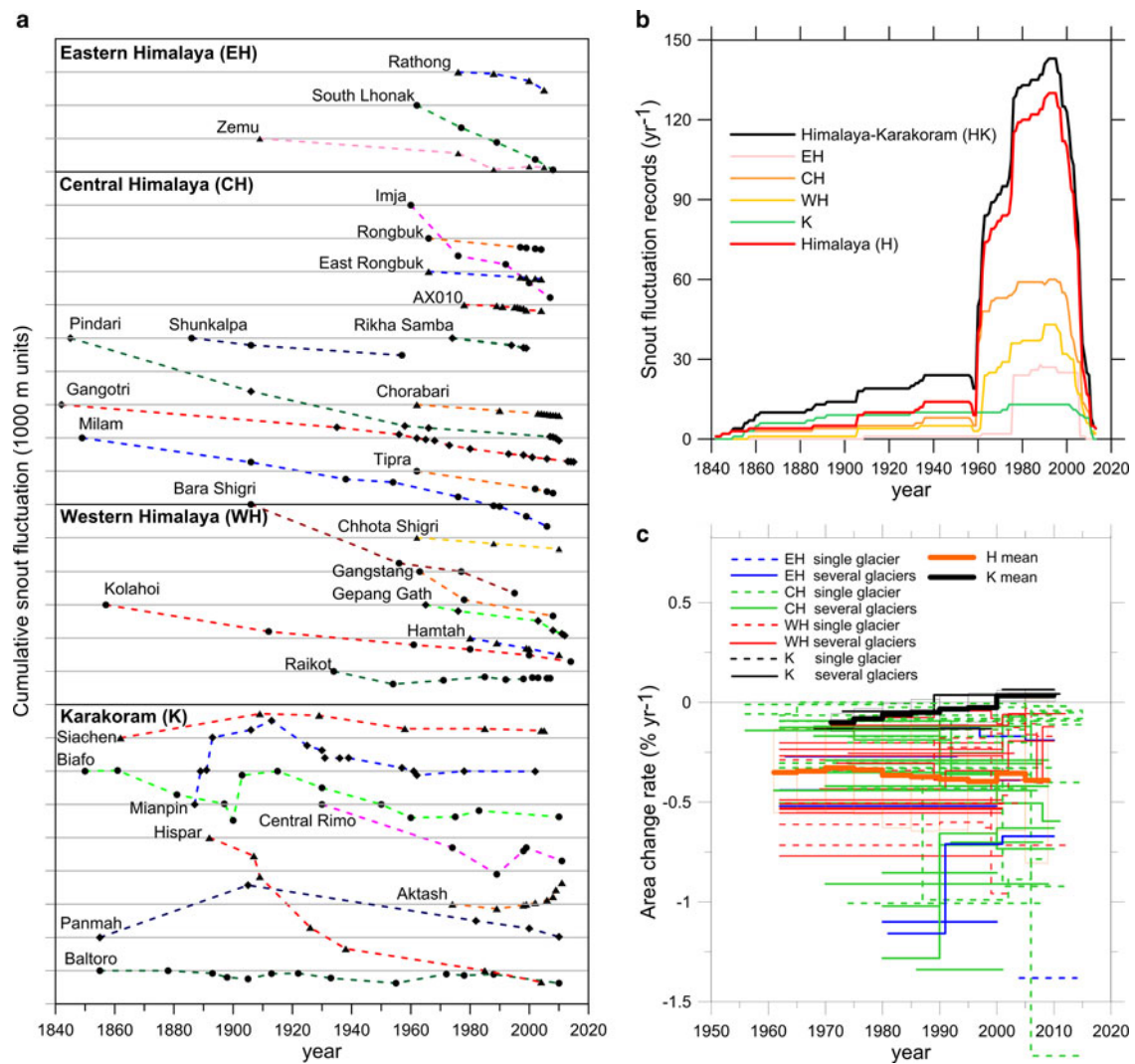


**Fig. 2.** (a) Length change of selected glaciers in the HK region over the last 170 years (b) Number of data records (c) Area change rates for HK region. The rates were calculated in percent change per year with respect to the initial observed area. Note that the unweighted mean area rates are calculated for 5-year period from a varying number of values depending on the period. The black and orange boxes represent the  $\pm 1$  Std dev. envelope for each 5-year mean area change rate and calculated from the area change rates available for the corresponding period. Data and references used in the figure are listed in Supplementary Table S2 and S3.

mass-balance changes at both glacier scale (from the glaciological method, geodetic method and model results) and regional scale (geodetic method).

The glaciological mass balance is an undelayed, direct response to meteorological changes (Oerlemans, 2001) and thus mass-balance observations are needed to study the climate change especially in remote areas such as the HK, where our knowledge of climate–glacier relationship is still partial. Regrettably only 24 glaciers, covering an area of  $\sim 112 \text{ km}^2$  ( $\sim 0.5\%$  of the total Himalayan glacierized area (Bolch and others, 2012)), have been surveyed in the Himalayan Range using the glaciological method (Supplementary Tables S4–S5), which is sparse in comparison with most other large glacierized regions of the world (Zemp and others, 2015). Glaciological mass-balance measurements in the Himalayan Range are often challenging because of the vast glacierized area, high altitude, rugged terrain, extreme climate, and political and cultural boundaries. In the Karakoram, where the challenges are the toughest, the glaciological measurements were performed only on the ablation area of Baltoro Glacier (Mayer and others, 2006). Since the first mass-balance observation on Gara Glacier in

1974/75, the annual mass balances in the Himalaya have mostly been negative, with only 16 positive annual mass-balance observations out of a total of 142 observations (see the unweighted mean mass-balance series in Fig. 3a and Supplementary Table S6). The longest continuous series is just 12 years for Chhota Shigri Glacier ( $-0.56 \pm 0.40 \text{ m w.e. a}^{-1}$  over 2002–14) (Azam and others, 2016).

Previous compilations of field-based mass balances (Cogley, 2011; Bolch and others, 2012) yielded regional mean mass balances for the Himalaya using all available glaciological mass-balance data without quality checks. As already highlighted (Gardner and others, 2013), this problem, combined with bias and lack of representativeness due to benchmark glacier selection, results in regional glaciological mass balances that are more negative compared with the values derived from remote-sensing data, and might lead to an overestimation of the sea-level rise contribution of Himalayan glaciers. The surveyed glaciers are generally chosen for their easy access, low altitudes, small sizes (mean area of surveyed glaciers is  $4.6 \text{ km}^2$ ; Supplementary Table S4) and low coverage by debris. Selection criteria introduce a strong bias toward rapid



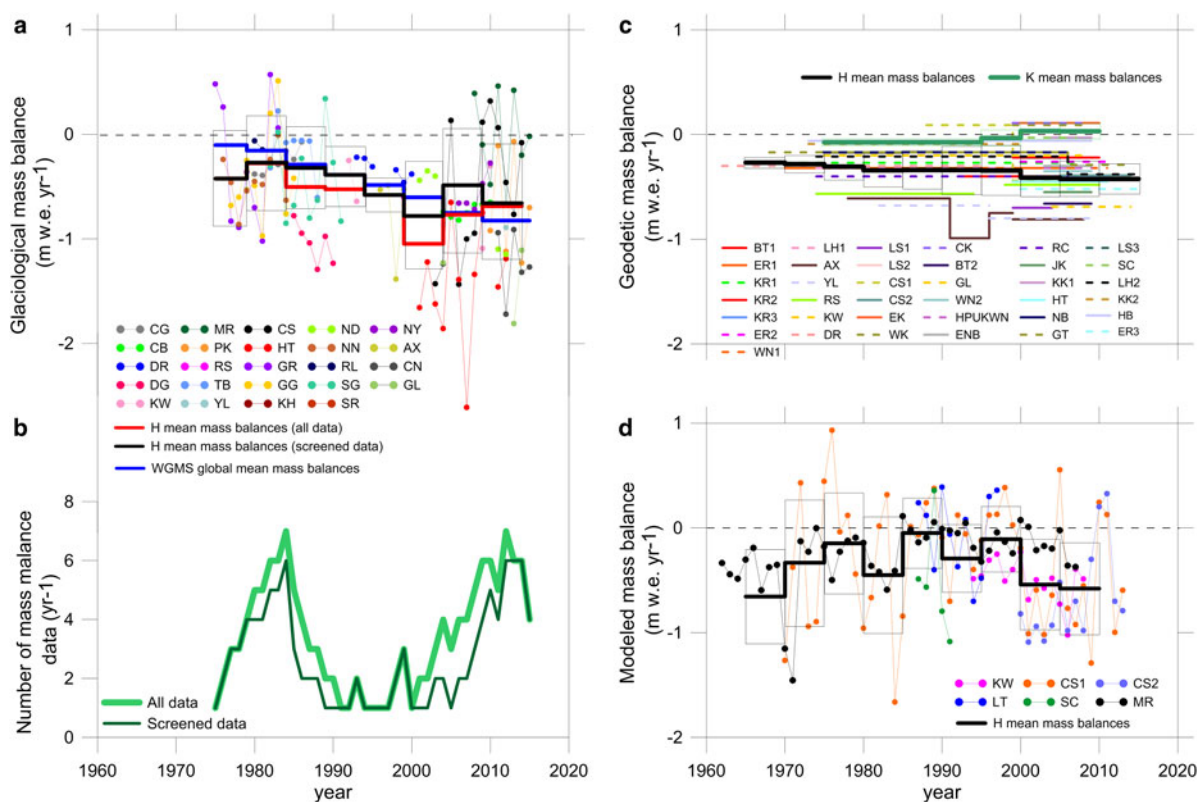


**Fig. 3.** Mass balances in the HK region. (a) Annual glaciological mass balances for all 24 glaciers. Red thick line is the mean mass balances for the Himalayan Range calculated using 24 glaciers' data, black thick line is the mean mass balances for the Himalayan Range calculated using 18 screened glaciers, and the blue thick line represents the global mean mass balances between 1975 and 2014 calculated from 37 reference glaciers of the World Glacier Monitoring Service (Zemp and others, 2012, WGMS 2013). (b) Number of data points available each year. (c) Geodetic mass balances. Black thick line is the mean geodetic mass balances for the Himalayan Range while green thick line is the mean geodetic mass balances for the Karakoram Range and (d) Annual modeled/hydrological mass balances. Black thick line is the mean modeled mass balances. Abbreviations in different panels are glacier/region names, available in Supplementary Tables S4, S8, and S9. Note that the mean mass balances are unweighted and calculated for the 5-year period from a varying number of mass balance values available for each period. The black boxes represent the  $\pm 1$  Std dev. envelope for each 5-year mean mass balance and calculated from the mass-balance values available for the corresponding period.

response type glaciers, or at least does not represent the population as a whole; representation is especially lacking for the large, complex glaciers, which dominate the total ice mass in the HK region. Further, almost half of the glaciological studies were conducted by the Geological Survey of India and are published in internal reports (Supplementary Table S4) and often lack the details of mass-balance observations (Supplementary Table S5). These problems make difficult the identification of the reliable mass-balance data series and extension of the data to represent the Himalayan region as a whole. The mass balances of the avalanche-fed Hamtah Glacier ( $-1.43 \text{ m w.e. a}^{-1}$  between 2000 and 2012) were already found to be negatively biased (Vincent and others, 2013). Therefore, we performed a detailed systematic check of the reliability of each mass-balance time series using several criteria, such as density of point measurement network, stake material, availability of snow density field measurements, error analysis in mass-balance estimates, map quality, debris-cover extent, avalanche contribution, verification of glaciological mass balance with geodetic mass balance and relationships of mass balances with equilibrium line altitude, temperature and precipitation, etc. and classify the mass-balance time series in four categories (excellent, good, fair and dubious; Supplementary Table S7) (details are in the Supplementary material).

Mass balances of six glaciers are dubious (Supplementary Table S7) and might have biases. Except for Kangwure Glacier, these glaciers either receive their accumulation through avalanches (Changmekhangpu, Dunagiri, Hamtah and Kolahoi glaciers) or are highly debris covered (50–80% debris-covered area on Changmekhangpu, Chorabari, Dunagiri, Hamtah glaciers) (Supplementary material). Due to steep topography, many HK glaciers receive a large part of their accumulation from avalanches (Racoviteanu and others, 2014), a mass input that has not been quantified yet (Laha and others, 2017). Avalanches sometimes destroy the ablation/accumulation stakes. Most accumulation is close to the glacier headwalls and cannot be safely monitored with the glaciological method. Full representation of all glacier types should include avalanche-fed glaciers, but for the preceding reasons, these glaciers themselves cannot be fully and correctly surveyed. The debris distribution on highly debris-covered glaciers is, generally, heterogeneous across the surface (often the stakes are installed over a few decimeter thick debris cover); hence the ablation measurement with stakes is location specific. Further, the stakes are generally installed at locations easy to access, and so the effects of supraglacial ponds or ice cliffs, known to be melt 'hot spot' (Sakai and others, 2002), is not included in the mass-balance estimates. In support of previous studies (Buri and others, 2016; Miles and others, 2016; Vincent and

others, 2016), we find that conventional glaciological mass-balance methods applied to highly debris-covered and avalanche-fed glaciers are error prone, but the selection of simple, safe, clean-ice glaciers might introduce a bias toward more negative regional assessments. Therefore, glacier-wide mass balance on highly avalanche-fed and debris-covered glaciers should be estimated by remote-sensing methods. Despite errors and biases, in situ glaciological data on avalanche-fed and debris-covered glacier are needed for ground truthing of remotely sensed data, modeling and process understanding (Banerjee and Shankar, 2013; Vincent and others, 2016). It is thus necessary to recognize and explain the biases pertaining to the benchmark glacier sample of the whole glacier population, versus biases which may render an individual glacier's data misleading and thus favoring exclusion.

Excluding these six dubious mass-balance series (total 37 annual mass-balance data points), the mean mass balances for the Himalayan range were less negative (Fig. 3a). The revised mean mass balance during 1975–2015 for 18 screened glaciers is  $-0.49 \text{ m w.e. a}^{-1}$  versus  $-0.59 \text{ m w.e. a}^{-1}$  for all 24 glaciers. These revised mean mass balances show a moderate wastage since 1975 that generally follows the global trend before 2000 (Fig. 3a). After 2000, a positive deviation of Himalayan mean mass balances from the increasingly negative global mean seems to be consistent with the regional satellite-based mass changes estimated over recent years that suggest two or three times less negative mass balances for the Pamir-Karakoram-Himalaya than for the global mean (Kääb and others, 2012; Gardelle and others, 2013). We note that our inference of reduced Himalayan glacier mass loss after 2000 is based on a changing sample of field-monitored glaciers and thus need to be confirmed in the future. In particular, rare remote-sensing mass-balance estimates for several periods do not show such a trend (Ragettli and others, 2016). However, remote-sensing estimates themselves carry their own uncertainty, as illustrated by the fact that the glacier-wide mass balance in the Langtang area (Nepal) had to be revisited by Ragettli and others (2016) compared with a similar earlier assessment by Pellicciotti and others (2015). Two major sources of uncertainty in DEM-based geodetic mass-balance estimates are the poor quality of DEM in the texture-less accumulation areas (Ragettli and others, 2016) and the unknown penetration of the SRTM C-band and X-band radar signal into dry snow and firn (Barandun and others, 2015; Kääb and others, 2015; Dehecq and others, 2016; Round and others, 2017).

With recent progress in satellite data acquisitions and processing, and the availability of declassified stereo images from spy satellites, several estimates provided the geodetic mass changes at glacier- or region-wide scale (Fig. 3c; Supplementary Table S8). Several comprehensive assessments of glacier mass changes in the HK have been obtained from 2003 to 2009 using ICESat laser altimetry (Kääb and others, 2012, 2015; Gardner and others, 2013; Neckel and others, 2014) and, despite differences, revealed a contrasted pattern of mass change in the HK with strong thinning in the south-east Tibetan Plateau and in the western Himalaya and no significant elevation change in the Karakoram and over the Western part of the Tibetan plateau. These ICESat-based mass-balance estimates tended to be more negative than the ones derived by comparing SPOT5 and SRTM DEMs for nine sub-regions of KH (Gardelle and others,

2013). The differences in these estimates are difficult to investigate as the study periods and sample regions are mismatched (Supplementary Table S8). However, the difficulty of accounting for the penetration of the SRTM radar signal into snow and ice may explain some of these differences (Kääb and others, 2015) and the varying treatment of errors (not all studies account for systematic errors), but we also note that at the error limits, the estimates overlap. Hence, we find an encouraging approach toward consistency. The contrasted pattern of change has recently been confirmed for a longer time period (2000–16) and at the scale of individual glaciers using multi-temporal analysis of 50 000 ASTER DEMs (Brun and others, 2017).

Measurement of the time-varying gravity fields by the GRACE (Gravity Recovery and Climate Experiment) satellites have led to varying estimates of glacier mass changes in our study region (Jacob and others, 2012; Gardner and others, 2013). However, they remain difficult to interpret glaciologically due to their coarse resolution, leakage of the strong signal of groundwater depletion from north India (Rodell and others, 2009), the fact that glacier meltwater may be stored in nearby glacier lakes (Song and others, 2014) and the apparent large positive mass change anomaly over the Tibetan Plateau (Yi and Sun, 2014), probably due to increased precipitation (Zhang and others, 2017). As an example, in their sea-level budget assessment during 2002–14, Reager and others (2016) were cautious not to use GRACE data to update glacier mass loss in High Mountain Asia, relying instead on the 2003–09 ICESat mass change estimates.

The individual geodetic mass balances are available at multiannual scale (Supplementary Table S8). The mean geodetic mass balance for the Himalayan Range was  $-0.37 \text{ m w.e. a}^{-1}$  between 1962 and 2015. Conversely, the Karakoram Range exhibited balanced mass budget with  $-0.01 \text{ m w.e. a}^{-1}$  between 1975 and 2010 against the mean mass balance of  $-0.37 \text{ m w.e. a}^{-1}$  for the Himalayan region over the same period. Therefore, the 'Karakoram Anomaly' can be extended back at least to the mid-1970s (Bolch and others, 2017; Zhou and others, 2017). The mean balanced mass over the Karakoram Range is consistent with recent glacier snout stability (Fig. 2a), whereas the continuing negative balances over the Himalaya are consistent with glacial lake growth since the early 1960s (Bajracharya and Mool, 2009).

Some discrepancies in glaciological and geodetic mean mass-balance estimates are obvious because of (i) selection bias and lack of representativeness of glaciers used for glaciological measurements (ii) different satellite data types and methodologies for geodetic mass balance and (iii) the larger area covered by geodetic estimates. Compared with mean mass balance of  $-0.59 \text{ m w.e. a}^{-1}$  for all 24 observed glaciers between 1975 and 2015, the screened mean mass balance of  $-0.49 \text{ m w.e. a}^{-1}$  over the same period is closer to the agreement with the geodetic mean mass balance of  $-0.37 \text{ m w.e. a}^{-1}$  for the Himalayan Range over 1975–2015. However, these screened glaciological mass balances remain too sparse in time and space to obtain a robust regional average and an unambiguous temporal trend. Our analysis highlights the sensitivity of the regional average to the addition/subtraction of just a few glaciological measurements. Glaciological measurements should be retained for the understanding of physical processes, validation of remotely sensed measurements, calibration/validation of

glacio-hydrological models and development of process-based models for future glacier changes. Our recommendation is that glaciological mass balances should not be used for the computation of regional mass balance (Sherpa and others, 2017) and for sea-level rise contribution from the Himalayan range. This recommendation is paired with suggested improvements in the benchmark glacier network.

Mass-balance modeling is becoming widely used in the HK region with growing satellite and recent in situ meteorological data availability. A few studies estimated mass balances using different models such as the hydrological model for Siachen Glacier; temperature index model for Chhota Shigri, Langtang and Mera glaciers; albedo model for Chhota Shigri and regression (mass balance-meteorological parameters) model for Kangwure Glacier (Fig. 3d; Supplementary Table S9). Modeling of mass balance over the historic period of observations using both in situ and satellite measurements may finally give high spatial and temporal resolution, long-term continuity and geographic completeness, thus filling data gaps and addressing current inhomogeneities (Supplementary Tables S4 and S8).

Based on in situ field measurements, Vincent and others (2013) showed that Chhota Shigri Glacier was near balanced conditions during the 1990s. The reconstructed mass change of Chhota Shigri Glacier corresponded to a moderate mass loss of  $-0.30 \pm 0.36$  m w.e.  $a^{-1}$  between 1969 and 2012, with, interestingly, no significant mass change between 1986 and 2000 ( $-0.01 \pm 0.36$  m w.e.  $a^{-1}$ ) (Azam and others, 2014a). Further, Mera Glacier mass-balance reconstruction over 1961–2007 showed strong similarities with the Chhota Shigri reconstruction with balanced conditions from the late 1980s to the early 1990s (Shea and others, 2015) (Fig. 3d, Table S10). Our glaciological mean mass balances for the Himalayan glaciers, do not show balanced conditions over the mid-1980s to the late 1990s (Fig. 3a). Few measurements are available for this period (Fig. 3b) when the glaciers may have been in balance. Supporting the modeling studies, only Tipra bank glaciological mass-balance series was close to steady state with mean mass balance of  $-0.14$  m w.e.  $a^{-1}$  between 1981 and 1988. The appearance of nearly balanced conditions on Chhota Shigri, Mera and Tipra Bank glaciers could be because of regional orography and glacier-specific dynamics. For instance, Mera Glacier showed almost no mass change ( $-0.02$  m w.e.  $a^{-1}$ ) between 2010 and 2015, while Pokalde and Changri Nup glaciers, in the nearby interior of the range, showed a rapid wastage of  $-0.63$  and  $-1.24$  m w.e.  $a^{-1}$ , respectively, over the same period (Supplementary Table S6, Sherpa and others, 2017). Given the limited number of modeled mass-balance series for mean mass-balances computation, we believe these means should not be considered as regional representative and must be handled cautiously.

## 5. GLACIER WASTAGE AND DEBRIS COVER

Debris-covered glaciers are widespread in the HK region (Scherler and others, 2011). Thermally insulating debris due to rugged topography and strong avalanche activity might slow the glacier mass wastage, thus resulting in longer timescales of mass loss (Rowan and others, 2015; Banerjee, 2017). This insulating effect has been recently quantified on Changri Nup Glacier (between 5240 and 5525 m a.s.l.) (Vincent and others, 2016) where the area-averaged ablation of the entire debris-covered area is

reduced by 1.8 m w.e.  $a^{-1}$ . Fine-grained thick and intact debris cover (0.5 m or more) nearly stop the surface ablation (Potter and others, 1998; Konrad and others, 1999). Further, a large number of glaciers in the HK region are avalanche-fed and accumulating debris continuously. Indeed such phenomena exert strong effects on glacier dynamics; the effects that are very poorly understood in the HK region (see Section 6). The role of supra-glacial debris cover and thus melt beneath debris cover has been investigated (Lejeune and others, 2013; Collier and others, 2015). A few recent studies also addressed the role of backwasting of supraglacial ice cliffs (Buri and others, 2016) and supraglacial ponds on melting of debris-covered glaciers (Miles and others, 2016; Watson and others, 2016). Furthermore, internal ablation (enlargement of englacial conduits) has both a direct and indirect effect on mass loss, through melting and collapse of ice surfaces (Thompson and others, 2016; Benn and others, 2017). Recent satellite observations of glacier dynamics (Scherler and others, 2011), supported by simplified models (Banerjee and Shankar, 2013), have shown that debris-covered glacier losses occur mostly by thinning without significant retreat in response to climatic warming (Rowan and others, 2015; Banerjee, 2017). Further, regional-scale studies have shown that the thinning rates of debris-free and debris-covered ice are not different (Kääb and others, 2012; Nuimura and others, 2012); this is ascribed to dynamics (Banerjee and Shankar, 2013; Banerjee, 2017) and strongly enhanced wastage at thermokarst features like supraglacial ponds, ice cliffs and pro-glacial lakes (Sakai and others, 2002; Buri and others, 2016; Miles and others, 2016; Watson and others, 2016), which counteract the effect of insulation by debris. Future investigations are needed to quantify the role of debris cover on HK glaciers.

As a result of mass wastage (Figs 3a, b), increasing supra-glacial debris-covered area was reported in the Himalaya (Scherler and others, 2011; Nuimura and others, 2012; Thakuri and others, 2014) over the last 5–6 decades. Conversely, in the Karakoram Range, the nearly balanced mass budget since the 1970s (Fig. 3b) are accompanied with nearly unchanged supraglacial debris-covered area between 1977 and 2014 (Herreid and others, 2015). Based on glaciers' response times, a study (Rankl and others, 2014) inferred a shift of the Karakoram glaciers from negative to balanced/positive mass budgets in the 1980s or 1990s, but recent findings (Bolch and others, 2017; Zhou and others, 2017) of steady-state mass balances since the 1970s suggest this shift to be during or preceding the 1970s.

## 6. ADJUSTING GLACIER DYNAMICS

Changes in mass balance (Figs 3c, d) influence the glacier dynamics (Cuffey and Paterson, 2010); hence, an adjustment in HK glacier flow is expected. There has been recent progress in regional satellite-based glacier velocity mapping (Dehecq and others, 2015; Bhattacharya and others, 2016). However, ice thickness data – also scarce in the HK – are needed with velocity measurements to study the glacier dynamics. On Chhota Shigri Glacier, field-based surface velocities and ice thickness were found to be reducing since 2003 (Supplementary material), which suggest that the glacier is adjusting its dynamics in response to its negative mass balances (Azam and others, 2012). Since the Little Ice Age, the mean ice thickness and surface velocities at Khumbu Glacier were also found to be decreasing,



suggesting that Khumbu Glacier is out of balance with climate (Rowan and others, 2015), consistent with a lengthy response time (Jóhannesson and others, 1989). The mean velocity on Gangotri Glacier decreased by  $\sim 6.7\%$  between 2006–14 and 1993–2006, a likely response to negative mass budget (Bhattacharya and others, 2016). To understand the impact of climate change on the HK glacier dynamics and to confirm these glacier-scale findings, more region-scale dynamics studies are urgently needed. Hitherto these handful studies on Chhota Shigri, Khumbu and Gangotri glaciers support the reduced glacier velocities found in response to the negative glacier mass balances in several regions of the world (Heid and Kääb, 2012). Recent accelerations of Baltoro Glacier (Karakoram, Pakistan) (Quincey and others, 2009) and other Karakoram glaciers may be linked with positive mass balances, but the surging phenomenon and a wide range of flow instabilities (Scherler and Strecker, 2012; Bhambri and others, 2017) complicate this relationship (Heid and Kääb, 2012).

## 7. GLACIER/CLIMATE RELATIONSHIP

Many glacial processes such as glacier surface mass balance and glacier runoff respond simultaneously with changes in climate; other responses such as length, area, ice velocity, ice thickness profiles are delayed. For example, a step change in climate may take a century or longer to manifest in an approach toward a new equilibrium glacier length, area and thickness profile (Jóhannesson and others, 1989). The glaciers in the region of low annual temperature range ( $10 < \Delta T < 20^\circ\text{C}$ ) such as in the Himalaya were found to have higher mass-balance sensitivity to climate (temperature and precipitation) change, while glaciers having a higher annual temperature range ( $20 < \Delta T < 30^\circ\text{C}$ ) such as in the Karakoram have lower climate sensitivity (Sakai and others, 2015). Accordingly, eastern and central Himalaya have a higher sensitivity than western Himalaya and Karakoram (Fujita, 2008; Sakai and others, 2015), a feature that alone explains a larger part of the contrasted pattern of mass loss measured using laser altimetry (Sakai and Fujita, 2017). Some studies attempted to understand the mass balances with local meteorological data (Azam and others, 2014a; Sherpa and others, 2017). The glacier wastage in the Himalayan Range is consistent with increasing temperature (Shrestha and others, 1999; Dash and others, 2007; Dimri and Dash, 2012; Banerjee and Azam, 2016) and decreasing precipitation (Bhutiyan and others, 2010; Dimri and Dash, 2012). For instance, on the East Rongbuk Glacier (Everest area) the decrease in snow accumulation from 1970 to 2000 (Kaspari and others, 2008) might be related to the weakening of the AM (Bingyi, 2005). An extremely ambitious global temperature rise of  $1.5^\circ\text{C}$  would lead to a warming of  $2.1 \pm 0.1^\circ\text{C}$  in HMA (including HK region) and that  $64 \pm 7\%$  of the present-day ice mass stored in the HMA glaciers will remain by the end of the century (Kraaijenbrink and others, 2017). Avalanche-fed glaciers in the HK region are sensitive to rising temperature not only through increased melting, but also through a rise in rain/snow transition elevation during the monsoon; this especially impacts avalanche-fed glaciers because their accumulation zones are relatively low due to the downward transfer of snow into avalanche cones (Benn and others, 2012). The conditions which make Karakoram and Himalayan glaciers different could be attributed to increasing winter precipitation in the former (Fowler and

Archer, 2005) or the weaker sensitivity of their winter accumulation to warming (Kapnick and others, 2014; Sakai and Fujita, 2017). Moreover, cooler summers, greater summer cloudiness and snow cover, and decreasing maximum and minimum temperatures (Fowler and Archer, 2005; Shekhar and others, 2010; Bashir and others, 2017; Forsythe and others, 2017) reduce the average ablation rates or the duration of the ablation season (Hewitt, 2005) thereby resulting in quasi-stable mass balance.

The physical basis of glacier/climate relationships can be understood by studying the glacier surface energy balance (SEB). In the HK, only a few SEB studies are available; therefore, we spread our area of interest to the whole HMA region. Generally, the SEB studies are restricted to understand the melt processes at point scale over clean glaciers during the summer-monsoon months (Supplementary Table S11). Some intrinsic discrepancies are evident in the comparison because of different models/methods for SEB calculations, time periods, or climatic conditions. Yet, similar to glaciers worldwide (Favier and others, 2004; Andreassen and others, 2008), net short wave radiation flux is the largest source of energy on glacier surfaces in the HMA region and mainly controls the temporal variability of melting, whereas net longwave radiation flux is the greatest energy sink. The net all-wave radiation flux provides the maximum energy flux with  $>80\%$  contribution to the glacier surface during the summer for the observed HMA glaciers except for Guxiang No. 3 (65%). Sensible turbulent heat flux, always positive over debris-free areas, complements the net radiation flux. Latent heat flux also brings some energy, at least during the core summer-monsoon period, in the form of re-sublimation/condensation of moisture on the glaciers directly affected by monsoonal activity like Chhota Shigri, AX010, Parlung No. 4 and Guxiang No. 3 (Supplementary Table S11). However, depending on the monsoon intensity, the duration of the re-sublimation period can vary from a few weeks (e.g., on Chhota Shigri (Azam and others, 2014b)) to a few days (on Parlung No. 4, where re-sublimation occurs on rare days (Zhu and others, 2015)). With continuous negative latent heat flux, sublimation prevails in the summer over the ablation zones of the glaciers less affected by the monsoon and more affected by drier conditions (e.g., Zhadang Glacier, central Tibetan Plateau (Zhu and others, 2015) and Baltoro Glacier in the Karakoram (Collier and others, 2013)). Therefore, dry climate conditions over the central Tibetan Plateau, Karakoram and northwest Himalaya (Ladakh, Zaskar regions) point toward mass loss through sublimation. For instance, on Puruogangri ice cap (north-central Tibetan Plateau), sublimation accounted for 66% of its total mass loss from October 2001 to September 2011 (Huintjes and others, 2015). The conductive heat flux or heat flux from precipitation is normally small compared with other terms of the SEB. Therefore, the glaciers under drier conditions seem to lose a significant mass fraction through sublimation, while condensation/re-sublimation dominates over glaciers directly influenced by the monsoon. However, we stress that these conclusions are based on a few sporadic studies and need to be confirmed in near future by developing more glacier-scale as well as region-scale SEB studies.

In the western Himalaya, SEB analysis on Chhota Shigri Glacier suggests a clear control of the summer monsoon on annual mass balance through surface albedo change (reduced absorption of solar radiation when monsoonal



snow falls occur) (Azam and others, 2014b). Handling large-scale circulation analysis over HMA, another study (Mölg and others, 2014) suggested that mass balance is mainly determined by the precipitation amounts in May–June and shaped by the intensity of summer-monsoon onset and WD dynamics.

## 8. HYDROLOGICAL REGIMES OF HK RIVERS

Glaciers in a basin can alter the river discharge characteristics at different temporal scales from daily to multi-century (Jansson and others, 2003). Glacier melt contribution to total river discharge depends on the percentage of glacierized area at any given basin outlet hence, going up in the basin, glacier melt contribution increases (Kaser and others, 2010). Glacier runoff contribution in the HK has strong seasonality and follows the seasonality of precipitation/glacier melt in the basins (Bookhagen and Burbank, 2010; Kaser and others, 2010). Total discharge at any basin outlet is the sum of rain runoff, snow melt, glacier melt and base flow (Lutz and others, 2014). A variety of methods with different complexity such as empirical relationships between precipitation and discharge (Thayyen and Gergan, 2010), ice ablation models (Racoviteanu and others, 2013), the hydrograph separation method (Mukhopadhyay and Khan, 2014a, 2015), chemical tracer methods (Racoviteanu and others, 2013) and distributed glacio-hydrological models (Lutz and others, 2014; Ragettli and others, 2015) are used to understand the discharge composition in the HK. Generally, the meteorological stations are installed at valley bottoms; knowledge of the precipitation distribution at glacier altitudes is nearly lacking, which makes it difficult to develop hydrological models. Few studies (Immerzeel and others, 2015; Sakai and others, 2015) used the glacier mass balances to inversely infer the precipitation at glacier altitudes. They generally suggest that the amount of precipitation required to sustain the observed mass balances is far beyond what is observed at valley stations or estimated by gridded precipitation data (Immerzeel and others, 2015). Another challenge in runoff modeling of the HK glaciers is the presence of debris cover. Detailed glacio-hydrological studies explaining the physical basis of discharge generation from debris-cover glaciers are still regionally sparse (Fujita and Sakai, 2014; Ragettli and others, 2015). Further, most models do not include sublimation and wind erosion in these methods/models, yet sublimation may be a vital share of the glacier mass wastage in the dry conditions of the Tibetan Plateau and parts of the Karakoram (see Section 7) or even on wind-exposed high-elevation slopes in the Himalaya due to strong winds mostly in winter (Wagnon and others, 2013).

The HK glaciers play a significant role with varying contributions of glacier and snow melt to the total discharge of HK rivers (Lutz and others, 2014; Pritchard, 2017). For instance, over 1998–2007, in the upper Indus Basin (whole basin excluding Indo-Gangetic plains) stream flow was dominated by glacier meltwater, contributing almost 41% of the total discharge, while in the upper Ganges and upper Brahmaputra basins (whole basins excluding Indo-Gangetic plains) contribution was much lower, i.e., ~12 and 16%, respectively (Lutz and others, 2014). In general, glacial melt dominates snow melt in all these basins (Lutz and others, 2014) but it varies intrabasinally. In the upper Indus Basin, glacial melt dominates in the Karakoram, while in

the western Himalaya, snow melt contributes more than glacial melt to the total discharge (Mukhopadhyay and Khan, 2015). Initially, the positive mass budgets of the central Karakoram (Gardelle and others, 2012) were linked with decreased river flow (Fowler and Archer, 2006). Recently, this relationship was questioned with the finding of increasing river flows in the central Karakoram during the melt season from 1985 to 2010 (Mukhopadhyay and Khan, 2014a) and the nearly balanced mass budgets (Kääb and others, 2015). The increasing river flows are now thought to be associated with increasing mass turnover as a result of increased temperature and precipitation, but under near-neutral mass balance (Mukhopadhyay and Khan, 2014b). Mass wastage over the Himalayan region is expected to modify the runoff regimes. The glacier-wastage contribution (net water withdrawal from glacier storage) is a moderate fraction of the total annual glacial meltwater (Kääb and others, 2012; Gardelle and others, 2013), hence, discharge composition and its seasonal variation will shift in the future due to changing climate, partly but not only because of changing glaciers.

Future expected temperature increase over the HK region will affect river hydrology in three ways: (i) phase change of precipitation from snow to rain directly contributes to the discharge, (ii) the reduced albedo because of less snow imparts more absorption of solar radiation and thus enhances melting, and (iii) earlier seasonal onset and later end of snow/ice melting. In the Shigar catchment (upper Indus basin), snowmelt is projected to occur earlier in the melting season (Soncini and others, 2015). In the HK region, the glacier melt contribution is projected to increase until 2050 and then decrease (Immerzeel and others, 2013; Soncini and others, 2015; Shea and Immerzeel, 2016). Discharge is projected to increase at catchment (Immerzeel and others, 2013; Soncini and others, 2015) and basin scales (Lutz and others, 2014) up to at least 2050 in HK rivers. The projected increase in discharge is mainly due to the enhanced melt for the Indus Basin and increase in precipitation for the Ganges and Brahmaputra basins (Lutz and others, 2014; Tahir and others, 2016). However, partly due to the large differences in glacier area/volume estimates, the future predictions inherit large uncertainties.

## 9. CONCLUSIONS AND OUTLOOK

With increasing recent attention of the scientific community, the understanding of the HK glaciers has grown swiftly, yet this understanding remains weak in spatial and temporal coverage compared with many other mountain ranges of the world. Most glaciers are retreating, shrinking and losing mass with variable rates along the Himalayan Range. These trends are generally consistent with climate warming and decreasing precipitation. The supraglacial debris-covered area in the Himalaya has increased due to glacier shrinkage and debris accumulation. Since the 1970s, the mass budget of Karakoram glaciers has been almost balanced, a global exception initially referred as the ‘Karakoram Anomaly’ and now known to extend to the west of the Tibetan Plateau (western Kunlun and eastern Pamir). This multi-decadal mass stability is in line with nearly unchanged debris-cover. The anomalous behavior of Karakoram glaciers can be linked with increased precipitation and cooler summers as well as their lower sensitivity to temperature change. Often, the climatic response of HK glaciers has been

analyzed using temperature and precipitation data generally from meteorological stations at low altitude. Glacier SEB studies, explaining the physical processes of mass change, are still sparse. We suggest that glaciers in dry regions lose a significant amount of mass through sublimation, while condensation/re-sublimation is dominant over glaciers more directly influenced by monsoons. Thus, sublimation should be included in hydrological modeling at least over dry regions, such as the northwest Himalaya and Karakoram, especially on the cold, dry Tibetan side.

Some glaciological measurements are likely errant and together they contribute to regional glaciological mass balances that are more negative than geodetically based measurements. Once the dubious glaciological data are excluded, the mean regional mass balance has better agreement with the geodetic mass balance in the Himalaya. Considering the deficient statistical representation of glaciers in glaciological mass-balance data, this improved agreement with geodetic mass balances could be somewhat fortuitous. Our screening of all 24 glaciological mass-balance series from the Himalaya identified possible biased series and the evidence suggests that the glaciological method is unsuitable if the glacier is highly debris-covered or surrounded by steep valley walls that induce avalanches. Yet, point mass-balance measurements on such glaciers are of great importance for process understanding and modeling. While most Himalayan glaciers have lost mass over the last 5–6 decades, a few showed steady-state mass-balance episodes. Temporal and spatial variability of mass balances relate to heterogeneous climatic conditions, which vary among or within mountain ranges, or even within the same valley. These findings pose vexing questions about the representativeness of benchmark glaciers and highlight the importance of selection of glaciers for field measurement.

Bolch and others (2012) tracked mass wastage from 1963 to 2010 and saw accelerating ice loss, especially after 1995, with the mean Himalayan glacier wastage trend generally following that of the global mean. Our unscreened dataset, covering a similar but updated time span, leads to a similar conclusion as that of Bolch and others (2012), but our screened data indicate either nearly constant magnitudes of wastage rate or at least less acceleration, in agreement with geodetic mass-balance estimates. Due to the scarcity and biases of glaciological measurements, remote-sensing methods should be preferred for the computation of sea-level rise contribution from the HK region.

Studies have shown decreasing glacier thickness and velocities due to mass wastage in the Himalaya, while in the Karakoram velocities are temporally more variable, but not much is known about local responses of glaciers in the HK range. Though melt contributions from the HK glaciers are projected to increase until 2050 and then decrease (Immerzeel and others, 2013; Soncini and others, 2015; Shea and Immerzeel, 2016), the wide range of area and volume estimates (glacier inventories still have ~30% range in estimates) introduces big uncertainties in runoff. Accurate glacier inventory and additional in situ measurements of glacier volumes are needed to validate the area-volume parameterizations and volume distribution models (Frey and others, 2014; Farinotti and others, 2017) used in hydrological modeling. These models are hampered by poor information on the amount, spatial distribution and phase state of high-elevation precipitation, and of permafrost in the HK.

The projected increase in discharge if coupled with extreme rainfall in the future may result in floods that may further induce rapid erosion, landslides, glacial lake outburst floods (GLOFs), etc. Such an event occurred in Kedarnath (Uttarakhand, India) during 15–17 June 2013 when extreme 1-day rainfall of 325 mm was recorded; this extreme event is believed to be a result of the summer monsoon and WD convergence (Bhambri and others, 2015). This rainfall event also caused the collapse of the moraine-dammed Chorabari Glacier Lake. The resulting flood devastated the Kedarnath valley and downstream, and killed hundreds of people (Dobhal and others, 2013). Several glacial lakes were found potentially dangerous in the HK (Bajracharya and Mool, 2009; Fujita and others, 2013), but the prediction of extreme rainfall events, the growth of possible future lakes (Linsbauer and others, 2016), related risks or GLOFs is still difficult because of limited regional forecasting abilities (Bookhagen, 2010). Sometimes glacial surges develop a natural dam and block the river streams that further result in outburst floods (Hewitt and Liu, 2010; Round and others, 2017).

Our mass-balance reliability assessment using scoring method highlights the weaknesses in available mass-balance series. We recommend long-term continuation and expansion of ongoing in situ glaciological observations in the HK so that these glaciers can be used for climate change and applications studies. Further, for ongoing or future observations, we suggest to systematically include uncertainty estimates, use an optimized density of ablation stakes, perform systematic accumulation measurements with appropriate methods (e.g., use of artificial layer to mark the glacier surface), and verify in situ glaciological mass balances with geodetic mass balances.

We also propose the establishment of a network of high altitude meteorological and discharge stations covering more glaciers/watersheds in the HK region, adoption of a holistic approach to understand mass-balance-climate/hydrology relationships, and development of data sharing policies among the HK countries so that the large-scale modeling of the future glacier and runoff evolution can be done with improved accuracy.

The pace of glacier change is fast enough that many applications and interests should consider climate-change induced glacier responses and associated hydrological changes, but is slow enough that well-planned and locally tailored approaches to adaptation are both possible and needed.

## SUPPLEMENTARY MATERIAL

The supplementary material for this article can be found at <https://doi.org/10.1017/jog.2017.86>

## AUTHOR CONTRIBUTIONS

MFA compiled and analyzed the data, generated the figures and wrote the review. All authors contributed significantly to writing and improving this review.

## ACKNOWLEDGEMENTS

MFA acknowledges the research grant from INSPIRE Faculty award (IFA-14-EAS-22) from Department of Science and Technology (India) and National Institute of Hydrology

(India) for hosting INSPIRE Faculty tenure. Thanks to Antoine Rabatel for his suggestions for mass-balance analysis, Argha Banerjee on his suggestions on debris cover section and Joseph Michael Shea for providing modeled mass balances on Mera Glacier. EB acknowledges support from the French Space Agency (CNES) through the TOSCA and ISIS programs and from the Programme National de Télédétection Spatiale (PNTS, <http://www.insu.cnrs.fr/pnts>), grant PNTS-2016-01. JSK acknowledges support as part of NASA's High Mountain Asia Team. KF acknowledges support from JSPS-KAKENHI grant number 26257202. We thank the scientific editor Hester Jiskoot and two anonymous reviewers for their constructive suggestions.

## REFERENCES

- Ageta Y and Higuchi K (1984) Estimation of mass balance components of a summer-accumulation type glacier in the Nepal Himalaya. *Geogr. Ann. Ser. Phys. Geogr.*, **66**, 249–255
- Andreassen LM, Van Den Broeke MR, Giesen RH and Oerlemans J (2008) A 5 year record of surface energy and mass balance from the ablation zone of Storbreen, Norway. *J. Glaciol.*, **54**(185), 245–258
- Azam MF and 9 others (2012) From balance to imbalance: a shift in the dynamic behaviour of Chhota Shigri glacier, western Himalaya, India. *J. Glaciol.*, **58**(208), 315–324
- Azam MF and 5 others (2014a) Reconstruction of the annual mass balance of Chhota Shigri glacier, Western Himalaya, India, since 1969. *Ann. Glaciol.*, **55**(66), 69–80
- Azam MF and 6 others (2014b) Processes governing the mass balance of Chhota Shigri Glacier (western Himalaya, India) assessed by point-scale surface energy balance measurements. *Cryosphere*, **8**(6), 2195–2217
- Azam MF and 10 others (2016) Meteorological conditions, seasonal and annual mass balances of Chhota Shigri Glacier, western Himalaya, India. *Ann. Glaciol.*, **57**, 328–338
- Bajracharya SR and Mool P (2009) Glaciers, glacial lakes and glacial lake outburst floods in the Mount Everest region, Nepal. *Ann. Glaciol.*, **50**(53), 81–86
- Banerjee A (2017) Brief communication: thinning of debris-covered and debris-free glaciers in a warming climate. *Cryosphere*, **11**(1), 133–138
- Banerjee A and Shankar R (2013) On the response of Himalayan glaciers to climate change. *J. Glaciol.*, **59**(215), 480–490
- Banerjee A and Azam MF (2016) Temperature reconstruction from glacier length fluctuations in the Himalaya. *Ann. Glaciol.*, **57**, 189–198
- Barandun M and 8 others (2015) Re-analysis of seasonal mass balance at Abramov glacier 1968–2014. *J. Glaciol.*, **61**(230), 1103–1117
- Bashir F, Zeng X, Gupta H and Hazenberg PA (2017) Hydro-meteorological perspective on the Karakoram Anomaly using unique valley-based synoptic weather observations. *Geophys. Res. Lett.*, **44**(20), 10,470–10,478 (doi: 10.1002/2017GL075284)
- Benn DI and 9 others (2012) Response of debris-covered glaciers in the Mount Everest region to recent warming, and implications for outburst flood hazards. *Earth-Sci. Rev.*, **114**, 156–174
- Benn DI and 5 others (2017) Structure and evolution of the drainage system of a Himalayan debris-covered glacier, and its relationship with patterns of mass loss. *Cryosphere*, **11**, 2247–2264
- Bhambri R and 5 others (2013) Heterogeneity in glacier response in the upper Shyok valley, northeast Karakoram. *Cryosphere*, **7**, 1385–1398
- Bhambri R and 6 others (2015) Devastation in the Kedarnath (Mandakini) Valley, Garhwal Himalaya, during 16–17 June 2013: a remote sensing and ground-based assessment. *Nat. Hazards*, **80**, 1801–1822
- Bhambri R, Hewitt K, Kawishwar P and Pratap B (2017) Surge-type and surge-modified glaciers in the Karakoram. *Sci. Rep.*, **7**(1), 15391 (doi: 10.1038/s41598-017-15473-8)
- Bhattacharya A and 5 others (2016) Overall recession and mass budget of Gangotri Glacier, Garhwal Himalayas, from 1965 to 2015 using remote sensing data. *J. Glaciol.*, **62**(236), 1115–1133
- Bhutiyan MR, Kale VS and Pawar NJ (2010) Climate change and the precipitation variations in the northwestern Himalaya: 1866–2006. *Int. J. Climatol.*, **30**(4), 535–548
- Bingyi W (2005) Weakening of Indian summer monsoon in recent decades. *Adv. Atmospheric Sci.*, **22**(1), 21–29
- Bolch T, Buchroithner M, Pieczonka T and Kunert A (2008) Planimetric and volumetric glacier changes in the Khumbu Himal, Nepal, since 1962 using Corona, Landsat TM and ASTER data. *J. Glaciol.*, **54**(187), 592–600
- Bolch T and 9 others (2012) The state and fate of Himalayan glaciers. *Science*, **336**(6079), 310–314
- Bolch T, Pieczonka T, Mukherjee K and Shea J (2017) Brief communication: glaciers in the Hunza catchment (Karakoram) have been nearly in balance since the 1970s. *Cryosphere*, **11**(1), 531
- Bookhagen B (2010) Appearance of extreme monsoonal rainfall events and their impact on erosion in the Himalaya. *Geomat. Nat. Hazards Risk*, **1**(1), 37–50
- Bookhagen B and Burbank DW (2010) Toward a complete Himalayan hydrological budget: spatiotemporal distribution of snowmelt and rainfall and their impact on river discharge. *J. Geophys. Res.: Earth Surf.*, **115**(F3), 1–25 (doi: 10.1029/2009JF 001426)
- Brun F, Berthier E, Wagnon P, Kääb A and Treichler D (2017) A spatially resolved estimate of High Mountain Asia glacier mass balances from 2000 to 2016. *Nat. Geosci.*, **10**, 668–673 (doi: 10.1038/ngeo2999)
- Buri P, Pellicciotti F, Steiner JF, Miles ES and Immerzeel WW (2016) A grid-based model of backwasting of supraglacial ice cliffs on debris-covered glaciers. *Ann. Glaciol.*, **57**(71), 199–211
- Chand P and Sharma MC (2015) Glacier changes in the Ravi basin, North-Western Himalaya (India) during the last four decades (1971–2010/13). *Glob. Planet. Change*, **135**, 133–147
- Cogley JG (2011) Present and future states of Himalaya and Karakoram glaciers. *Ann. Glaciol.*, **52**(59), 69–73
- Cogley JG (2016) Glacier shrinkage across High Mountain Asia. *Ann. Glaciol.*, **57**(71), 41–49
- Cogley JG, Kargel JS, Kaser G and van der Veen CJ (2010) Tracking the source of glacier misinformation. *Science*, **327**(5965), 522
- Collier E and 5 others (2013) High-resolution interactive modelling of the mountain glacier–atmosphere interface: an application over the Karakoram. *Cryosphere*, **7**(3), 779–795
- Collier E and 5 others (2015) Impact of debris cover on glacier ablation and atmosphere–glacier feedbacks in the Karakoram. *Cryosphere*, **9**(4), 1617–1632
- Cuffey KM and Paterson WSB (2010) *The physics of glaciers*, 4<sup>th</sup> edn. Butterworth-Heinemann, Oxford
- Dash SK, Jenamani RK, Kalsi SR and Panda SK (2007) Some evidence of climate change in twentieth-century India. *Clim. Change*, **85**(3), 299–321
- Dehecq A, Gourmelen N and Trouvé E (2015) Deriving large-scale glacier velocities from a complete satellite archive: application to the Pamir–Karakoram–Himalaya. *Remote Sens. Environ.*, **162**, 55–66
- Dehecq A, Millan R, Berthier E, Gourmelen N and Trouve E (2016) Elevation changes inferred from TanDEM-X data over the Mont-Blanc area: impact of the X-band interferometric bias. *IEEE J-STARS*, **9**(8), 3870–3882 (doi: 10.1109/JSTARS.2016.2581482)
- Dimri AP and Dash SK (2012) Wintertime climatic trends in the western Himalayas. *Clim. Change*, **111**(3–4), 775–800
- Dimri AP and Mohanty UC (2009) Simulation of mesoscale features associated with intense western disturbances over western Himalayas. *Meteorol. Appl.*, **16**(3), 289–308
- Dobhal DP, Gupta AK, Mehta M and Khandelwal DD (2013) Kedarnath disaster: facts and plausible causes. *Curr. Sci.*, **105**, 171–174



- Farinotti D and 37 others (2017) How accurate are estimates of glacier ice thickness? Results from ITMIX, the Ice thickness models intercomparison eXperiment. *Cryosphere*, **11**, 949–970
- Favier V, Wagnon P, Chazarin J-P, Maisincho L and Coudrain A (2004) One-year measurements of surface heat budget on the ablation zone of Antizana Glacier 15, Ecuadorian Andes. *J. Geophys. Res. Atmos.*, **109**(D18), 1–15
- Forsythe N, Fowler HJ, Li X-F, Blenkinsop S and Pritchard D (2017) Karakoram temperature and glacial melt driven by regional atmospheric circulation variability. *Nat. Clim. Chang.*, **7**(9), 664–+ (doi: 10.1038/NCLIMATE3361)
- Fowler HJ and Archer DR (2005) Hydro-climatological variability in the Upper Indus Basin and implications for water resources. *Reg. Hydrol. Impacts Clim. Chang. Assess. Decis. Mak.*, **295**, 131–138
- Fowler HJ and Archer DR (2006) Conflicting signals of climatic change in the Upper Indus Basin. *J. Clim.*, **19**(17), 4276–4293
- Frey H and 9 others (2014) Estimating the volume of glaciers in the Himalayan–Karakoram region using different methods. *Cryosphere*, **8**(6), 2313–2333
- Fujita K (2008) Effect of precipitation seasonality on climatic sensitivity of glacier mass balance. *Earth Planet. Sci. Lett.*, **276**(1), 14–19
- Fujita K and Sakai A (2014) Modelling runoff from a Himalayan debris-covered glacier. *Hydrol. Earth Syst. Sci.*, **18**(7), 2679
- Fujita K and 6 others (2013) Potential flood volume of Himalayan glacial lakes. *Nat. Hazards Earth Syst. Sci.*, **13**(7), 1827
- Gardelle J, Berthier E and Arnaud Y (2012) Slight mass gain of Karakoram glaciers in the early twenty-first century. *Nat. Geosci.*, **5**(5), 322–325
- Gardelle J, Berthier E, Arnaud Y and Kääb A (2013) Region-wide glacier mass balances over the Pamir-Karakoram-Himalaya during 1999–2011. *Cryosphere*, **7**, 1885–1886
- Gardner AS and 9 others (2013) A reconciled estimate of glacier contributions to sea level rise: 2003 to 2009. *Science*, **340** (6134), 852–857
- Heid T and Kääb A (2012) Repeat optical satellite images reveal widespread and long term decrease in land-terminating glacier speeds. *Cryosphere*, **6**(2), 467–478
- Herreid S and 6 others (2015) Satellite observations show no net change in the percentage of supraglacial debris-covered area in northern Pakistan from 1977 to 2014. *J. Glaciol.*, **61**(227), 524–536
- Hewitt K (2005) The Karakoram anomaly? Glacier expansion and the ‘elevation effect’ Karakoram Himalaya. *Mt. Res. Dev.*, **25** (4), 332–340
- Hewitt K and Liu J (2010) Ice-dammed lakes and outburst floods, Karakoram Himalaya: historical perspectives on emerging threats. *Phys. Geogr.*, **31**(6), 528–551
- Huintjes E, Neckel N, Hochschild V and Schneider C (2015) Surface energy and mass balance at Purogangri ice cap, central Tibetan Plateau, 2001–2011. *J. Glaciol.*, **61**(230), 1048–1060
- Huss M and Hock R (2015) A new model for global glacier change and sea-level rise. *Front. Earth Sci.*, **3**, 1–22
- Immerzeel WW, Van Beek LP and Bierkens MF (2010) Climate change will affect the Asian water towers. *Science*, **328**(5984), 1382–1385
- Immerzeel WW, Pellicciotti F and Bierkens MFP (2013) Rising river flows throughout the twenty-first century in two Himalayan glacierized watersheds. *Nat. Geosci.*, **6**, 742–745
- Immerzeel WW, Wanders N, Lutz AF, Shea JM and Bierkens MFP (2015) Reconciling high-altitude precipitation in the upper Indus basin with glacier mass balances and runoff. *Hydrol. Earth Syst. Sci.*, **19**(11), 4673
- Jacob T, Wahr J, Pfeffer WT and Swenson S (2012) Recent contributions of glaciers and ice caps to sea level rise. *Nature*, **482**(7386), 514–518
- Jansson P, Hock R and Schneider T (2003) The concept of glacier storage: a review. *J. Hydrol.*, **282**(1), 116–129
- Jóhannesson T, Raymond C and Waddington ED (1989) Time-scale for adjustment of glaciers to changes in mass balance. *J. Glaciol.*, **35**(121), 355–369
- Kääb A, Berthier E, Nuth C, Gardelle J and Arnaud Y (2012) Contrasting patterns of early twenty-first-century glacier mass change in the Himalayas. *Nature*, **488**(7412), 495–498
- Kääb A, Treichler D, Nuth C and Berthier E (2015) Brief communication: contending estimates of 2003–2008 glacier mass balance over the Pamir–Karakoram–Himalaya. *Cryosphere*, **9** (2), 557–564
- Kapnick SB, Delworth TL, Ashfaq M, Malyshev S and Milly PC (2014) Snowfall less sensitive to warming in Karakoram than in Himalayas due to a unique seasonal cycle. *Nat. Geosci.*, **7**(11), 834–840
- Kaser G, Großhauser M and Marzeion B (2010) Contribution potential of glaciers to water availability in different climate regimes. *Proc. Natl. Acad. Sci.*, **107**(47), 20223–20227
- Kaspari S and 5 others (2008) Snow accumulation rate on Qomolangma (Mount Everest), Himalaya: synchronicity with sites across the Tibetan Plateau on 50–100 year timescales. *J. Glaciol.*, **54**(185), 343–352
- Khanal NR and 6 others (2015) A comprehensive approach and methods for glacial lake outburst flood risk assessment, with examples from Nepal and the transboundary area. *Int. J. Water Resour. Dev.*, **31**(2), 219–237
- Konrad SK and 5 others (1999) Rock glacier dynamics and paleo-climatic implications. *Geology*, **27**(12), 1131–1134
- Kraaijenbrink PDA, Bierkens MFP, Lutz AF and Immerzeel WW (2017) Impact of a global temperature rise of 1.5 degrees Celsius on Asia’s glaciers. *Nature*, **549**, 257–260
- Kulkarni AV and 6 others (2007) Glacial retreat in Himalaya using Indian remote sensing satellite data. *Curr. Sci.*, **92**, 69–74
- Laha S and 7 others (2017) Evaluating the contribution of avalanching to the mass balance of Himalayan glaciers. *Ann. Glaciol.*, **1–9**. (doi: 10.1017/aog.2017.27)
- Lang TJ and Barros AP (2004) Winter storms in the central Himalayas. *J. Meteorol. Soc. Japan*, **82**, 829–844
- Lejeune Y, Bertrand J-M, Wagnon P and Morin S (2013) A physically based model of the year-round surface energy and mass balance of debris-covered glaciers. *J. Glaciol.*, **59**(214), 327–344
- Linsbauer A and 5 others (2016) Modelling glacier-bed overdeepenings and possible future lakes for the glaciers in the Himalaya–Karakoram region. *Ann. Glaciol.*, **57**(71), 119–130
- Lutz AF, Immerzeel WW, Shrestha AB and Bierkens MFP (2014) Consistent increase in high Asia’s runoff due to increasing glacier melt and precipitation. *Nat. Clim. Chang.*, **4**, 587–592
- MauSSION F and 5 others (2014) Precipitation seasonality and variability over the Tibetan plateau as resolved by the high Asia reanalysis. *J. Clim.*, **27**(5), 1910–1927
- Mayer C, Lambrecht A, Belo M, Smiraglia C and Diolaiuti G (2006) Glaciological characteristics of the ablation zone of Baltoro glacier, Karakoram, Pakistan. *Ann. Glaciol.*, **43**(1), 123–131
- Miles ES and 5 others (2016) Refined energy-balance modelling of a supraglacial pond, Langtang Khola, Nepal. *Ann. Glaciol.*, **57**(71), 29–40
- Mölg T, MauSSION F and Scherer D (2014) Mid-latitude westerlies as a driver of glacier variability in monsoonal high Asia. *Nat. Clim. Change*, **4**(1), 68–73
- Mukhopadhyay B and Khan A (2014a) A quantitative assessment of the genetic sources of the hydrologic flow regimes in Upper Indus Basin and its significance in a changing climate. *J. Hydrol.*, **509**, 549–572
- Mukhopadhyay B and Khan A (2014b) Rising river flows and glacial mass balance in central Karakoram. *J. Hydrol.*, **513**, 192–203
- Mukhopadhyay B and Khan A (2015) A reevaluation of the snow-melt and glacial melt in river flows within Upper Indus Basin and its significance in a changing climate. *J. Hydrol.*, **527**, 119–132
- Neckel N, Bolch T and Hochschild V (2014) Glacier mass changes on the Tibetan plateau 2003? 2009 derived from ICESat laser altimetry measurements. *Environ. Res. Lett.*, **9**(1), 014009
- Nepal S, Krause P, Flügel W-A, Fink M and Fischer C (2014) Understanding the hydrological system dynamics of a glaciated

- alpine catchment in the Himalayan region using the J2000 hydrological model. *Hydrol. Process.*, **28**(3), 1329–1344
- Nuimura T, Fujita K, Yamaguchi S and Sharma RR (2012) Elevation changes of glaciers revealed by multitemporal digital elevation models calibrated by GPS survey in the Khumbu region, Nepal Himalaya, 1992–2008. *J. Glaciol.*, **58**(210), 648–656
- Oerlemans J (2001) *Glaciers and climate change*. A.A. Balkema, Lisse
- Ojha S and 6 others (2016) Glacier area shrinkage in eastern Nepal Himalaya since 1992 using high-resolution inventories from aerial photographs and ALOS satellite images. *J. Glaciol.*, **62**(233), 512–524
- Pellicciotti F, Stephan C, Miles E, Immerzeel WW and Bolch T (2015) Mass-balance changes of the debris-covered glaciers in the Langtang Himal, Nepal, from 1974 to 1999. *J. Glaciol.*, **61**(226), 373–386
- Potter N and 5 others (1998) Galena Creek rock glacier revisited—new observations on an old controversy. *Geogr. Ann.: Ser. A, Phys. Geo.*, **80**(3–4), 251–265
- Pritchard HD (2017) Asia's glaciers are a regionally important buffer against drought. *Nature*, **545**(7653), 169–174
- Quincey DJ and 5 others (2009) Ice velocity and climate variations for Baltoro Glacier, Pakistan. *J. Glaciol.*, **55**(194), 1061–1071
- Racoviteanu AE and Bahuguna IM (2014) Himalayan glaciers (India, Bhutan, Nepal), chapter 24. In Kargel JS, Leonard GJ, Bishop MP, Kääb A and Raup B eds. *Global land Ice measurements from space*. Springer-Praxis, Heidelberg, 549–582
- Racoviteanu AE, Armstrong R and Williams MW (2013) Evaluation of an ice ablation model to estimate the contribution of melting glacier ice to annual discharge in the Nepal Himalaya. *Water Resour. Res.*, **49**(9), 5117–5133
- Racoviteanu AE, Arnaud Y, Williams MW and Manley WF (2015) Spatial patterns in glacier characteristics and area changes from 1962 to 2006 in the Kanchenjunga-Sikkim area, eastern Himalaya. *Cryosphere*, **9**, 505–523
- Ragetli S and 9 others (2015) Unraveling the hydrology of a Himalayan catchment through integration of high resolution in situ data and remote sensing with an advanced simulation model. *Adv. Water Resour.*, **78**, 94–111
- Ragetli S, Bolch T and Pellicciotti F (2016) Heterogeneous glacier thinning patterns over the last 40 years in Langtang Himal. *Cryosphere*, **10**, 2075–2097
- Rankl M, Kienholz C and Braun M (2014) Glacier changes in the Karakoram region mapped by multimission satellite imagery. *Cryosphere*, **8**(3), 977–989
- Reager JT and 5 others (2016) A decade of sea level rise slowed by climate-driven hydrology. *Science*, **351**(6274), 699–703
- Rodell M, Velicogna I and Famiglietti JS (2009) Satellite-based estimates of groundwater depletion in India. *Nature*, **460**, 999–1002
- Round V, Leinss S, Huss M, Haemmig C and Hajnsek I (2017) Surge dynamics and lake outbursts of Kyagar Glacier, Karakoram. *Cryosphere*, **11**(2), 723–739 (doi: 10.5194/tc-11-723-2017)
- Rowan AV, Egholm DL, Quincey DJ and Glasser NF (2015) Modelling the feedbacks between mass balance, ice flow and debris transport to predict the response to climate change of debris-covered glaciers in the Himalaya. *Earth Planet. Sci. Lett.*, **430**, 427–438
- Sakai A and Fujita K (2017) Contrasting glacier responses to recent climate change in high-mountain Asia. *Sci. Rep.*, **7**(1), 13717 (doi: 10.1038/s41598-017-14256-5)
- Sakai A, Nakawo M and Fujita K (2002) Distribution characteristics and energy balance of ice cliffs on debris-covered glaciers, Nepal Himalaya. *Arctic, Antarct. Alp. Res.*, **34**, 12
- Sakai A and 5 others (2015) Climate regime of Asian glaciers revealed by GAMDAM glacier inventory. *Cryosphere*, **9**(3), 865–880
- Salerno F, Buraschi E, Bruccoleri G, Tartari G and Smiraglia C (2008) Glacier surface-area changes in Sagarmatha national park, Nepal, in the second half of the 20th century, by comparison of historical maps. *J. Glaciol.*, **54**(187), 738–752
- Scherler D and Strecker MR (2012) Large surface velocity fluctuations of Biafo Glacier, central Karakoram, at high spatial and temporal resolution from optical satellite images. *J. Glaciol.*, **58**(209), 569–580
- Scherler D, Bookhagen B and Strecker MR (2011) Spatially variable response of Himalayan glaciers to climate change affected by debris cover. *Nat. Geosci.*, **4**, 156–159
- Schmidt S and Nüsser M (2012) Changes of high altitude glaciers from 1969 to 2010 in the Trans-Himalayan Kang Yatze Massif, Ladakh, northwest India. *Arct. Antarct. Alp. Res.*, **44**(1), 107–121
- Shangguan D and 9 others (2014) Glacier changes in the Koshi River basin, central Himalaya, from 1976 to 2009, derived from remote-sensing imagery. *Ann. Glaciol.*, **55**(66), 61–68
- Shea JM and Immerzeel WW (2016) An assessment of basin-scale glaciological and hydrological sensitivities in the Hindu Kush–Himalaya. *Ann. Glaciol.*, **57**(71), 308–318
- Shea JM, Immerzeel WW, Wagnon P, Vincent C and Bajracharya S (2015) Modelling glacier change in the Everest region, Nepal Himalaya. *Cryosphere*, **9**(3), 1105–1128
- Shekhar MS, Chand H, Kumar S, Srinivasan K and Ganju A (2010) Climate-change studies in the western Himalaya. *Ann. Glaciol.*, **51**(54), 105–112
- Sherpa SF and 8 others (2017) Contrasted surface mass balances of debris-free glaciers observed between the southern and the inner parts of the Everest region (2007–15). *J. Glaciol.*, **63**(240), 637–651
- Shrestha AB, Wake CP, Mayewski PA and Dibb JE (1999) Maximum temperature trends in the Himalaya and its vicinity: an analysis based on temperature records from Nepal for the period 1971–94. *J. Clim.*, **12**(9), 2775–2786
- Soncini A and 9 others (2015) Future hydrological regimes in the upper Indus basin: a case study from a high-altitude glacierized catchment. *J. Hydrometeorol.*, **16**(1), 306–326
- Song C, Huang B, Richards K, Ke L and Hien Phan V (2014) Accelerated lake expansion on the Tibetan Plateau in the 2000s: induced by glacial melting or other processes? *Water Resour. Res.*, **50**(4), 3170–3186
- Tahir AA, Adamowski JF, Chevallier P, Haq AU and Terzago S (2016) Comparative assessment of spatiotemporal snow cover changes and hydrological behavior of the Gilgit, Astore and Hunza River basins (Hindukush–Karakoram–Himalaya region, Pakistan). *Meteorol. Atmos. Phys.*, **128**(6), 793–811
- Thakuri S and 6 others (2014) Tracing glacier changes since the 1960s on the south slope of Mt. Everest (central Southern Himalaya) using optical satellite imagery. *Cryosphere*, **8**, 1297–1315
- Thayyen RJ and Gergan JT (2010) Role of glaciers in watershed hydrology: a preliminary study of a 'Himalayan catchment'. *Cryosphere*, **4**, 115–128
- Thompson S, Benn DI, Mertes J and Luckman A (2016) Stagnation and mass loss on a Himalayan debris-covered glacier: processes, patterns and rates. *J. Glaciol.*, **62**(233), 467–485
- Vaughan DG and 13 others (2013) Observations: Cryosphere. In Stocker TF, Qin D, Plattner G-K, Tignor M, Allen SK, Boschung J, Nauels A, Xia Y, Bex V and Midgley PM eds. *Climate Change: The Physical Science Basis. Contribution of Working Group I to the Fifth Assessment Report of the Intergovernmental Panel on Climate Change*. 317–382, Cambridge University Press, Cambridge, UK and New York, NY, USA
- Vincent C and 9 others (2013) Balanced conditions or slight mass gain of glaciers in the Lahaul and Spiti region (northern India, Himalaya) during the nineties preceded recent mass loss. *Cryosphere*, **7**(2), 569–582
- Vincent C and 10 others (2016) Reduced melt on debris-covered glaciers: investigations from Changri Nup Glacier, Nepal. *Cryosphere*, **10**, 1845–1858
- Wagnon P and 9 others (2013) Seasonal and annual mass balances of Mera and Pokalde glaciers (Nepal Himalaya) since 2007. *Cryosphere*, **7**(6), 1769–1786

- Watson CS, Quincey DJ, Carrivick JL and Smith MW (2016) The dynamics of supraglacial ponds in the Everest region, central Himalaya. *Glob. Planet. Change*, **142**, 14–27
- Yi S and Sun W (2014) Evaluation of glacier changes in high-mountain Asia based on 10 year GRACE RL05 models. *J. Geophys. Res. Solid Earth*, **119**(3), 2504–2517
- Zemp M and 6 others (2012) *Fluctuations of glaciers 2005–2010, volume X*. ICSU (WDS)/IUGG (IACS)/UNEP/UNESCO/WMO, World Glacier Monitoring Service, Zurich, Switzerland
- WGMS (2013) Glacier Mass Balance Bulletin No. 12 (2010–2011). Zemp, M., Nussbaumer, S. U., Naegeli, K., Gärtner-Roer, I., Paul, F., Hoelzle, M., and Haeberli, W. (eds.), ICSU(WDS)/IUGG (IACS)/UNEP/ UNESCO/WMO, World Glacier Monitoring Service, Zurich, Switzerland, 106 pp., publication based on database version: doi:10.5904/wgms-fog-2013-11.
- Zemp M and 38 others (2015) Historically unprecedented global glacier decline in the early 21st century. *J. Glaciol.*, **61**(228), 745–762
- Zhang G and 13 others (2017) Lake volume and groundwater storage variations in Tibetan plateau's endorheic basin. *Geophys. Res. Lett.*, **44**(11), 5550–5560 (doi: 10.1002/2017GL073773)
- Zhou Y, Li Z and Li J (2017) Slight glacier mass loss in the Karakoram region during the 1970s to 2000 revealed by KH-9 images and SRTM DEM. *J. Glaciol.*, **63**(238), 331–342
- Zhu M and 5 others (2015) Energy-and mass-balance comparison between Zhadang and Parlung No. 4 glaciers on the Tibetan Plateau. *J. Glaciol.*, **61**(227), 595–607

*MS received 11 August 2017 and accepted in revised form 4 December 2017; first published online 9 January 2018*



Supplementary materials for  
**Review of the status and mass changes of Himalayan-Karakoram  
glaciers**

**Mohd Farooq AZAM<sup>\*1</sup>, Patrick WAGNON<sup>2,3</sup>, Etienne BERTHIER<sup>4</sup>, Christian  
VINCENT<sup>2</sup>, Koji FUJITA<sup>5</sup> and Jeffrey S. KARGEL<sup>6</sup>**

*<sup>1</sup>National Institute of Hydrology, Roorkee, Uttarakhand, India*

*<sup>2</sup>Univ. Grenoble Alpes, CNRS, IRD, IGE, F-38000 Grenoble, France*

*<sup>3</sup>International Centre for Integrated Mountain Development, Kathmandu, Nepal*

*<sup>4</sup>LEGOS, Université de Toulouse, CNES, CNRS, IRD, UPS, (Toulouse), France*

*<sup>5</sup>Graduate School of Environmental Studies, Nagoya University, Nagoya, Japan*

*<sup>6</sup>Department of Hydrology and Atmospheric Sciences, University of Arizona, Tucson, AZ, USA*

**\*corresponding author. Email: [farooqaman@yahoo.co.in](mailto:farooqaman@yahoo.co.in)**

## **Supplementary Text**

### **Glacier area and volume estimates**

Recent glacierized area estimates for the HK region varies from 36 845 to 50 750 km<sup>2</sup> (Table S1). These large differences among glacier inventories could be due to different geographical demarcation of the mountain ranges, different maps and satellite images used, cloud cover in satellite imagery, different methods (manual or semi-automatic methods of delimitation), inclusion or not of steep avalanche walls, shading effects on glaciers, difficulty to identify debris-covered part of glaciers etc. For example, steep avalanche walls over which snow cannot accumulate were deliberately excluded in the GAMDAM glacier inventory (Nuimura and others, 2015), explaining the smaller glacierized area of the HK range in this inventory. Conversely, in Kääb and others (2012), ice areas from steep terrains and small snow and ice patches present in satellite images with the minimal snow cover were included explaining the largest glacier area in this inventory. However, Kääb and others (2012) stressed that the steep areas and ice patches included in their area estimates might not be included in conventional map-based glacier inventories.

One comprehensive HK-wide (plus Hindu Kush) inventory (Bajracharya and Shrestha, 2011) usefully broke down the data by sub-basins and provided detailed analysis such as glacier number, hypsography, clean-ice and debris-covered glaciers' area, and ice volumes. Unfortunately, the field based ice thickness measurements, needed for ice volume model validation, are extremely limited and most were not available at the time of ICIMOD report (Gärtner-Roer and others, 2014; Vincent and others, 2016) and therefore ice volumes in Bajracharya and Shrestha (2011) were estimated using an empirical relationship between glacier ice thickness and area, derived from the Tian Shan mountain region. A recent study estimated the ice volumes for the Himalaya and Karakoram using the glacier inventory of Bolch and others (2012) and local ice thickness measurements on a few HK glaciers (Frey and others, 2014). Depending upon the adopted approach, the published volume estimates range from 2 955 to 4 737 km<sup>3</sup>. This wide range indicates the need for improvements in ice volume models and a requirement for in-situ glacier ice thickness data. Recently an international vast initiative was undertaken to inter-compare the ice volume estimates of glaciers worldwide (Farinotti and others, 2017).

### **Glacier fluctuations and area changes**

Historical snout fluctuations and area shrinkage are often estimated comparing the Survey of India (SOI) maps with the recent satellite images (Table S2 and S3). The surveying and

mapping of the Himalayan glaciers were started in the early 19<sup>th</sup> century using the plane-table survey and heavy theodolites (Purdon, 1861; Godwin-Austen, 1864). Since the beginning of the 20<sup>th</sup> century, SOI together with the Geological Survey of India (GSI) produced topographic maps at different scales for several glaciers using plane table, terrestrial photogrammetry and aerial photographs combined with field work (Longstaff, 1910; Auden, 1937; Chaujar, 1989; Survey of India, 2005). However, these maps are not in the public domain and some contain errors due to the seasonal snow cover that led to some erroneous glacier delineations (Bhambri and Bolch, 2009; Raina, 2009). Therefore, the uncertainties of mapped glacier outlines are unclear and rarely accounted for in snout fluctuation or glacier area change estimates. Some revised studies (Chand and Sharma, 2015; Nainwal and others, 2016) indicated an overestimation of area shrinkage and snout retreat in the older studies. Starting in the 1960s, satellites have delivered images of glacierized areas around the globe. Comparison of the latest satellite-based images with old maps and photographs allowed researchers to quantify the glacier snout fluctuations or area changes. Some recent studies (Table S3) estimated the area change using different satellite-only data sets and methodologies.

From available literature, we calculate the snout retreat in m per year for 152 glaciers and 2 basins (Table S2) and rate of area change in percent per year for 24 glaciers and 47 basins (Table S3) with respect to the initial observed area following equation 1:

$$\dot{A} = \frac{1}{A_0} \left[ \frac{A_1 - A_0}{y_1 - y_0} \right] 100$$

where  $\dot{A}$  is the shrinkage rate (% yr<sup>-1</sup>),  $A_0$  and  $A_1$  are the initial and final observed areas (km<sup>2</sup>),  $y_0$  and  $y_1$  represent the initial and final integer years of observation (which is strictly relevant when complete hydrological years are involved). Basin- and region-wide studies cover a few to few thousands of glaciers (Table S3). Therefore, calculation of area change rates in percent per year are necessary to justify inter comparisons (Cogley, 2016). Often the basin- and region-wide studies used a range of years because of image availability from different years; in such situations the mean year of range was assigned to the measurement. We assess all the length and area change studies and assign ‘caution flags’ to all calculated rates based on quality of topographic maps, resolution of satellite images, dates of map/image, and uncertainty assessment in original sources.

## **Glaciological mass changes**



In the HK range, the first glaciological mass balance study was started on Gara Glacier (western Himalaya) in September 1974 by GSI (Raina and others, 1977). Gradually, GSI selected more glaciers in India, under different climatic regimes, from the eastern, central and western parts of the Himalaya. During the late 1970s, Japanese teams also conducted some pioneering mass balance surveys in the Nepalese Himalaya on AX010, Yala and on Rikha Samba glaciers (Ageta and others, 1980; Ageta and Higuchi, 1984; Fujita and Nuimura). In the whole HK region, glaciological mass balance series have been mainly reported from India (western as well as parts of central and eastern Himalaya) and Nepal (central Himalaya). The mass balance series are often less than 10 years long. Kolahoi, Shishram, Rikha Samba, and Yala glaciers were surveyed just for one hydrological year (Table S4) whereas Triloknath Glacier was surveyed just for one ablation period (Swaroop and others, 1995). During the 1990s, the number of mass balance observations were small and available only for the AX010, Rikha Samba, Kangwure and Dokriani glaciers but, unfortunately, these measurements were either short (<5 years) or discontinuous (Dokriani) and provided an incomplete picture of glacier change (Table S4 and S6). In recent years, several new mass balance series started in the Indian, Nepalese and Bhutanese Himalaya (Table S4).

### **Reliability of glaciological mass balance data**

Several mass balance compilations were made at regional scales (Vincent and others, 2013; Pratap and others, 2016; Singh and others, 2016) or covered the whole HK range (Dyurgerov and Meier, 2005; Cogley, 2011; Bolch and others, 2012). Some studies used all mass balance data without checking their reliability and computed mean mass balances for the Himalayan range (Cogley, 2011; Bolch and others, 2012). Therefore, resulting mean mass balances may be biased. We carefully check the reliability of each mass balance series. Then the mean mass balances (Fig. 3a) for the Himalayan range are calculated excluding the dubious mass balance series.

Almost half of the available glaciological annual mass balance data series from the HK range were collected by GSI (Table S4). These mass balance data were published in GSI annual expedition reports or short abstracts. Previous compilations often used secondary sources for these data. Here we collected all these reports/abstracts directly from GSI libraries. However, there are still some unpublished reports not available to the scientific community. GSI used the conventional glaciological method (Ostrem and Stanley, 1969), but the published literature sometimes lacks the details about stake network, methodology for accumulation measurements, density measurements, base map details, and dates of

measurements. In our analysis, an attempt is made to extract the GSI general guidelines for mass balance estimation from different reports/abstracts (Table S5) and briefly recalled here:

1. According to glacier's shape and size, a stake network was planned usually with  $\sim 10$  stakes per  $1 \text{ km}^2$  of glacierized area. Stakes were installed by manual drilling, power drilling or steam drilling in ablation area while in accumulation area stakes were either inserted by pushing or hammering.
2. Often stakes of aluminum pipes with rubber bases were used. Sometimes wooden (probably bamboo) stakes were also used.
3. Stakes were often monitored sub-monthly during the summer months (May to September).
4. Accumulation was estimated at accumulation stakes or by digging up a few pits in the accumulation area. Density profiling was also done to find out the stratigraphy along the depth of the pit.
5. For annual mass balance estimation, ablation and accumulation measurements were carried out at the end of ablation season ( $\sim 30$  September).
6. Point mass balance measurements were converted into water equivalents and isolines were plotted on a large scale contoured map (1:10,000 to 1:20,000).
7. The point mass balances were plotted against elevation to get the elevation corresponding to zero mass balance (Equilibrium Line Altitude, ELA).

GSI standard operating procedure seems to be quite robust except for the use of metallic stakes that accelerate melting because of heat conduction. However, the use of rubber bases at the bottom of stakes might have reduced the amount of stake sinking due to conduction. A typical example of stakes and accumulation pits network designed by GSI on Gara Glacier (GSI, 1977) is given in Fig. S1. A network of 34 stakes in the ablation and 13 in the accumulation area were installed during the first glaciological expedition in 1974 by GSI on Gara Glacier ( $5.2 \text{ km}^2$ ). In September 1975, besides measuring the ablation and accumulation from stakes, four pits were also dug in the accumulation area for annual accumulation estimation (Raina and others, 1977). The pits were dug using shovels until the previous year's summer surface (a thick layer of superimposed ice that could not be dug through) was reached and then the densities along the pit were determined. The selection of last summer layer by this method might lead to selection of an incorrect layer, hence erroneous accumulations (Basantes-serrano and others, 2016). As already discussed, the accuracy of the maps used by GSI is unclear and may lead to errors in the glacier-wide mass balance estimates.

In GSI mass balance measurements, error analysis was not performed while in other mass balance series error estimation was occasionally included (Table S4). It is well known that glaciological mass balances are subjected to the potential systematic biases and thus their validation with geodetic mass balance is necessary (Zemp and others, 2013). Harsh conditions of the HK region limit the number of point accumulation measurements; therefore, it becomes even more crucial to check the biases in glaciological mass series. It is not possible to estimate the geodetic mass balances for every glacier in the past because of the date-specific requirement of satellite images. Therefore, an alternative analysis is developed for the assessment of the quality and reliability of all available mass balance series. In our analysis, the criteria are (1) the mass balance-ELA relationship, (2) the mass balance relationships with annual/seasonal meteorological parameters, (3) mass balance behaviours within a climatic setting/basin, (4) debris-cover extent, (5) avalanche contribution (6) spatial density of measurement network (ablation and accumulation points), (7) ablation stake material, (8) field-based snow density measurements, (9) quality of map to get the glacier hypsometry, and (10) verification of glaciological mass balance series with geodetic mass balance (Table S7). For each criterion, a score is attributed (e.g. score = 1 if the in-situ mass balance series is validated with the geodetic method, 0 otherwise; see details in Table S7). The final score, indicative of the mass balance series quality, is computed by dividing the sum of all intermediate scores with the number of available parameters for corresponding mass balance series.

First, a thorough compilation of all the possible information related to mass balance is made from published reports and literature (Table S4, S5 and S6). Besides the limited available information, other challenges are short lengths of the mass balance series and different observation periods. We select the groups of glaciers from similar climatic settings/basin and analyze their mass balance behaviours. However, it is not possible or beneficial to include or group all the glaciers, as some glaciers were either surveyed for only a year or two, or were the only ones in their corresponding climatic settings/basin. The lack of mass balance error estimates in source studies prevents us from making a purely quantitative analysis, but our scoring method based on maximum possible information allows (1) highlighting the mass balance series possessing likely biases in order to avoid the percolation of biased mass balance data in the future scientific analysis; (2) classifying all the mass balance series in four categories: excellent (score > 0.60), good (0.45<score<0.60), fair (0.30<score<0.45), and dubious (score < 0.30) (Table S7); and (3) drawing some useful conclusions about HK mass balances using what are, likely, the most reliable data.

The ELA of a glacier is the altitude where mass balance is zero and it fluctuates corresponding to the mass balance of the individual year (Rabatel and others, 2012). Higher ELA corresponds to a more negative mass balance or vice-versa. Whenever available in the literature, we plot ELA against annual mass balances of the glaciers. Further, the annual mass balances are compared with the annual and seasonal anomalies of meteorological data. The ERA-interim reanalysis data are used for this purpose (Dee and others, 2011). ERA-interim data have been available at daily time scale since 1979. Mass balances for three glaciers (Gara, Gor Garang and Neh Nar) are available only before 1979. For these glaciers, we use the meteorological data from India Water Portal (IWP) (<http://www.indiawaterportal.org/>). IWP provides the district wise mean monthly meteorological data for the whole of India between 1901 and 2002. Daily temperatures from ERA-interim data are extracted at the median elevation of each glacier (Sakai and others, 2015), whereas the district wise data from IWP are used.

**1. Eastern Himalayan glaciers:** Changmekhangpu (India) and Gangju La (Bhutan) are the only glaciers surveyed in the eastern Himalaya (GSI, 2001; Tshering and Fujita, 2016). Changmekhangpu (5.6 km<sup>2</sup>) is a debris-covered glacier and Gangju La is a small, clean glacier (0.3 km<sup>2</sup>) (Fig. S2). The mass wastage was moderate on Changmekhangpu with annual mean mass balance of  $-0.26 \text{ m w.e. yr}^{-1}$  between 1979 and 1986 whereas the mass balance was strongly negative on Gangju La at  $-1.38 \pm 0.18 \text{ m w.e. yr}^{-1}$  between 2003 and 2014 (mass balance was measured using the glaciological method for three years: 2003-2004 and 2012-2014 only and then the in-situ geodetic method was used for different periods between 2003 and 2014). The correlations between annual mass balances of Gangju La glacier were the best with summer precipitation and summer temperature anomalies (Fig. S3) suggesting a clear control of summer season on this glacier. The observed mass-balance profiles suggest that the ELA has been higher than the top of Gangju La glacier since 2003 (Tshering and Fujita, 2016) which explains its high mass wastage. Thus this glacier seems to be out of balance with the recent climate and is likely to disappear in the near future. However, a longer time series is needed to confirm this. The strong measurement network and good mass balance-climatic parameter correlations on Gangju La suggest the mass balances on this glacier are of excellent quality (Table S7). On Changmekhangpu, ELA information was available for the 1980-1983 period when it showed weak correlation ( $r^2 = 0.11$ ) with annual mass balances (Fig. S3b). This relationship is unexpected as more negative mass balances were associated with lower



ELAs (Fig. S3b), from which we infer the dubiousness of the Changmekhangpu mass balances series. Further, the annual mass balances of Changmekhangpu showed very weak correlations with temperature and precipitation anomalies at annual as well as seasonal scale (Fig. S3). The mass balance estimates on Changmekhangpu could have been biased because of the steepness of its upper reaches that probably provided the accumulation mainly through avalanches (Fig. S2). Moreover, the stakes' installation over the thick and widespread debris cover (50% of total area) may also have been biased to cover the relatively gentle slope where stakes could be installed easily, while the melting at ice cliffs was not monitored. Changmekhangpu mass balance series receive a low assessment score and falls in 'dubious' category (Table S7).

## 2. Central Himalayan glaciers:

**Dudh Koshi Basin (Nepal):** Four debris-free glaciers (AX010, Mera, Pokalde and West Changri Nup) were surveyed in the Dudh Koshi Basin. All these glaciers are clean glaciers (Fig. S2). A Japanese team performed the mass balance observations on AX010 (0.6 km<sup>2</sup>) for 1978-1979 year (Ageta and others, 1980). Later on the mass balance observations were also conducted during the 1995-1999 period for AX010 (Fujita and others, 2001a). The mean annual mass balance was  $-0.69 \text{ m w.e. yr}^{-1}$  for all five observed years between 1978 and 1999. AX010 mass balances show a strong correlation with annual precipitation anomaly but weak correlations with annual temperature anomalies and seasonal precipitation and temperature anomalies (Fig. S4). The information about stake material, number of accumulation sites, ELA were not reported (Table S5), and AX010 scores for 'fair' category (Table S7).

Annual and seasonal mass balance observations on Mera were started in 2007, Pokalde in 2009 and West Changri Nup in 2010 and are still going on (Wagnon and others, 2013; Sherpa and others, 2017). Mera (5.1 km<sup>2</sup>) Glacier showed steady state between 2007 and 2015 ( $-0.03 \pm 0.28 \text{ m w.e. yr}^{-1}$ ) while Pokalde (0.1 km<sup>2</sup>) and West Changri Nup (0.9 km<sup>2</sup>) glaciers showed rapid mass wastage for 2009-2015 ( $-0.69 \pm 0.28 \text{ m w.e. yr}^{-1}$ ) and 2010-2015 ( $-1.24 \pm 0.27 \text{ m w.e. yr}^{-1}$ ), respectively. The high mass wastage on Pokalde and West Changri Nup glaciers is due to their lower maximum elevations and the smaller accumulation areas that in some years become zero when their ELAs jump above the highest altitudes of the glaciers (Wagnon and others, 2013). Glaciological mass balances on West Changri Nup are checked and found consistent with geodetic mass balance (Sherpa and others, 2017), suggesting no large bias in this series (Zemp and others, 2013). Furthermore, over the common observation periods, centered mass balances (annual –

mean value over the common period) of three glaciers were strongly correlated (Fig. S4a). This good agreement, which has already been observed in the Alps over longer time periods (Vincent and others, 2005; Huss and others, 2010); our reliability scores of these show that the mass balances of Mera, Pokalde and West Changri Nup glaciers contain a common signal in response to regional climate fluctuations.

The annual mass balances of Mera and Pokalde glaciers show strong correlation with the corresponding ELAs ( $r^2 = 0.92$ ;  $r^2 = 0.99$ , respectively) whereas West Changri Nup annual mass balances show very weak relationship with corresponding ELAs ( $r^2 = 0.01$ ). In general, Pokalde Glacier shows the good correlations with precipitation and temperature anomalies at annual as well as seasonal scales, while good correlations of summer precipitation and summer temperature anomalies with annual mass balances of all glaciers (Fig. S4) highlight that the summer season is more important for these glaciers. Based on the total score for each mass balance series, Pokalde series is categorized as ‘excellent’, Mera and West Changri Nup glaciers in the ‘good’ category (Table S7).

**Rikha Samba (Hidden Valley):** Mass balance observations on Rikha Samba Glacier were conducted for 1998-1999 year ( $-0.60 \pm 0.03$  m w.e.). This glacier ( $4.6 \text{ km}^2$ ) is clean with gentle slopes (Fig. S2). A total of 8 stakes were drilled on the central line from lowest to highest altitude for the estimation of ablation as well as accumulation (Fujita and others, 2001b). Information about stake material, accumulation sites and ELA are not available (Table S5) and the total score suggests this series to be ‘good’ (Table S7).

**Yala (Langtang Valley):** Yala is a small ( $1.6 \text{ km}^2$ ), clean glacier (Fig. S2). This glacier was first observed for summer mass balance in 1996 (Fujita and others, 1998) and annual mass balance studies were started in 2011. The mass balance of Yala Glacier was negative with a value of  $-0.89$  m w.e. and corresponding ELA of 5455 m a.s.l. for 2011-2012 (Baral and others, 2014). The ablation was measured at 6 stakes while accumulation was estimated using density profile method at each stake by digging pits (Baral and others, 2014). The monitoring network on Yala is strong (Table S5) and therefore this mass balance series is ‘excellent’ (Table S7).

**Kangwure (Shishapangma Mountains):** Kangwure is a small ( $1.9 \text{ km}^2$ ), clean glacier (Fig. S2) towards the Tibet side of the central Himalaya. Annual mass balances of this glacier are available for 1991-1993 and 2008-2010 periods (Liu and others, 1996; Yao and others, 2012). The mean mass balance was  $-0.69$  m w.e.  $\text{yr}^{-1}$  for all four observed years.

Annual mass balances show very weak correlations ( $\approx 0.01$ ) with annual and seasonal precipitation and temperature anomalies (Fig. not shown). Total score for this mass balance series is very low, thus classifying as ‘dubious’ (Table S7).

**Garhwal Himalaya:** In Garhwal Himalaya, four glaciers; Dunagiri, Tipra Bank, Chorabari, and Dokriani were surveyed for their annual mass balances (Fig. S5a). All these glaciers are debris covered with minimum on Dokriani (6%) to maximum on Dunagiri ( $\sim 80\%$ ) (Fig. S2) and have a similar area ( $\sim 7 \text{ km}^2$ ), except Dunagiri glacier which is smaller ( $2.6 \text{ km}^2$ ).

Tipra Bank was close to balance conditions with mean annual mass balance of  $-0.14 \text{ m w.e. yr}^{-1}$  over 1981–1988 while Dunagiri showed a mean annual mass wastage of  $-1.04 \text{ m w.e. yr}^{-1}$  over 1984–1990. Over the common observed period of 1985–1988, centered mass balances of both the glaciers were satisfactorily correlated ( $r^2 = 0.75$ ) (Fig. S5a) suggesting that interannual mass balance fluctuations of both the glaciers were quite similar and indicating that the mass balances of both Tipra Bank and Dunagiri glaciers give similar climatic signals. Both the mass balance series show very weak relationships with the annual precipitation anomalies and average correlations with temperature anomalies, while Tipra Bank shows the best correlation with winter temperature anomaly and Dunagiri with winter precipitation anomaly (Fig. S5). The main mass balance controlling season is hard to find with these correlations. However, the rapid wastage of Dunagiri Glacier (mass balances are  $0.82 \text{ m w.e. yr}^{-1}$  more negative on Dunagiri than Tipra Bank between 1985 and 1988) and weak mass balance-ELA correlation ( $r^2 = 0.23$ ) on Dunagiri Glacier compared to Tipra Bank ( $r^2 = 0.49$ ) motivated us to analyze these mass balances further. Dunagiri Glacier high mass wastage seems to be linked with its topographical settings in the upper reaches. The accumulation area (6.4% of its total area between 4900 and 5150 m a.s.l.) is bounded by steep head walls (GSI, 1992). From Fig. S2, it seems that Dunagiri is a highly avalanche fed glacier, although avalanche contributions are not included for mass balance estimation (GSI, 1992). Moreover, more than 80% of debris covered area of Dunagiri Glacier compared to 15% on Tipra Bank (Table S4) is in support of the high avalanche activity in the accumulation area. Therefore, annual mass balances of Dunagiri Glacier seem to be biased due to lack of measurements of the accumulation input from avalanches. Thus, Dunagiri mass balance series is in the ‘dubious’ category, Tipra Bank in the ‘fair’ category (Table S7).

Dokriani Glacier mass balance is available intermittently for 1992-1995 ( $-0.25$  m w.e.  $\text{yr}^{-1}$ ) and 1997-2000 ( $-0.39$  m w.e.  $\text{yr}^{-1}$ ) periods. Annual mass balances show strong correlation ( $r^2 = 0.90$ ) with ELA, weak correlation with the precipitation and temperature anomalies at annual scale but fair correlations with winter precipitation anomaly and summer temperature anomaly (Fig. S5). Dokriani Glacier's mass balance series is in the 'fair' category (Table S7).

The annual mass balances of Chorabari Glacier ( $-0.73$  m w.e.  $\text{yr}^{-1}$ ; 2003-2010) show a weak ( $r^2 = 0.26$ ) and opposite relationship with the corresponding ELAs. Higher ELAs are associated with higher mass balances (Fig. S5b), which is the first caution flag that possibly this dataset is unreliable. The correlations with precipitation and temperature were also very weak at annual and seasonal scale except for winter precipitation anomaly when annual mass balances showed fair correlation (Fig. S5). Further, Chorabari Glacier is highly debris covered (53% of its total area). Applying the glaciological method over debris cover tongues may not be a good option because of large spatial variability of ablation over debris covered areas that is hard to capture by ablation stakes. Such conditions provide very low score and put this mass balance series to be in the 'dubious' category (Table S7). However, this series is continuous since 2003 and we recommend this glacier to be checked and reanalyzed using geodetic mass balance in the future (Zemp and others, 2013).

### 3. Western Himalayan glaciers:

**Lahaul and Spiti Valley:** In Lahaul and Spiti valley, two neighboring glaciers: Chhota Shigri ( $15.5 \text{ km}^2$ ) and Hamtah ( $3.2 \text{ km}^2$ ) have been under survey since the early 2000s. Chhota Shigri is an almost clean glacier (3.4% debris covered area) while Hamtah is heavily debris covered ( $\sim 70\%$  debris covered) (Fig. S2). The mean mass balance of Hamtah Glacier ( $-1.43$  m w.e.  $\text{yr}^{-1}$ ) was two and half times more negative than Chhota Shigri ( $-0.59$  m w.e.  $\text{yr}^{-1}$ ) over the common observed period between 2003 and 2012. The annual mass balances show average correlations with the summer precipitation and temperature anomalies (Fig. S6) suggesting that summer is the main mass balance driving season for these glaciers. The centered mass balances of both the glaciers were also fairly correlated ( $r^2 = 0.37$ ) (Fig. S6a).

Chhota Shigri Glacier's mass balance series has been reanalyzed using an updated glacier hypsometry and also validated against geodetic mass balance (Azam and others, 2016). The statistical agreement between the glaciological and geodetic mass balances of



Chhota Shigri suggested that the present stake and accumulation site network on this glacier is suitable and able to capture the spatial variability of mass balance over the glacier. Moreover, Chhota Shigri annual mass balances show strong correlation ( $r^2 = 0.94$ ) with corresponding ELAs (Fig. S6b) and detailed analyses of annual (since 2002) as well as seasonal mass balances (since 2009) with meteorological parameters showed that the summer monsoon snowfalls are the main driver of the interannual variability of annual mass balance through controlling the summer mass balances of this glacier (Azam and others, 2014b; 2016). Based on the high score (0.63), Chhota Shigri mass balance series belongs to the ‘excellent’ category (Table S7). Hamtah Glacier’s strong negative mass balances ( $-1.43 \text{ m w. e. yr}^{-1}$  during 2000–2012) were found three-fold more negative than a satellite-based estimate of the geodetic mass balance ( $-0.45 \pm 0.16 \text{ m w. e. yr}^{-1}$ ; 1999–2011) (Vincent and others, 2013). The upper reaches (above 4600 m a.s.l.) of Hamtah Glacier are bounded by steep head walls and the whole ablation area is highly debris covered. Indeed, these conditions make this glacier unsuitable for glaciological method. As already inferred (Vincent and others, 2013), most probably Hamtah Glacier was surveyed only in its lower part and contribution of avalanches was not included in mass balance estimation (Banerjee and Shankar, 2014). Hamtah mass balance series scores the lowest (0) and is classified as ‘dubious’ (Table S7).

**Jhelum Basin:** In Jhelum Basin, three debris-free glaciers have been surveyed (Table S4; Fig. S2): Neh Nar ( $1.3 \text{ km}^2$ ), Kolahoi ( $11.9 \text{ km}^2$ ) and Shishram ( $9.9 \text{ km}^2$ ). Kolahoi and Shishram glaciers were just surveyed for one hydrological year of 1983/84 and showed a moderate and almost same mass losses of  $-0.27$  and  $-0.29 \text{ m w.e. yr}^{-1}$ , respectively. Both glaciers were also surveyed for winter balances by measuring ablation stakes and making almost 40 pits in April 1984 (Kaul, 1986), but most of the information about annual mass balance is missing. Kolahoi mass balance series is thus ‘dubious’ while Shishram is ‘fair’ (Table S7).

Neh Nar Glacier showed a mean wastage of  $-0.43 \text{ m w.e. yr}^{-1}$  over 1975–1984 period with maximum wastage ( $-0.86 \text{ m w.e.}$ ) in 1977/78 and an almost balanced condition ( $-0.1 \text{ m w.e.}$ ) in 1982/83 (GSI, 2001). The Neh Nar mass balance series was started in 1975; therefore we use the meteorological data from IWP. The temperature and precipitation anomalies are computed for the nearest district of Anantnag. Neh Nar annual mass balances are fairly well correlated with temperature anomaly at annual and seasonal scales, while the correlation is only fair with winter precipitation anomalies (Fig. S7). Though

ELA information is not available, the strong measurement network helps this glacier time series to rank as ‘good’ (Table S7).

**Baspa Basin:** In Baspa Basin (Kinnaur district, Himachal Pradesh), four glaciers; Gara, Gor Garang, Shaune Garang and Naradu were surveyed. All these glaciers are of similar area ( $\sim 5 \text{ km}^2$ ) except Gor Garang ( $2.0 \text{ km}^2$ ). The lower ablation areas of Gara and Shaune Garang glaciers are debris covered (17 and 24% of total area, respectively), whereas Gor Garang and Naradu glaciers are highly debris covered ( $\sim 60\%$ ) (Fig. S2 and Table 4). Gara ( $-0.27 \text{ m w.e. yr}^{-1}$ ; 1974–1983), Gor Garang ( $-0.38 \text{ m w.e. yr}^{-1}$ ; 1976–1985) and Shaune Garang ( $-0.42 \text{ m w.e. yr}^{-1}$ ; 1981–1991) glaciers had mostly negative mass balances with some sporadic positive mass balance years (Fig. S8a). The annual mass balances of these three glaciers show good correlation with the corresponding ELAs (Fig. S8b). Further, during the overlapping periods of observation, the centered mass balances of Shaune Garang and Gor Garang glaciers are synchronous. Gara and Gor Garang centered mass balances (1977 to 1983) as well as Gor Garang and Shaune Garang centered mass balances (1982 to 1985) are well correlated ( $r^2 = 0.81$  and  $0.98$ , respectively) (Fig. S8a). This consistency suggests that the interannual mass balance variability were similar on these glaciers and all these glaciers responded similarly to regional climate. Gara and Gor Garang observations were started in 1975 and 1977, respectively therefore, for these glaciers, precipitation and temperature anomalies are computed using IWP data at Kinnaur district. Annual as well as seasonal temperature anomalies show average correlation with the annual mass balances of these three glaciers while weak correlations were observed with precipitation anomalies except Gor Garang mass balance series that showed an average correlation with winter precipitation anomaly (Fig. S8). Although Gor Garang is a highly debris covered glacier, its mass balance consistency with neighboring Gara glacier could be because of its strong stake network ( $12 \text{ stakes km}^{-2}$ ) distributed over the ablation area that was able to capture the spatial mass balance variability. Based on total score for all three glaciers they are classified as ‘fair’ (Table S7).

Mass balance observations on Naradu Glacier showed a mean wastage of  $-0.40 \text{ m w.e. yr}^{-1}$  between 2000 and 2003 (Koul and Ganjoo, 2010). Over the same period, annual mass balances were averagely correlated with corresponding ELAs (Fig. S8). Later on, the observations were again started in 2010 by another team when the higher mean mass wastage of  $-1.12 \text{ m w.e. yr}^{-1}$  was observed over 2010-2012 (Kumar and others, 2014). The details of their methodology are not available. Similar to other glaciers in Baspa Basin, annual mass balances of Naradu also show weak correlations with precipitation anomalies

however the correlations with annual and winter temperatures were good (Fig. S8). Based on its total score, this intermittent mass balance series falls in the ‘fair’ category.

**Rulung (Zaskar Range):** Rulung is a small (1.1 km<sup>2</sup>), relatively flat and clean glacier (Fig. S2). This glacier was surveyed for just two years (−0.11 m w.e. yr<sup>−1</sup>; 1979–1981) by GSI (Shrivastava and others, 2001). A strong network of wooden stakes and well documented details of ablation and accumulation as a function of altitude (Shrivastava and others, 2001) leads to a high score for this series, hence it is classified as ‘excellent’ (Table S7).

**Naimona’nyi (Karnali Basin):** Naimona’nyi is a clean glacier with an area of 7.8 km<sup>2</sup> (Fig. S2). The mean mass balance was −0.56 m w.e. yr<sup>−1</sup> between 2005 and 2010. The mass balance studies were started in 2005 with a network of 16 stakes (Yao and others, 2012) and available up to 2010. No measurements could be performed in 2006; therefore a mean mass balance for 2005–2007 was estimated in 2007. The mass balances and ELAs are well correlated ( $r^2 = 0.91$ ; Fig. not shown) between 2007 and 2010. Annual mass balances between 2007 and 2010 were well correlated with winter precipitation anomaly ( $r^2 = 0.75$ ), annual temperature anomaly ( $r^2 = 0.84$ ) and winter temperature anomaly ( $r^2 = 0.64$ ; Fig. not shown). The details of map used, stakes’ material and accumulation pits were not found in the sources. This mass balance series is thus in the ‘fair’ category (Table S7).

### Modelled mass changes

Recent mass balance modelling studies were available for our review at glacier-wide scale (Table S8). Due to limited in-situ meteorological data availability, statistical or semi-distributed methods were used for mass balance reconstruction. The Kangwure mass balance series was reconstructed using a regression equation based on the meteorological data (annual air temperature and precipitation) at Dingri meteorological station (about 100 km away from the Kangwure Glacier) and 5-year in-situ mass balance observations (Yao and others, 2012), and therefore may have some biases. The mean mass balance for Siachen Glacier between 1986 and 1991 was found to be −0.51 m w.e. yr<sup>−1</sup> using a hydrological (water balance) method (Bhutiya, 1999). Recently, this mass balance series was suggested to be negatively biased due to exclusion of a ~249 km<sup>2</sup> area; the revised estimates were thus suggested to be between +0.22 and −0.23 m w.e. yr<sup>−1</sup> over 1986–1991 (Zaman and Liu, 2015). We note that these mass balances are consistent with near zero mass balances (−0.03 ± 0.21 m w.e. yr<sup>−1</sup>) between 1999 and 2007 for Siachen Glacier (Agarwal and others, 2016).

### **Dynamic behavior of Chhota Shigri Glacier**

The ice flux through a glacier cross section is equal to the upstream mass balance at that cross section if the glacier is in steady-state. A negative (positive) mass balance will result in decreased (increased) ice fluxes through changes in glacier ice thickness and velocity. To our knowledge, Chhota Shigri Glacier field dataset, even though not very long, provides the best dataset to understand its dynamic behavior. The mean glaciological mass balance on this glacier was negative ( $-0.56 \text{ m w.e. yr}^{-1}$ ) between 2002 and 2014 (Azam and others, 2016). The thickness changes of the Chhota Shigri Glacier between 1988 and 2010 were also determined using in-situ geodetic measurements (Vincent and others, 2013). An overall uniform decrease in thickness changes with increasing altitude was observed, with thinning ranging from  $\sim 8 \text{ m}$  at  $4500 \text{ m a.s.l.}$  to  $5 \text{ m}$  at  $5100 \text{ m a.s.l.}$  (Vincent and others, 2013). Here we measured the surface velocities from stake displacement method using differential GPS for 2012/13 and compared with 2003/04 velocities. Though measurements have not been performed at exactly the same locations (Fig. S9), the reduced surface velocities in both eastern and western flanks were found since 2003 (Fig. S10). In main glacier body (eastern flank), the velocities below  $4650 \text{ m a.s.l.}$  reduced by  $\sim 10 \text{ m yr}^{-1}$  between 2003/04 and 2012/13 however; at higher altitudes  $4900 \text{ m a.s.l.}$  the velocities were almost same (Fig. S10). These reducing velocities and thickness (Azam and others, 2012) on Chhota Shigri Glacier suggest that the glacier is adjusting its dynamics in response to its negative mass balances.



## Supplementary Figures

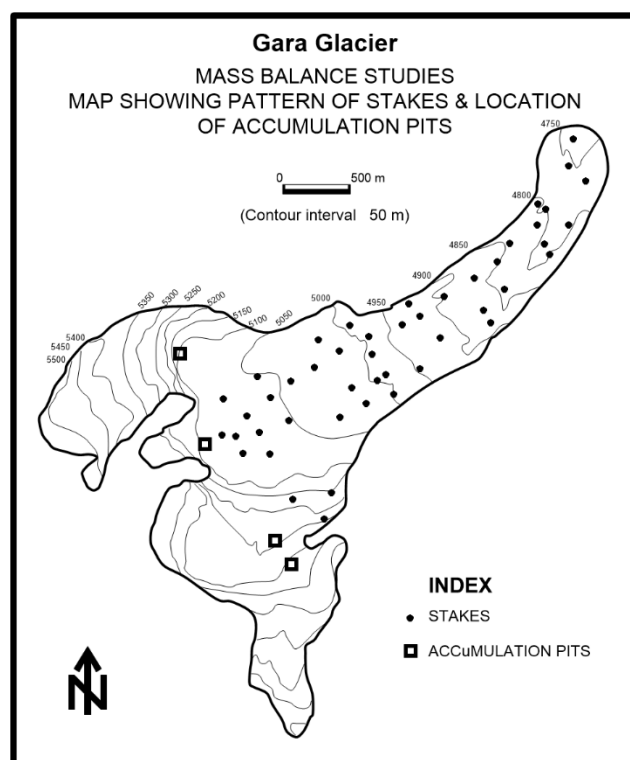


**Fig. S1.** Positions of stakes and accumulation pits on Gara Glacier (western Himalaya). The map is modified after a 1:15000 scale map (GSI, 1977).

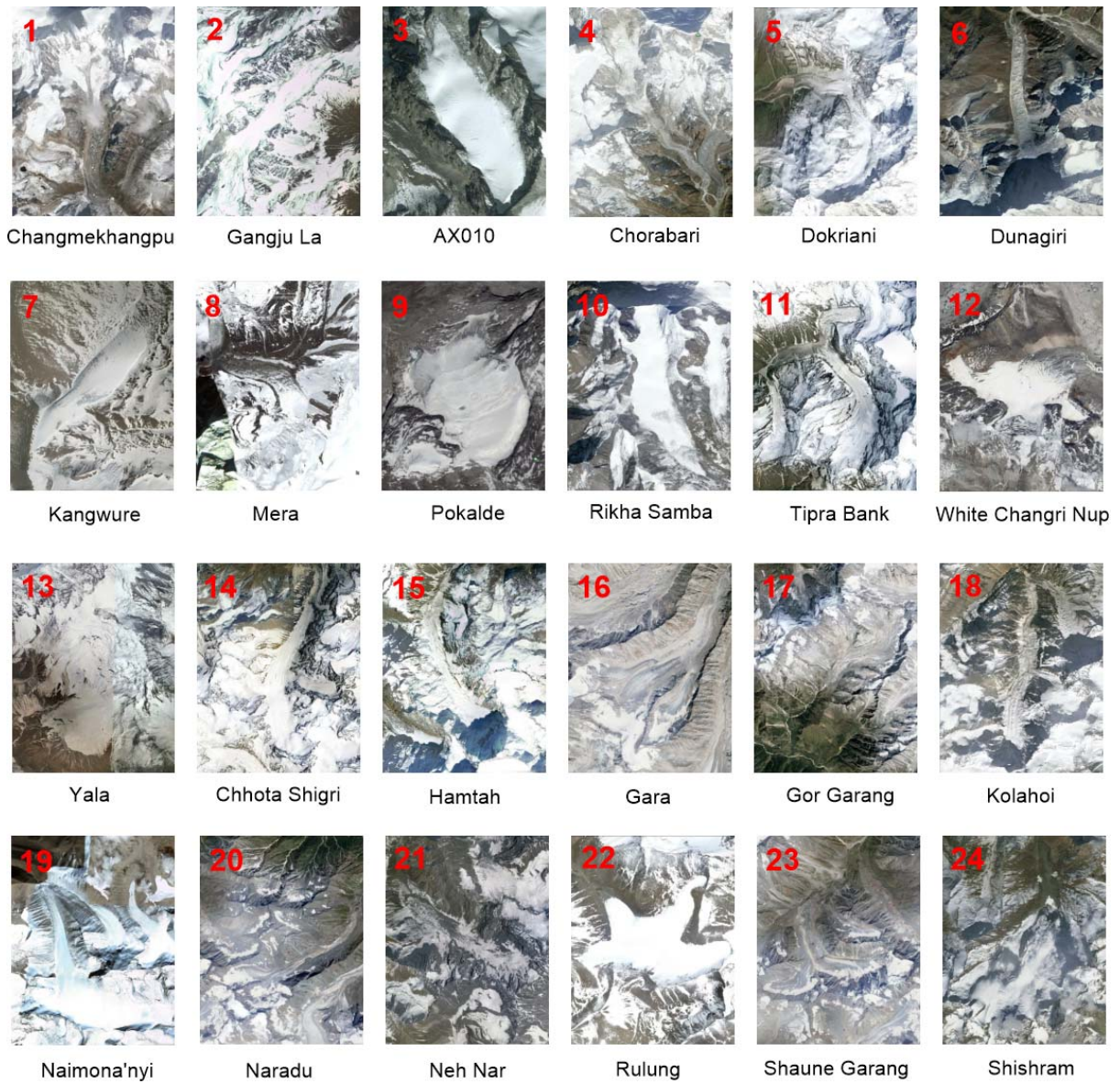


**Fig. S2.** Google Earth images showing all 24 surveyed glaciers by glaciological method in the HK range. The panels are shown following the sequence in Table S4. Note: the images are not to scale.

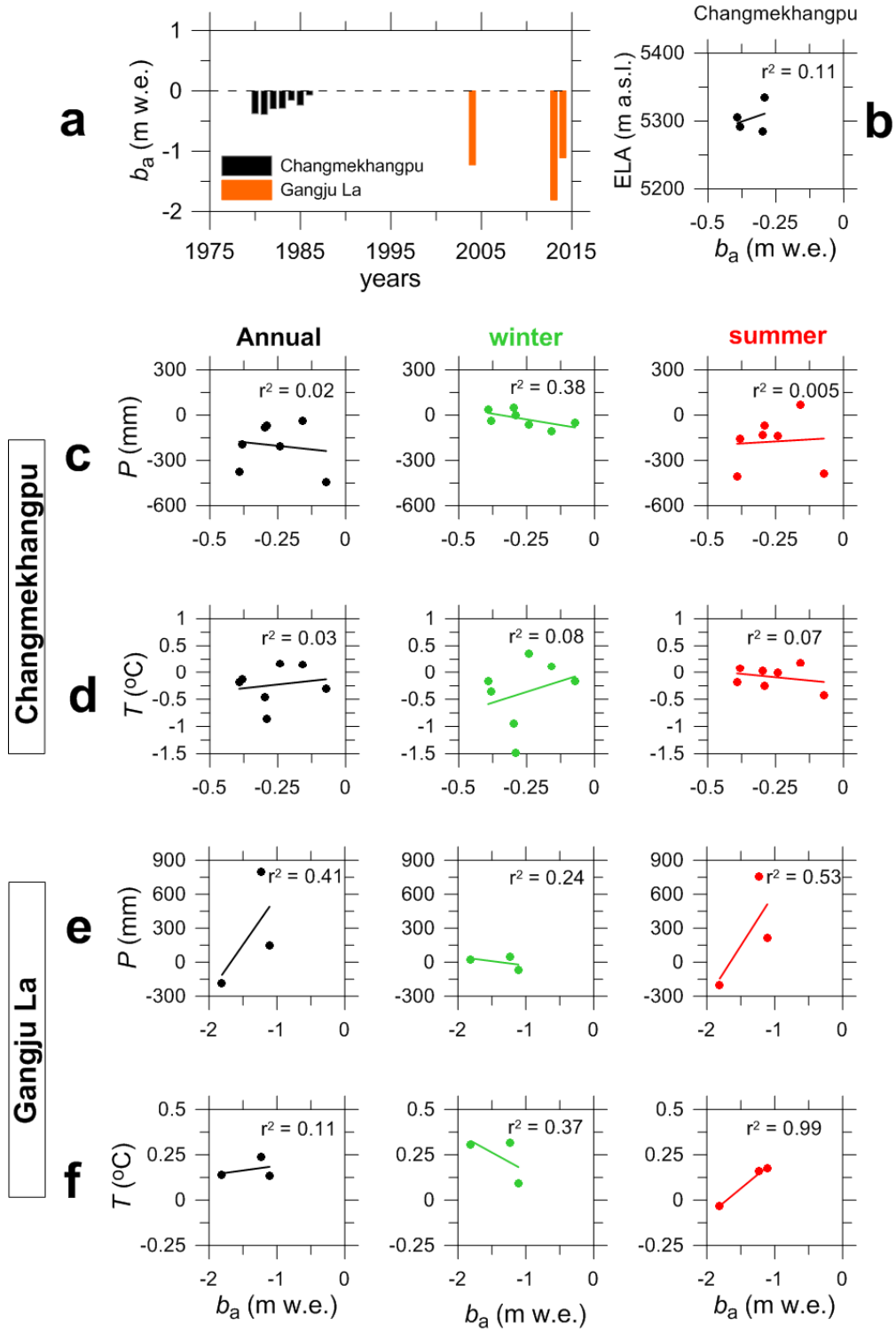


**Fig. S3.** (a) Annual mass balances ( $b_a$ ) of Changmekhangpu and Gangju La glaciers in the eastern Himalaya. (b)  $b_a$  as a function of ELA for 1980-1983 period for Changmekhangpu Glacier. (c)  $b_a$  of Changmekhangpu as a function of annual, winter and summer precipitation ( $P$ ) anomalies, (d)  $b_a$  of Changmekhangpu as a function of annual, winter and summer temperature ( $T$ ) anomalies, (e)  $b_a$  of Gangju La as a function of annual, winter and summer  $P$  anomalies, and (f)  $b_a$  of Gangju La as a function of annual, winter and summer  $T$  anomalies.

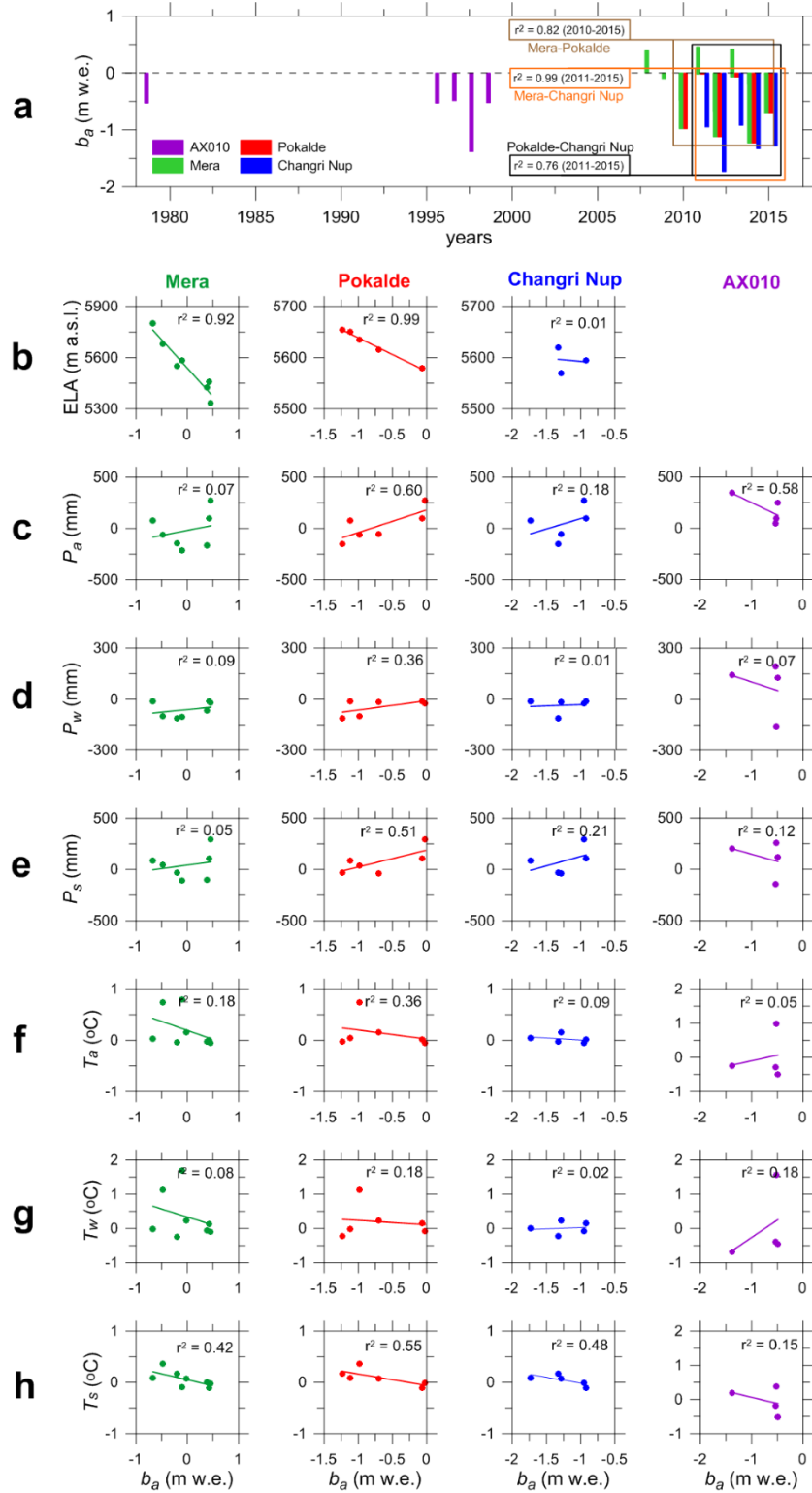


**Fig. S4.** (a) Annual mass balances ( $b_a$ ) of Mera, Pokalde, White Changri Nup and AX010 glaciers in the Dudh Koshi Basin. (b)  $b_a$  as a function of ELA, (c) as a function of annual precipitation anomalies ( $P_a$ ), (d) as a function of winter precipitation anomalies ( $P_w$ ), (e) as a function of summer precipitation anomalies ( $P_s$ ), (f) as a function of annual temperature anomalies ( $T_a$ ), (g) as a function of winter temperature anomalies ( $T_w$ ), (h) and as a function of summer temperature anomalies ( $T_s$ ).



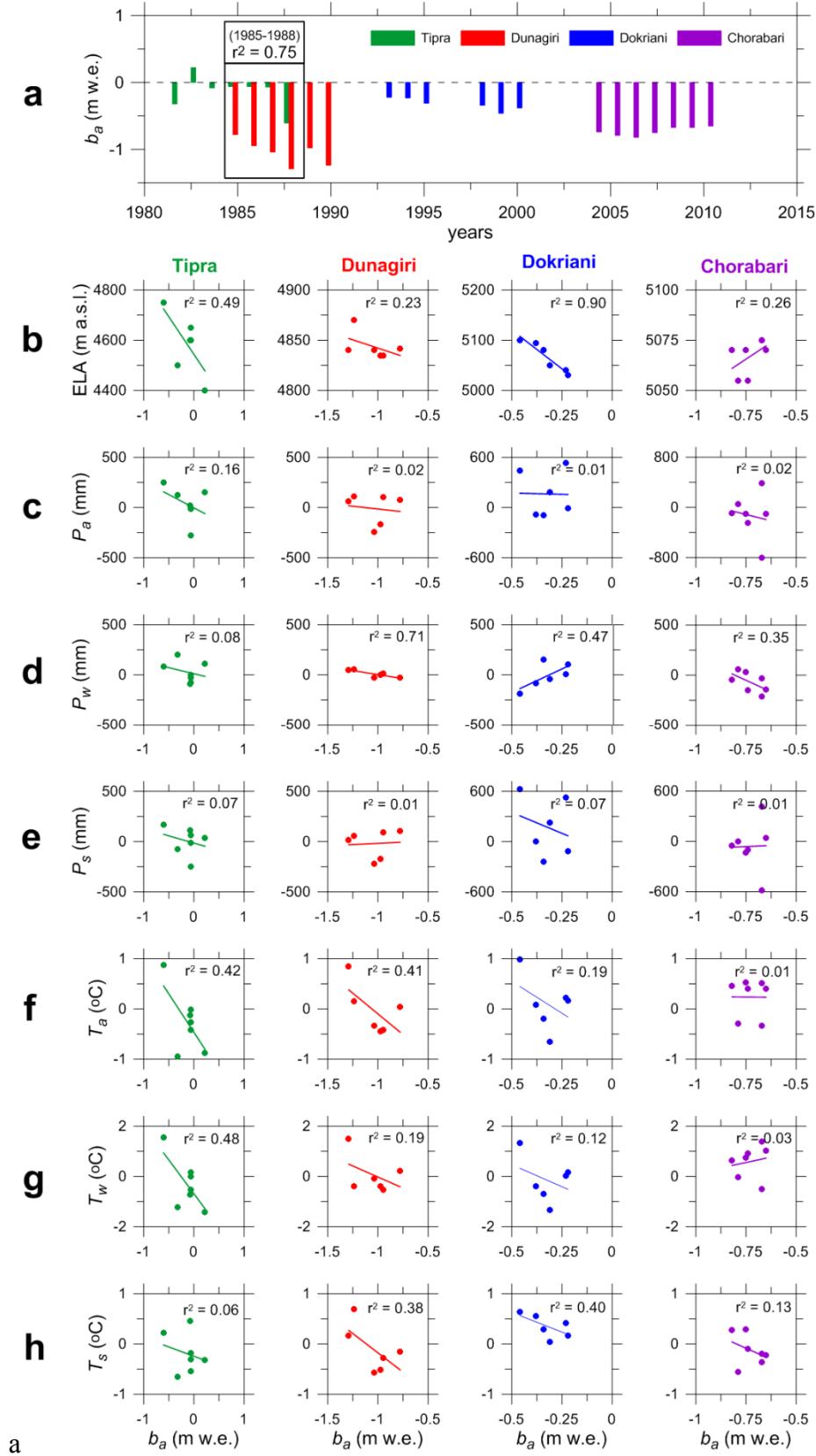


**Fig. S5. (a)** Annual mass balances ( $b_a$ ) of Tipra Bank, Dunagiri, Dokriani and Chorabari glaciers in the Garhwal Himalaya. **(b)**  $b_a$  as a function of ELA, **(c)** as a function of  $P_a$ , **(d)** as a function of  $P_w$ , **(e)** as a function of  $P_s$ , **(f)** as a function of  $T_a$ , **(g)** as a function of  $T_w$ , and **(h)** as a function of  $T_s$ .

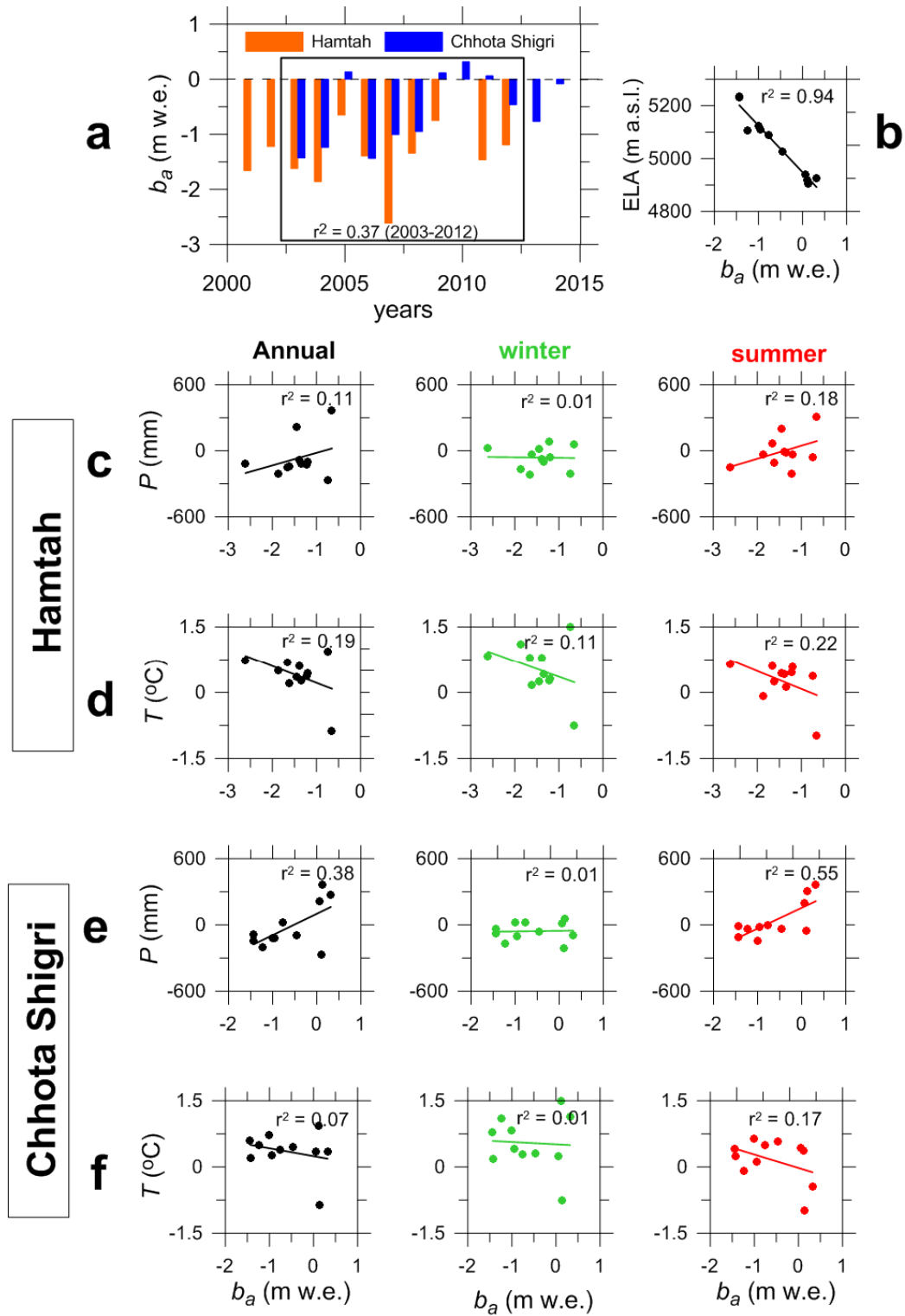


**Fig. S6.** (a) Annual mass balances ( $b_a$ ) of Hamtah and Chhota Shigri glaciers in the Lahaul and Spiti Valley of western Himalaya. (b) ELA- $b_a$  correlation for 2002-2014 period for Chhota Shigri Glacier, (c)  $b_a$  of Hamtah as a function of annual, winter and summer precipitation anomalies, (d)  $b_a$  of Hamtah as a function of annual, winter and summer temperature anomalies, (e)  $b_a$  of Chhota Shigri as a function of annual, winter and summer precipitation anomalies, and (f)  $b_a$  of Chhota Shigri as a function of annual, winter and summer temperature anomalies.

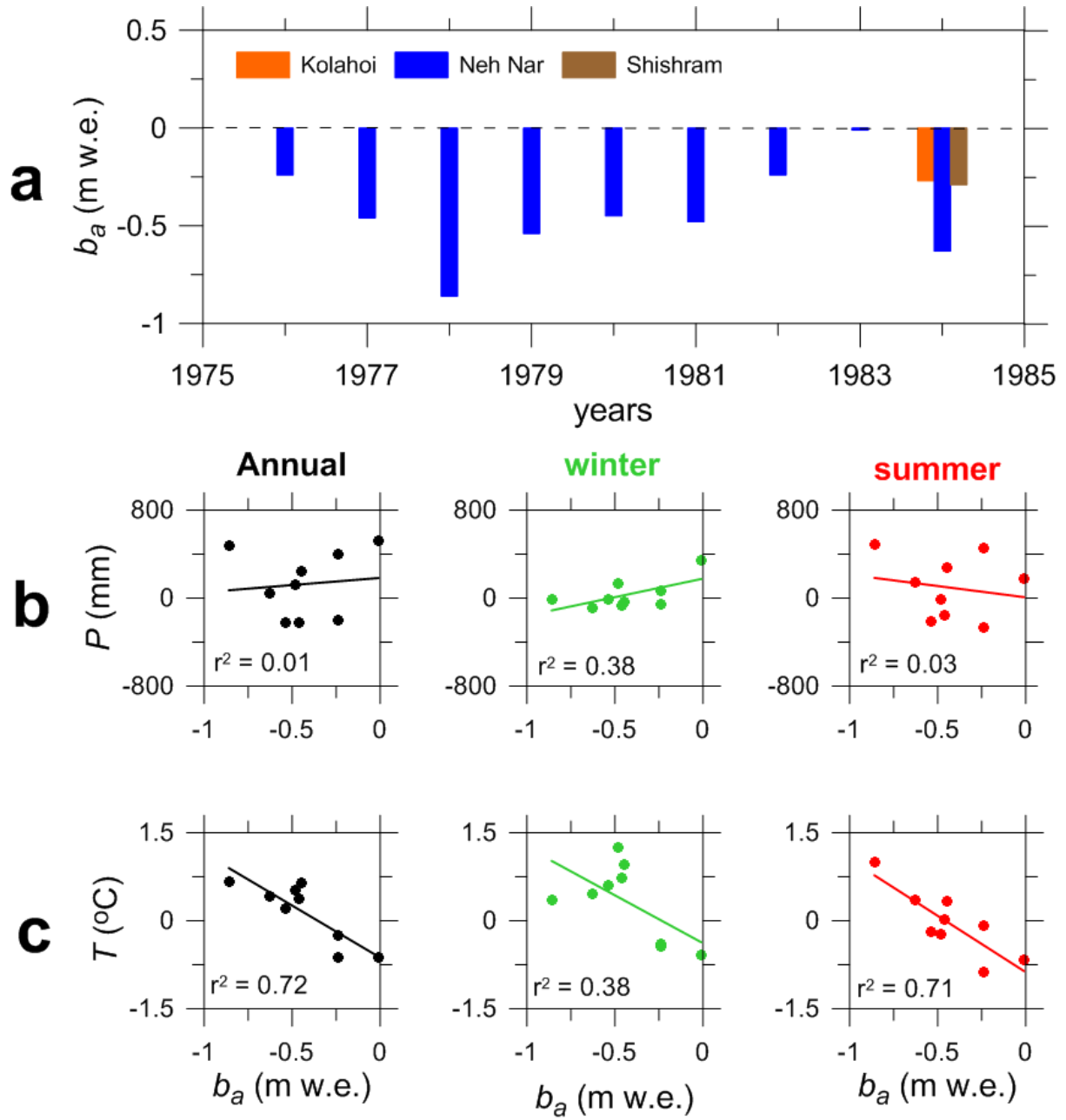


**Fig. S7.** (a) Annual mass balances ( $b_a$ ) of Kolahoi, Neh Nar and Shishram glaciers in the Jhelum Basin of the western Himalaya. (b)  $b_a$  of Neh Nar as a function of annual, winter and summer precipitation anomalies, and (c)  $b_a$  of Neh Nar as a function of annual, winter and summer temperature anomalies.

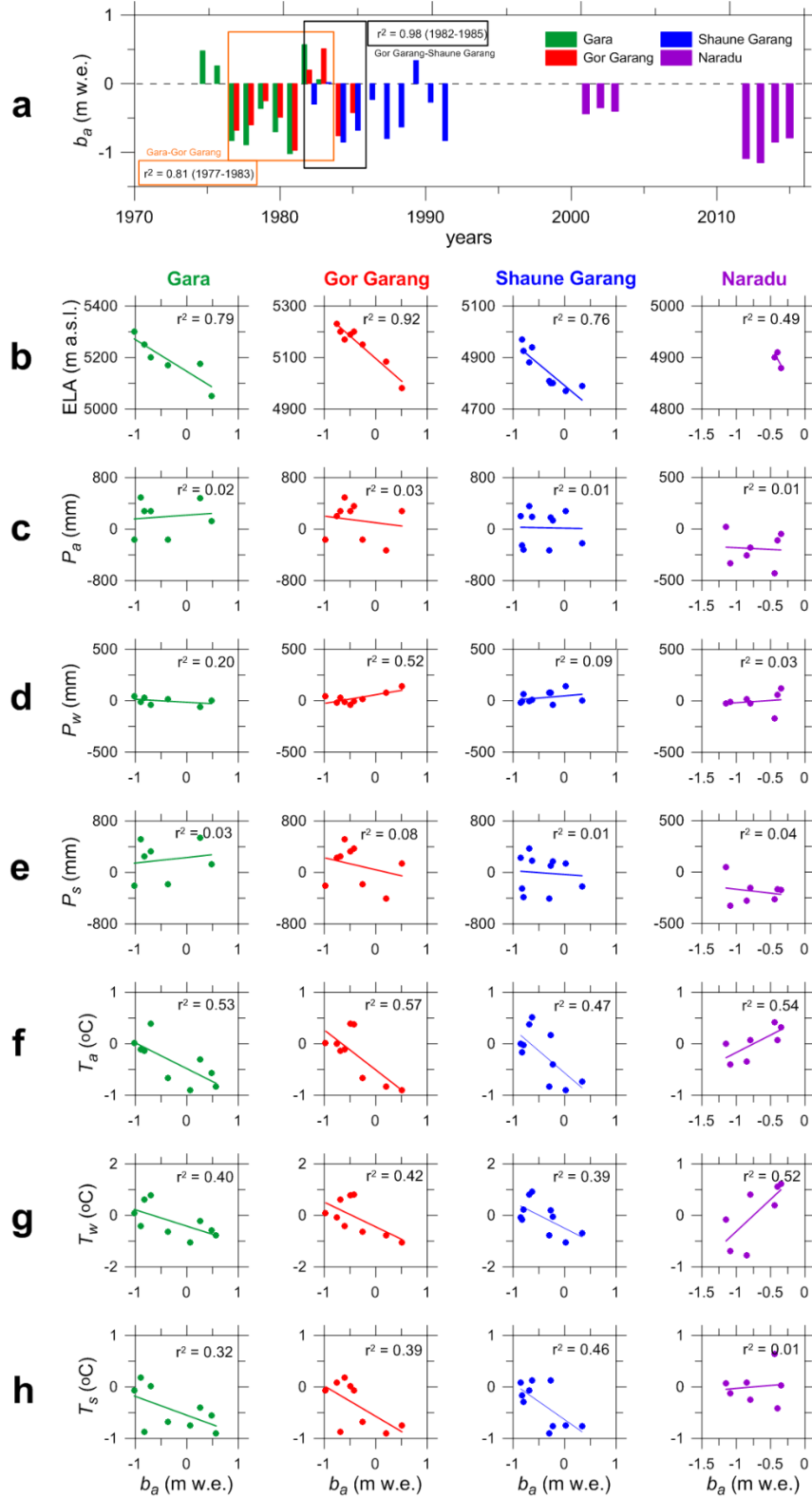


**Fig. S8.** (a) Annual mass balances ( $b_a$ ) of Gara, Gor Garang, Shaune Garang and Naradu glaciers in the Baspa Basin. (b)  $b_a$  as a function of ELA, (c) as a function of annual precipitation anomalies, (d) as a function of winter precipitation anomalies, (e) as a function of summer precipitation anomalies, (f) as a function of annual temperature anomalies (g) as a function of winter temperature anomalies, and (h) as a function of summer temperature anomalies.

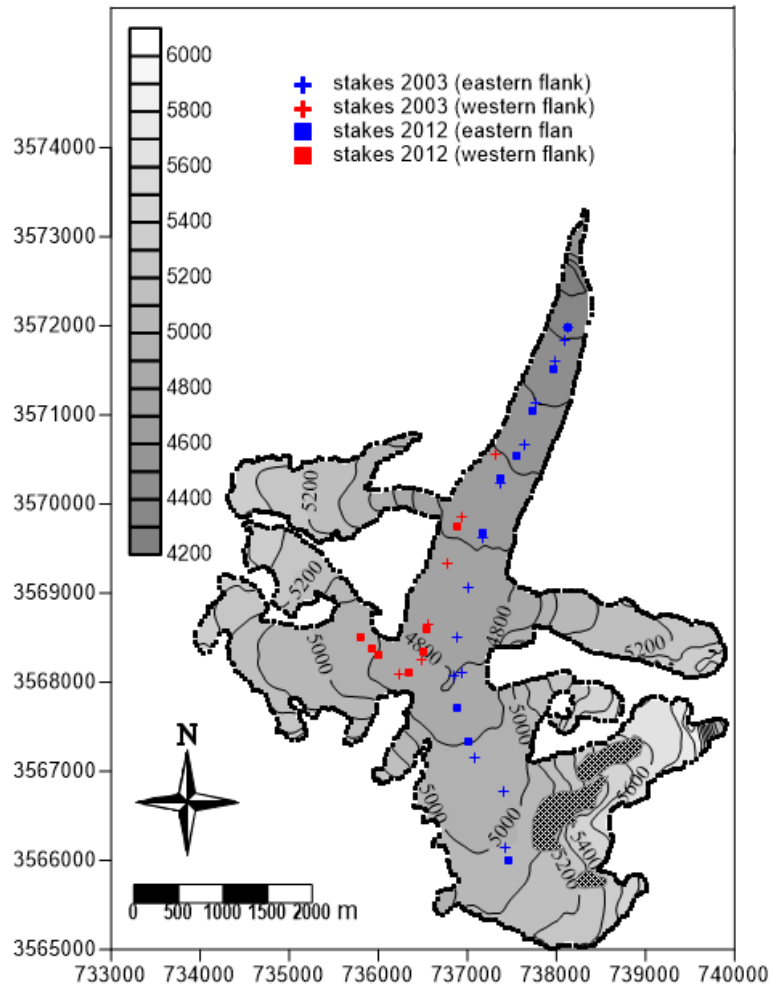


**Fig. S9.** Map of Chhota Shigri Glacier showing the stakes' positions in 2003 (blue crosses for eastern flank, main glacier body, and red crosses for western flank) and 2012 (blue squares for eastern flank and red squares for western flank). The map coordinates are in the UTM 43 (north) World Geodetic System 1984 (WGS84) reference system.

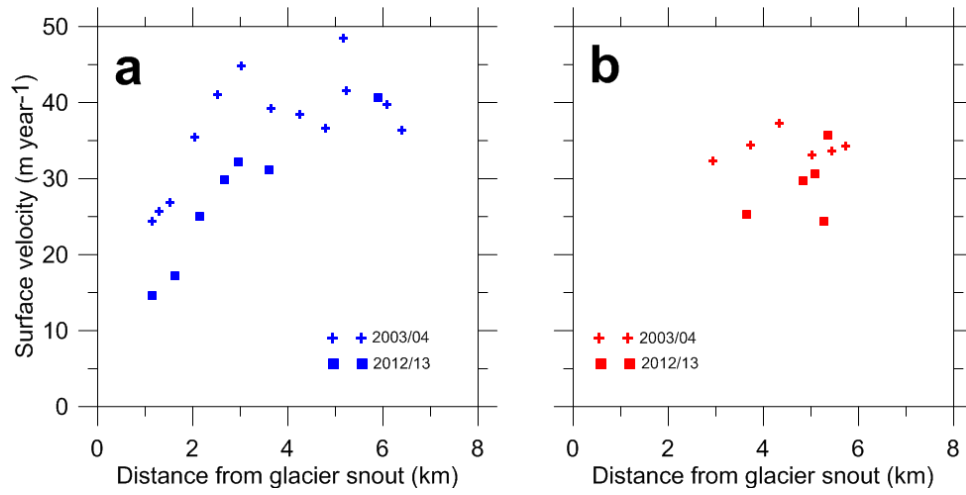


**Fig. S10.** Surface velocities for 2003/04 and 2012/2013 years from stake displacement method. Velocities in eastern flank (main glacier) (a) and in western flank (b).



## Supplementary Tables

**Table S1:** Recent estimates of glacierized area for Himalaya-Karakoram region.

Glacierized area (km <sup>2</sup> )			
Himalaya	Karakoram	Himalaya-Karakoram	Reference
21,973	21,205	43,178	Cogley (2011)
22,829	17,946	40,775	Bolch and others (2012)
29,000	21,750	50,750	Kääb and others (2012)
19,460	17,385	36,845	Nuimura and others (2015)

**Table S2:** The available data for snout fluctuation in the whole HK region. The mean recession rates are calculated using the best available data for each glacier.

s. no.	Glacier	Basin/region	Period of measurements	Number of measurements	Total recession (m)	Mean recession rate (m yr <sup>-1</sup> )	References
<b>Eastern Himalaya</b>							
1	Changme	Sikkim Himalaya	1976-2005	4	-78	-2.6**	Raina (2009)
2	Changsang	Sikkim Himalaya	1976-2005	4	-671	-22.4**	Raina (2009)
3	Chuma	Sikkim Himalaya	1976-2005	4	-247	-8.2**	(Raina (2009)
4	E. Langpo	Sikkim Himalaya	1976-2005	4	-719	-24.0**	Raina (2009)
5	Gyamtang	Sikkim Himalaya	1976-2005	4	-360	-12.0**	Raina (2009)
6	Jongsang	Sikkim Himalaya	1976-2005	4	-1146	-38.2**	Raina (2009)
7	Jumthul	Sikkim Himalaya	1976-2005	4	-355	-11.8**	Raina (2009)
8	Kangkyong	Sikkim Himalaya	1976-2005	4	-230	-7.7**	Raina (2009)
9	Lohank	Sikkim Himalaya	1976-2005	4	-813	-27.1**	Raina (2009)
10	N. Lhoank	Sikkim Himalaya	1976-2005	4	-398	-13.3**	Raina (2009)
11	Onglaktang	Sikkim Himalaya	1976-2005	4	-298	-9.9**	Raina (2009)
12	Rathong	Sikkim Himalaya	1976-2005	4	-546	-18.2**	Raina (2009)
13	Rula	Sikkim Himalaya	1976-2005	4	-546	-18.2**	Raina (2009)
14	S. Simpu	Sikkim Himalaya	1976-2005	4	-58	-1.9**	Raina (2009)
15	Talung	Sikkim Himalaya	1988-2005	3	-133	-7.8**	Raina (2009)
16	Tasha	Sikkim Himalaya	1988-2005	3	-63	-3.7**	Raina (2009)
17	Tasha 1	Sikkim Himalaya	1976-2005	4	-123	-4.1**	Raina (2009)
18	Tenbawa	Sikkim Himalaya	1976-1988	2	-124	-10.3**	Raina (2009)
19	Theukang	Sikkim Himalaya	1976-2005	4	-283	-9.4**	Raina (2009)
20	Tista	Sikkim Himalaya	1976-2005	4	-445	-14.8**	Raina (2009)
21	Toklung	Sikkim Himalaya	1976-2005	4	-331	-11.0**	Raina (2009)
22	Tongshong	Sikkim Himalaya	1976-2005	4	-420	-14.0**	Raina (2009)
23	Umaram	Sikkim Himalaya	1976-2005	4	-421	-14.0**	Raina (2009)
24	Yulhe	Sikkim Himalaya	1976-2005	4	39	1.3**	Raina (2009)
25	Zemu	Sikkim Himalaya	1909-2005	5	-863	-9.0**	Raina (2009)
	Mean of Sikkim glaciers (1-25)	Sikkim Himalaya	1976-2005	-	-	-12.6**	
26	Gangju La	Bhutan Himalaya	2004-2014	4	-108	-10.8	Tshering and Fujita (2016)
27	Luggye	Bhutan Himalaya	1984-1995	2	-300	-27.3**	GSI (1995)
28	Raphsthreng	Bhutan Himalaya	1984-1995	2	-250	-22.7**	GSI (1995)
29	S. Lhoank	Sikkim Himalaya	1962-2008	5	-1941	-42.2**	Govindha Raj and others, (2013)
<b>Central Himalaya</b>							
30	Adikailesh	Kuthiyankti	1962-2002	2	-524	13.1**	GSI (2002)
31	Amadabalam	Dudh Koshi	1960-2000	4	-474	-11.9**	Bajracharya and Mool (2009)
32	AX000	Shorong	1978-1989	2	-160	-14.5*	Yamada and others, (1992)
33	AX010	Shorong	1978-2004	9	-174	-6.7*	Fujita and others (2001a); Shrestha and Shrestha (20014)
34	AX030	Shorong	1978-1989	2	0	0.0*	Yamada (1992)
35	Bandarpunch	Tons Basin	1960-1999	3	-995	-25.5**	Sangewar (2012)
36	Bharigupanth	Bhagirathi Basin	1962-1995	2	-550	-16.7**	Srivastava (2001)
37	Bhagirathi Kharak	Alaknanda Basin	1936-2013	7	-539	-7.0*	Nainwal and others (2016)
38	Bhote Koshi	Dudh Koshi	1960-2001	4	-645	-15.7**	Bajracharya and Mool (2009)
39	Burphu	Goriganga Basin	1966-1997	2	-150	-4.8**	GSI (1997)
40	Chhule	Dudh Koshi	1960-2006	5	-942	-20.5**	Bajracharya and Mool (2009)
41	Chipa	Dauliganga Basin	1961-2000	4	-1050	-26.9**	Sangewar (2011)
42	Cholo	Dudh Koshi	1960-2006	5	-934	-20.3**	Bajracharya and Mool (2009)
43	Chorabari	Mandakani Basin	1962-2010	10	-327	-6.8*	Dobhal and others (2013)
44	Dakshini Rishi Bank	Alaknanda Basin	1960-2003	2	-731	-17**	Sangewar and Kulkarni (2011)
45	Dakshini Nanda Devi Bank	Alaknanda Basin	1960-2003	2	-559	-13**	Sangewar and Kulkarni (2011)
46	Dasuopu	Xixiabangma	1968-1997	2	-116	-4.0*	Jiawen and others (2006)
47	Devasthan Bank	Alaknanda Basin	1960-2003	2	-1118	-26**	Sangewar and Kulkarni (2011)
48	Dokriani	Bhagirathi Basin	1962-2007	4	-751	-16.7*	Dobhal and Mehta (2010)
49	Dunagiri	Dauliganga Basin	1992-1997	2	-15	-3.0**	GSI (1997)
50	East Rongbuk	Qomolangma	1966-2004	5	-226	-6.0*	Jiawen and others (2006)
51	Far East Rongbuk	Qomolangma	1966-1997	2	-229	-7.4*	Jiawen and others (2006)
52	Gangotri	Bhagirathi Basin	1842-2015	14	-1724	-10.0*	Auden (1937); Naithani and others (2001); Srivastava and others (2004); Bhattacharya and others (2016)
53	Glacier No. 3 Arwa valley	Alaknanda Basin	1932-1956	2	-198	-8.3**	Vohra and others (1981)
54	Imja	Dudh Koshi	1960-2006	5	-2784	-60.5**	Bajracharya and Mool (2009)
55	Inkhu	Dudh Koshi	1960-2001	5	-1049	-22.8**	Bajracharya and Mool (2009)

56	Jhajju Bamak	Tons Basin	1962-2010	2	-700	-14.6*	Mehta and others (2013)
57	Jhulang	Dauliganga Basin	1962-2000	2	-400	10.5**	GSI (2000)
58	Kafani	Pindar Basin	1976-2009	5	-533	-16.1*	WWF (2009)
59	Kangwure	Xixiabangma	1991-2001	2	-52	-5.2*	Jiawen and others (2006)
60	Khumbu	Dudh Koshi	1960-2006	5	-842	-18.3**	Bajracharya and Mool (2009)
61	kdugr 167	Dudh Koshi	1960-2000	4	-749	-18.7**	Bajracharya and Mool (2009)
62	Kdugr 221	Dudh Koshi	1960-2001	3	-1526	-37.2**	Bajracharya and Mool (2009)
63	Kdugr 233	Dudh Koshi	1960-2001	4	-641	-15.6**	Bajracharya and Mool (2009)
64	Kyashar	Dudh Koshi	1960-2006	4	-668	-14.5**	Bajracharya and Mool (2009)
65	Langdak	Dudh Koshi	1960-2006	5	-666	-14.5**	Bajracharya and Mool (2009)
66	Langmuche	Dudh Koshi	1960-2006	5	-822	-17.9**	Bajracharya and Mool (2009)
67	Lhotse	Dudh Koshi	1960-2006	5	-535	-11.6**	Bajracharya and Mool (2009)
68	Lumding	Dudh Koshi	1960-2006	5	-1760	-38.3**	Bajracharya and Mool (2009)
69	Lumsamba	Dudh Koshi	1960-2001	4	-545	-13.3**	Bajracharya and Mool (2009)
70	Melung	Dudh Koshi	1960-2006	5	-1492	-32.4**	Bajracharya and Mool (2009)
71	Meola	Dauliganga Basin	1961-2000	3	-1350	-34.6**	GSI (2000)
72	Meru	Bhagirathi Basin	1977-2000	3	-395	-17.2**	Chitranshi and others (2003)
73	Milam	Goriganga Basin	1849-2006	9	-2662	-17.0**	Cotter (1906); Mason (1938); Jangpangi and Vohra (1959); Govindha Raj (2011)
74	Ngojumba	Dudh Koshi	1960-2006	5	-875	-19.0**	Bajracharya and Mool (2009)
75	Nikarchu	Kuthiyankti	1962-2002	2	-375	9.4**	GSI (2002)
76	North Jaunder Bamak	Tons Basin	1990-2010	4	-872	-43.6*	Mehta and others (2013)
77	Nuptse	Dudh Koshi	1960-2006	5	-432	-9.4**	Bajracharya and Mool (2009)
78	Ombigaichain	Dudh Koshi	1960-2006	5	-2077	-45.2**	Bajracharya and Mool (2009)
79	Pindari	Alaknanda Basin	1845-2010	8	-3080	-18.7**	Cotter (1906); Tewari (1966); Bali and others (2010, 2013)
80	Poting	Karnali Basin	1906-1957	2	-262	-5.1**	Vohra (1980)
81	Ramganga	Kuthiyankti	1962-2002	2	-2000	50.0**	GSI (2002)
82	Rikha Samba	Hidden Valley	1974-1999	4	-300	-12.0*	Fujita and others (2001b)
83	Rongbuk	Qomolangma	1966-2004	5	-334	-8.8*	Jiawen and others (2006)
84	Sabai (Sha)	Dudh Koshi	1960-2001	4	-599	-14.6**	Bajracharya and Mool (2009)
85	Satopanth	Alaknanda Basin	1936-2013	7	-747	-9.7*	Nainwal and others (2016)
86	Setta	Dudh Koshi	1960-2000	4	-404	-10.1**	Bajracharya and Mool (2009)
87	Shunkalpa (Ralam)	Karnali Basin	1886-1957	4	-518	-7.3**	Cotter (1906); Mason (1938)
88	South Jaundar Bamak	Tons Basin	1960-2010	6	-1709	-34.2*	Mehta and others (2013); (Shukla and others 2001)
89	Tilku	Tons Basin	1962-2010	2	-800	-16.7*	Mehta and others (2013)
90	Tipra Bank	Alaknanda Basin	1962-2008	4	-663	-14.4*	Mehta and others (2011)
91	Trisul Bank	Alaknanda Basin	1960-2003	2	-946	-22.0**	Sangewar and Kulkarni (2011)
92	Uttari Rishi Bank	Alaknanda Basin	1960-2003	2	-1462	-34.0**	Sangewar and Kulkarni (2011)
93	W. Chamjang	Dudh Koshi	1960-2001	5	-2367	-51.5**	Bajracharya and Mool (2009)
94	W. Lhotse	Dudh Koshi	1960-2006	5	-388	-8.4**	Bajracharya and Mool (2009)
<b>Western Himalaya</b>							
95	Bara Shigri	Chandra Basin	1906-1995	4	-2650	-29.8**	GSI (1999)
96	Baspa Bamak	Baspa Basin	1962-1997	2	-380	-10.9*	Kulkarni and Bahuguna (2002)
97	Beas Kund	Beas Basin	1963-2003	2	-750	-18.8**	GSI (2003)
98	Bilare Bange	Baspa Basin	1962-1997	2	-90	-2.6*	Kulkarni and Bahuguna (2002)
99	Chhota Shigri	Chandra Basin	1962-2010	3	-334	-7.0*	GSI (1999); Azam and others (2012)
100	Drang Drung	Zaskar	1975-2008	10	-311	-9.4*	Kamp and others (2012)
101	Gangstang	Bhaga Basin	1963-2008	3	-1335	-29.7**	Sangewar and Kulkarni (2011)
102	Gepang Gath	Chandra Basin	1965-2012	6	-926	-19.7*	Mukhtar and Prakash (2013)
103	Hamtah	Chandra Basin	1980-2010	5	-504	-16.8**	GSI (2011)
104	Janapa Garang	Baspa Basin	1962-1997	2	-690	-19.7*	Bahuguna and others (2004)
105	Jobri	Beas Basin	1963-2003	2	-100	-2.5	GSI (2003)
106	Jorya Garang	Baspa Basin	1962-1997	2	-425	-12.1*	Kulkarni and Bahuguna (2002)
107	Karu Garang	Baspa Basin	1962-1997	2	-800	-22.9*	Kulkarni and Bahuguna (2002)
108	Kolahoi	Jhelum Basin	1857-1961	7	-3423	-21.8**	Odell (1963); Shukla and others (2017)
109	Machoi	Jhelum Basin	1906-1957	2	-457	-9.0**	Shukla and others (2017)
110	ManiMahesh	Ravi Basin	1973-2013	4	-157	-3.7*	Chand and Sharma (2015)
111	Mantalai Glacier No. 115	Parvati Basin	1989-2004	2	-350	-23.3**	GSI (2004)
112	Mean of 121 glaciers	Kang Yatze Massif	1969-2010	2	-125	-3.0	Schmidt and Nüsser (2012)
113	Miyar	Chandra Basin	1961-1996	4	-575	-16.4**	Obero and others (2001)
114	Mulkila	Bhaga Basin	1963-2006	2	-635	-14.8**	Srivastava (2001)
115	Nagpo Tokpo	Sutlej Basin	1963-1998	2	-2300	-65.7**	GSI (1997)
116	Naradu Garang	Baspa Basin	1962-1997	2	-550	-15.7*	Kulkarni and Bahuguna (2002)
117	Parcachik	Zaskar	1990-2003	8	146	11.2*	Kamp and others (2011)
118	Panchi nala I	Bhaga Basin	1963-2007	3	-465	-10.6**	Sangewar and Kulkarni (2011)
119	Panchi nala II	Bhaga Basin	1963-2007	3	-525	-11.9**	Sangewar and Kulkarni (2011)

120	Parbati	Beas Basin	1962-2001	5	-6569	-168.4**	Kulkarni and others (2005)
121	Raikot	Nange Parbat massif	1934-2007	10	-207	-2.8*	Schmidt and Nüsser (2009)
122	Samudra Tapu	Chandra Basin	1962-2000	4	-741	-19.5*	Kulkarni and others (2006)
123	Sara Umga Glacier No. 25	Beas Basin	1963-2004	3	-1700	-41.5**	Sangewar and Kulkarni (2011)
124	Shaune Garang	Baspa Basin	1962-1997	2	-925	-26.4*	Bahuguna and others (2004)
125	Sonapani	Chandra Basin	1906-1957	2	-898	-17.6*	Vohra (1980)
126	Tal	Ravi Basin	1973-2013	4	-45	-1.1*	Chand and Sharma (2015)
127	Tingal Goh	Bhaga Basin	1963-2008	3	-720	-16.0**	Sangewar and Kulkarni (2011)
128	Triloknath	Chandra Basin	1969-1995	2	-400	-15.4**	GSI (1995)
129	Yoche Lungpa	Bhaga Basin	1963-2006	2	-840	-19.5**	Srivastava (2001)
130	53I1008	Baspa Basin	1962-1997	2	-585	-16.7*	Kulkarni and Bahuguna (2002)
131	Zaskar Glacier 1	Zaskar	1999-2004	6	-116	-23.2*	Kamp and others (2011)
132	Zaskar Glacier 3	Zaskar	1990-2003	3	-280	-21.5*	Kamp and others (2011)
133	Zaskar Glacier 4	Zaskar	1975-2003	7	-745	-26.6*	Kamp and others (2011)
134	Zaskar Glacier 5	Zaskar	1990-2003	7	-52	-4.0*	Kamp and others (2011)
135	Zaskar Glacier 6	Zaskar	1990-2003	5	-377	-29.0*	Kamp and others (2011)
136	Zaskar Glacier 7	Zaskar	1975-2003	7	-229	-8.2*	Kamp and others (2011)
137	Zaskar Glacier 8	Zaskar	1975-2003	7	-16	-0.6*	Kamp and others (2011)
138	Zaskar Glacier 9	Zaskar	1975-2006	9	-979	-31.6*	Kamp and others (2011)
139	Zaskar Glacier 10	Zaskar	1975-2006	9	-1887	-60.9*	Kamp and others (2011)
140	Zaskar Glacier 12	Zaskar	1990-2003	6	-48	-3.7*	Kamp and others (2011)
141	Zaskar Glacier 13	Zaskar	1975-2006	7	14	0.5*	Kamp and others (2011)
<b>Karakoram</b>							
142	Aktash	Shyok Basin	1974-2011	9	643	17.4	Bhambri and others (2013)
143	Baltoro	Shigar Basin	1855-2010	13	-375	-2.4**	Hewitt (2011)
144	Batura	Hunza Basin	1860-2010	9	-4030	-26.9**	Hewitt (2011)
145	Biafo	Shigar Basin	1850-2010	13	-1375	-8.6**	Hewitt (2011)
146	Central Rimo	Shyok Basin	1930-2011	6	-1700	-21.0	Bhambri and others (2013)
147	Chogo Lungma	Shigar Basin	1860-2010	6	-2985	-19.9**	Hewitt (2011)
148	Ghulkin	Hunza Basin	1883-2007	11	500	4.0**	Hewitt (2011)
149	Hispar	Hunza Basin	1892-2004	7	-4345	-38.8**	Hewitt (2011)
150	Kichik Kumdan	Shyok Basin	1974-2011	6	-89	-2.4	Bhambri and others (2013)
151	Liligo	Shigar Basin	1971-2001	6	2040	68.0	Beló and others (2008)
152	Minapin	Hunza Basin	1887-2002	16	990	8.6**	Hewitt (2011)
153	Panmanh	Shigar Basin	1855-2010	5	20	0.1**	Hewitt (2011)
154	Siachen	Shyok Basin	1862-2005	7	218	1.5**	Ganjoo (2010)

\*Mean length change rates are estimated combining high resolution satellite images with old topographic maps/coarse resolution satellite images; \*\*Mean rates are highly uncertain as estimated from old topographic maps/coarse resolution satellite images.

**Table S3:** Glacier/glacierized area shrinkage rates over the HK range. The rates are calculated in percent change per year with respect to the initial observed area.

Glacier/Catchment	No of glaciers	Data used	Observation Period	Time Period (observations)	Initial Area km <sup>2</sup>	Final Area km <sup>2</sup>	Mean Area km <sup>2</sup>	Area Change km <sup>2</sup>	Area Change km <sup>2</sup> yr <sup>-1</sup>	Area Change % yr <sup>-1</sup>	References
<b>Eastern Himalaya</b>											
1. Bhutan Himalaya	66	Map, SPOT	1963-1993	30 (2)	146.87	134.94	2.2	-11.9	-0.40	-0.27 <sup>+</sup>	Karma (2003)
2. Bhutan Himalaya	-	Landsat TM/ETM+	1980-2000	20 (2)	-	-	-	-	-	-1.10±0.20	Frauenfelder and Käab (2009)
3. Bhutan Himalaya	817	Landsat	1980-2010	30 (4)	837.6±28.81	642.1±16.12	1.03	-195.5	-6.52	-0.78 <sup>+</sup>	Bajracharya and Shrestha (2014)
4. Gangju La	1	ALOS PRISM, DGPS	2004-2014	10 (4)	0.29	0.25	0.29	-0.04	-0.004	-1.38 <sup>+</sup>	Tshering and Fujita (2016)
5. Nepal (Tamor and Arun basins)	68	Corona KH4, Landsat ETM+, ASTER	1962-2000	38 (2)	323.9±10	269.1±16	4.8	-54.8±19	-1.44	-0.44±0.20	Racoviteanu and others (2015)
6. Sikkim, Tista Basin	38	Landsat TM/ETM+, LISS III	1989/90-2009/10	20 (4)	201.91±7.09	195.31±7.13	5.3	-6.85±1.50	-0.34±0.07	-0.16±0.10	Basnett and others (2013)
7. Sikkim, Tista Basin	57	LISS-IV, Pan and LISS-III	1997-2004	7 (2)	403.0	392.0	7.1	-11.0	-1.57	-0.39 <sup>+</sup>	Kulkarni and others (2011)
8. Sikkim, Tista Basin	164	Corona KH4, Landsat ETM+, ASTER	1962-2000	38 (2)	634.7±19	507.0±35	3.9	-127.7±42	-3.36	-0.52±0.20	Racoviteanu and others (2015)
<b>Central Himalaya</b>											
9. Alaknanda Basin	69	Corona, ASTER, Landsat TM	1968-2006	38 (3)	324.77	306.35	4.7	-18.42	-0.48	-0.15±0.07	Bhambri and others (2011)
10. Bhagirathi Basin	13	Corona, ASTER, Landsat TM	1968-2006	38 (3)	275.15	266.17	21.2	-8.98	-0.24	-0.09±0.07	Bhambri and others (2011)
11. Bhagirathi Basin	212	Map, LISS III	1962-2001	39 (2)	1365	1178	6.4	-187.0	-4.79	-0.35 <sup>+</sup>	Kulkarni and others (2011)
12. Bhagirathi Kharak	1	Maps, Landsat ETM+, DGPS	1956-2013	57 (4)	31	30.83	31.0	-0.17 ± 0.04	-0.003	-0.01 <sup>+</sup>	Nainwal and others (2016)
13. Dokriani, Bhagirathi Basin	1	Maps	1962-1995	33 (2)	7.78	7	7.8	-0.78	-0.02	-0.30 <sup>+</sup>	Dobhal and others (2004)
14. Gandaki Basin	1071	Map, Landsat ETM+	~1970-2009	39 (2)	2030	-	1.9	-	-	-0.91 <sup>++</sup>	Bajracharya and others (2011)
15. Gangotri, Bhagirathi Basin	1	Map, LISS III, Cartosat-1	1962-2006	44 (2)	-	-	-	-	-	-0.14 <sup>++</sup>	Negi and others (2012)
16. Garhwal Himalaya	82	Corona, ASTER, Landsat TM	1968-2006	38 (2)	599.9±15.6	572.5±18.0	7.3	-27.4±16.8	-0.72	-0.12±0.07	Negi and others (2012)
17. Ghanna, Langtang Basin	1	Hexagon, SPOT, Cartosat, World view, ALOS, Pleiades	1974-2015	41 (3)	1.56	1.35	1.5	-0.21	-0.01	-0.33±0.12	Ragetti and others (2014)
18. Goriganga Basin	41	Map, LISS III	1962-2001	39 (2)	335	269	8.2	-66.0	-1.69	-0.51 <sup>+</sup>	Kulkarni and others (2011)
19. Hidden Valley, Kaligandagi Basin	9	Landsat, ASTER	~1980s-2010	30 (4)	19.79	15.46	2.2	-4.3	-0.14	-0.73 <sup>++</sup>	Lama and others (2015)
20. Jaundar, Tons Basin	1	Map, Landsat TM/ETM, GPS	1962-2010	48 (2)	56.8	55.0	56.8	-1.8	-0.04	-0.06 <sup>+</sup>	Mehta and others (2013)
21. Jahjiu, Tons Basin	1	Map, Landsat TM/ETM, GPS	1962-2010	48 (2)	6.2	5.9	6.2	-0.3	-0.01	-0.09 <sup>+</sup>	(Mehta and others (2013)
22. Kangwure	1	Map, GPS, ALOS	1974-2008	34 (2)	2.98	1.96	3.0	-1.02	-0.03	-1.01 <sup>+</sup>	Ma and others (2010)
23. Karnali Basin	1361	Map, Landsat ETM+	~1970-2009	39 (2)	1739	-	1.3	-	-	-0.29 <sup>++</sup>	Ye and others (2009)
24. Khumbu region, Dudh Koshi Basin	20	Corona, Landsat TM, ASTER	1962-2005	43 (4)	92.26	87.39	4.6	-4.87	-0.11	-0.12	Bolch and others (2008)
25. Khumbu region, Dudh Koshi Basin	29	Maps	1956-1990	34 (2)	403.9	384.6	13.9	-19.3	-0.57	-0.14 <sup>+</sup>	Salerno and others (2008)
26. Kimoshung, Langtang Basin	1	Hexagon, SPOT, Cartosat, World view, ALOS, Pleiades	1974-2015	41 (3)	4.51	4.38	4.445	-0.13	0.00	-0.07±0.02	Ragetti and others (2016)
27. Koshi Basin	779	Map, Landsat ETM+	~1970-2009	39 (2)	1413	-	1.8	-	-	-0.42 <sup>++</sup>	Ye and others (2009)
28. Koshi Basin	2206	Map, Landsat MSS, TM, TM+, ETM+	1976-2009	33 (3)	4000.5±196.0	3225.1±90.3	1.8	775.4	23.50	-0.59±0.17	Shangguan and others (2014)
29. Mt Everest region, Dudh Koshi Basin	29	Maps, Corona, Landsat MSS/TM/ETM+, ALOS	1962-2011	49 (6)	404.6	351.8	14.0	-52.8	-1.08	-0.27±0.06	Thakuri and others (2014)
30. Khumbu region, Dudh Koshi Basin	-	Model	1961-2007	46	499	398	-	-101.0±11.4	-2.20	-0.44	Shea and others (2015)
31. Langtang, Langtang Basin	1	Hexagon, SPOT, Cartosat, World view, ALOS, Pleiades	1974-2015	41 (3)	49.15	46.05	47.6	-3.10	-0.08	-0.15±0.02	Ragetti and others (2016)
32. Langshisha, Langtang Basin	1	Hexagon, SPOT, Cartosat, World view, ALOS, Pleiades	1974-2015	41 (3)	16.78	16.17	16.47	-0.61	-0.01	-0.09±0.04	Ragetti and others (2016)
33. Lirung, Langtang Basin	1	Hexagon, SPOT, Cartosat, World view, ALOS, Pleiades	1974-2015	41 (3)	6.95	6.45	6.7	-0.50	-0.01	-0.18±0.08	Ragetti and others (2016)
34. Mt. Qomolangma (Everest) Region	74	Landsat MSS/TM/ETM+, ASTER, ALOS/AVNIR-2	1974-2008	34 (2)	144.14	129.13	1.9	-15.01	-0.44	-0.31 <sup>+</sup>	Ye and others (2009)
35. Nepal	3430	Landsat	~1980-2010	30 (4)	5168.3	3902.4	1.5	-1265.9	-42.20	-0.82 <sup>++</sup>	Bajracharya and others (2014)
36. Nepal (eastern)	1034	Maps, Landsat TM, ALOS	1992-2006/10	49 (6)	495.72	440.2	0.43	-55.5	-3.47	-0.70±0.10	Ojha and others (2016)
37. Rataban, Alaknanda Basin	1	Map, LISS III, GPS	2002-2008	6 (3)	7.5	7.4	7.5	-0.1	-0.01	-0.17 <sup>+</sup>	Mehta and others (2011)
38. Shailbachum, Langtang Basin	1	Hexagon, SPOT, Cartosat, World view, ALOS, Pleiades	1974-2015	41 (3)	10.48	10.17	10.325	-0.31	-0.01	-0.07±0.04	Ragetti and others (2016)
39. Tilku, Tons Basin	1	Map, Landsat TM/ETM, GPS	1962-2010	48 (2)	2.7	2.3	2.7	-0.4	-0.01	-0.33 <sup>+</sup>	Mehta and others (2013)
40. Tipra, Alaknanda Basin	1	Map, LISS III, GPS	1962-2008	46 (5)	10.2	7.5	10.2	-2.7	-0.06	-0.57 <sup>+</sup>	Mehta and others (2011)
41. Northwest Himalaya (north of Everest)	197	Landsat TM/ETM+	1980-2000	20 (2)	449.4	372.6	2.3	-76.8	-3.84	-0.85 <sup>+</sup>	Frauenfelder and Käab (2009)

42. Pumqu (Arun) Basin	999	Map, ASTER, CBERS	1970-2001	31 (2)	1462±9	1330±8	1.5	-132.0	-4.26	-0.29 <sup>*</sup>	Jin and others (2005)
43. Pumqu (Arun) Basin	999	Map, ASTER, CBERS, Landsat8OLI/TIRS	1970-2013	43 (3)	1461.84	1183.4	1.5	-278.4	-6.48	-0.44 <sup>*</sup>	Che and others (2014)
44. Poiqu (Bhote-Sun Koshi) Basin	153	Landsat	1986-2001	15 (2)	229.0	183	1.5	-46.0	-3.07	-1.34 <sup>**</sup>	Chen and others (2007)
45. Satopanth	1	Maps, Landsat ETM+, DGPS	1956-2013	57 (6)	21.0	20.73		-0.27 ± 0.05	-0.005	-0.02 <sup>*</sup>	Nainwal and others (2016)
46. Yala, Langtang Basin	1	Hexagon, SPOT, Cartosat, World view, ALOS, Pléiades	1974-2015	41 (3)	2.21	1.59	1.9	-0.62	-0.02	-0.68±0.16	Ragettli and others (2016)
<b>Western Himalaya</b>											
47. Baspa Basin	19	Map, LISS III	1962-2001	39 (2)	173	140	9.1	-33.0	-0.85	-0.49 <sup>*</sup>	Kulkarni and others (2011)
48. Baspa, Chenab and Parbati basins	466	Map, LISS III, LISS IV, GPS	1962-2001	39 (2)	2077	1628	4.5	-449	-11.51	-0.55 <sup>*</sup>	Kulkarni and others (2007)
49. Beas Basin	224	Landsat MSS/TM/ETM+, LISS III	1972-2006	34 (3)	419	371	1.9	-48	-1.41	-0.34 <sup>*</sup>	Dutta and others (2012)
50. Bhaga Basin	111	Map, LISS III	1962-2001	39 (2)	363	254	3.3	-109.0	-2.79	-0.77 <sup>*</sup>	Kulkarni and others (2011)
51. Bhut Basin	189	Map, LISS III	1962-2001	39 (2)	469	420	2.5	-49.0	-1.26	-0.27 <sup>*</sup>	Kulkarni and others (2011)
52. Chandra Basin	116	Map, LISS III	1962-2001	39 (2)	696	554	6.0	-142.0	-3.64	-0.52 <sup>*</sup>	Kulkarni and others (2011)
53. Chandra-Bhaga Basin	15	Landsat MSS/TM, LISS III, AWiFS	1980-2010	30(10)	377.6±5.7	368.2±14.7	25.1	-9.3±0.5	-0.31	-0.08 <sup>*</sup>	Panday and Venkataraman (2013)
54. Hamtah, Chandra Basin	1	Map, Landsat TM/ETM+, ASTER, LISS III, AWiFS	1963-2010	47 (5)	3.4	3.0	3.4	-0.42	-0.01	-0.26 <sup>*</sup>	Panday and Venkataraman (2013)
55. Kolahoi, Jhelum Basin	1	Map, LISS III	1963-2005	42(2)	13.6	10.7	13.6	-2.9	-0.07	-0.51 <sup>*</sup>	Kanth and others (2011)
56. Miyar Basin	166	Map, LISS III	1962-2001	39 (2)	568	523	3.4	-45.0	-1.15	-0.20 <sup>*</sup>	Kulkarni and others (2011)
57. Naimona'nyi region	53	Landsat MSS/TM, ASTER	1976-2003	27 (4)	84.41	77.29	1.6	-7.12	-0.26	-0.31 <sup>*</sup>	Ye and others (2006)
58. Parbati, Beas Basin	1	Map, LISS II, LISS III, Landsat TM	1962-2001	39 (5)	48.4	36.9	48.4	-11.6	-0.30	-0.61 <sup>*</sup>	Kulkarni and others (2005)
59. Parbati Basin	90	Map, LISS III	1962-2001	39 (2)	493	390	5.5	-103.0	-2.64	-0.54 <sup>*</sup>	Kulkarni and others (2011)
60. Pensilungpa	1	Map, Landsat MSS/TM/ETM+, LISS III, AWiFS	1962-2012	50 (2)	23.82	15.3	23.8	-8.5	-0.17	-0.72 <sup>*</sup>	Ghosh and Pandey (2013)
61. Ravi Basin	157	Landsat ETM+ / Aster GDEM/Korona KH 4B/World view/Landsat 8 OLI TRIS	1971-2010/13	41 (3)	125.9±1.9	120±4.8	0.8	-5.9±5.2	-0.14±0.12	-0.1±0.1	Chand and Sharma (2015)
62. Samudra Tapu, Chandra Basin	1	Map, IRS PAN, LISS III	1962-2000	38 (2)	73	65	73.0	-8	-0.21	-0.29 <sup>*</sup>	Kulkarni and others (2006)
63. Warwan Basin	253	Map, LISS III	1962-2001	39 (2)	847	672	3.3	-175.0	-4.49	-0.53 <sup>*</sup>	Kulkarni and others (2011)
64. Zaskar Basin (Doda Valley)	13	Map, Landsat MSS/TM/ETM+, LISS III, GPS	1962-2001	39 (2)	363.4	291.2	28.0	-72.1	-1.85	-0.51 <sup>*</sup>	Rai and others (2013)
65. Zaskar Basin (Kang Yatze massif)	121	Corona, SPOT, Landsat TM/ETM+	1969-2010	41 (4)	96.4	82.6	0.8	-13.8	-0.34	-0.35 <sup>*</sup>	Schmidt, M. Nüsser (2012)
66. Zaskar Basin	671	Map, LISS III	1962-2001	39 (2)	1023	929	1.5	-94.0	-2.41	-0.24 <sup>*</sup>	Kulkarni and others (2011)
67. Mapam Yumco Basin	--	--	1974-2003	29 (4)	108	100		-8.0	-0.28	-0.26 <sup>*</sup>	Ye and others (2008)
<b>Karakoram</b>											
68. Central Karakoram	711	Landsat TM/ETM+	2001-2010	9 (2)	4587±18	4613±38	6.5	26.6±42	2.96	0.06 <sup>*</sup>	Minora and others (2013)
69. Shyok Valley	136	Hexagon KH 9, Landsat TM/ETM+	1973-2011	38(4)	1613.6±43.6	1615.8±35.5	11.9	2.2±56.2	0.06	0.01±3.5	Bhambri and others (2013)
70. Yarkant Basin	565	Map, Landsat TM/ETM+	1968-1999	31 (2)	2707.3	2596.2	4.8	-111.1	-3.58	-0.13 <sup>*</sup>	Liu and others (2006)
71. Siachen	1	Cartosat-1, KH-9 Hexagon, Landsat TM/ETM+, SRTM	1980-2014	34 (5)	936.7	936.2	936.7	-0.5	-0.01	-0.002	Agarwal and others (2016)

<sup>\*</sup> Estimates are based on topographic maps/coarse resolution satellite images and uncertainty not assessed; <sup>\*\*</sup> Highly uncertain as estimates are based on topographic maps, dates are not fixed and uncertainty not assessed.



**Table S4:** Glaciological mass balance observations in the Himalayan range. The error estimations in mass balances were given when calculated in the original source.

Glacier name (region/country)	Location	Area (km <sup>2</sup> )	Debris cover area (%)	Aspect	MB Period	Mass balance (m w.e. yr <sup>-1</sup> )	Reference
<b>Eastern Himalaya</b>							
1. Changmekhangpu (CG), Sikkim, India	27°57'N 88°41'E	5.6	50	S	1979-1986	-0.26	GSI (2001)
2. Gangju La (GL) Pho Chhu, Bhutan	27°94'N 89°95'E	0.3	clean	NE	2003-2004; 2012-2014	-1.38±0.18	Tshering and Fujita (2016)
<b>Central Himalaya</b>							
3. AX010 (AX), Shorang Himal, Nepal	27°43'N 86°33'E	0.6	clean	SE	1978-1979; 1995-1999	-0.69±0.08	Fujita and others (2001a)
4. Chorabari (CB), Garhwal Himalaya, India	30°74'N 79°09'E	6.7	53	S	2003-2010	-0.73	Dobhal and others (2013)
5. Dokriani (DR), Garhwal Himalaya, India	30°50'N 78°50'E	7.0	6	NW	1992-1995; 1997-2000;	-0.32	Dobhal and others (2008)
6. Dunagiri (DG), Garhwal Himalaya, India	30°33'N 79°54'E	2.6	~80	N	1984-1990	-1.04	GSI (1991)
7. Kangwure (KW), Xixiabangma, China	28°28'N 85°49'E	1.9	clean	NE	1991-1993; 2008-2010	-0.57	Liu and others (1996); Yao and others (2012)
8. Mera (MR), Dudh Koshi Basin, Nepal	27°43'N 86°52'E	5.1	clean	N	2007-2015	-0.03±0.28	Wagnon and others, (2013); Sherpa and others (2017)
9. Pokalde (PK), Dudh Koshi Basin, Nepal	27°55'N 86°50'E	0.1	clean	NW	2009-2015	-0.69±0.28	Wagnon and others, (2013); Sherpa and others (2017)
10. Rikha Samba (RS), Hidden Valley, Nepal	28°50'N 83°30'E	4.6	clean	S	1998-1999	-0.60±0.03	Fujita and others (2001b)
11. Tipra Bank (TB), Garhwal Himalaya, India	30°44'N 79°41'E	7.0	15	NW	1981-1988	-0.14	Gautam and Mukherjee (1992)
12. West Changri Nup (CN), Dudh Koshi Basin, Nepal	27°98'N 86°77'E	0.9	clean	NE	2010-2015	-1.24±0.27	Wagnon and others, (2013); Sherpa and others (2017)
13. Yala (YL), Langtang Valley, Nepal	28°14'N 85°36'E	1.6	clean	S	2011-2012	-0.89	Baral and others (2014)
<b>Western Himalaya</b>							
14. Chhota Shigri (CS), Lahaul-Spiti, India	32°28'N 77°52'E	15.5	3.4	N	2002-2014	-0.56±0.40	Wagnon and others (2007); Azam and others (2012; 2016)
15. Hamtah (HT), Lahaul-Spiti, India	32°24'N 77°37'E	3.2	~70	N	2000-2009; 2010-2012	-1.43	GSI (2011); Mishra and others (2014)
16. Gara (GR), Baspa basin, India	31°28'N 78°25'E	5.2	17	NE	1974-1983	-0.27	Raina (1977); Sangewar and Siddiqui (2007)

17. Gor Garang (GG), Baspa basin, India	31°37'N 78°49'E	2.0	~60	S	1976-1985	-0.38	Sangewar and Siddiqui (2007)
18. Kolahoi (KH), Jhelum Basin, India	34°20'N 75°47'E	11.9	clean	N	1983-1984	-0.27	Kaul (1986)
19. Naimona'nyi (NN), Karnali Basin, China	30°27'N 81°20'E	7.8	clean	N	2005-2010	-0.56	Yao and others (2012)
20. Naradu (ND), Baspa Basin, India	31°20'N 78°27'E	4.6	~60	N	2000-2003; 2011-2015	-0.72	Koul and Ganjoo (2010)
21. Neh Nar (NN), Jhelum Basin, India	34°09'N 75°31'E	1.3	clean	N	1975-1984	-0.43	GSI (2001)
22. Rulung (RL), Zaskar Range, India	33°07'N 78°26'E	1.1	clean	NE	1979-1981	-0.11	Srivastava (2001); Sangewar and Siddiqui (2007)
23. Shaune Garang (SG), Baspa basin, India	31°17'N 78°20'E	4.9	24	N	1981-1991	-0.42	GSI (1992); Sangewar and Siddiqui (2007)
24. Shishram (SR), Jhelum Basin, India	34°20'N 75°43'E	9.9	clean	N	1983-1984	-0.29	Kaul (1986)

**Table S5:** The details of mass balance observations on all the observed glaciers. The related references can be found in table S4.

Glacier	Map used	No. of stakes	stake material	No. of acc* site	Method of acc	Density measurement	Measurement frequency
1. Changmekhangpu	n/a	17-50	n/a	3 to 6	pit	yes	sub-monthly
2. Gangju La	ALOS PRISM 2010	8-10	n/a	n/a	n/a	yes	annual
3. AX010	n/a	14	n/a	n/a	pit	yes	annual
4. Chorabari	Landsat ETM+ 2005	44	bamboo	4	pit	yes	sub-monthly
5. Dokriani	SOI (1:10000)	22	iron <sup>a</sup>	5 to 6	pit	yes	sub-monthly
6. Dunagiri	SOI (1:20000)	30	aluminium	n/a	pit	yes	sub-monthly
7. Kangwure	n/a	14-27	n/a	n/a	n/a	n/a	annual
8. Mera	Pleiades-1A 2012	28-45	bamboo	6	core	yes	seasonal
9. Pokalde	SPOT5 2011	5	bamboo	1	core	yes	seasonal
10. Rikha Samba	n/a	8	n/a	n/a	pit	yes	annual
11. Tipra Bank	n/a	43	aluminium	n/a	pit	yes	sub-monthly
12. West Changri Nup	Pleiades-1A 2013	9	bamboo	n/a	n/a	yes	seasonal
13. Yala	Rapid Eye 2010	6	bamboo	6	pit	yes	annual
14. Chhota Shigri	SPOT5 2005	22	bamboo	5	core	yes	sub-monthly
15. Hamtah	n/a	n/a	aluminium	n/a	n/a	n/a	sub-monthly
16. Gara	SOI (1:15000)	47	aluminium	4	pit	yes	sub-monthly
17. Gor Garang	SOI (1:20000)	24	aluminium	n/a	pit	yes	sub-monthly
18. Kolahoi	SOI (1:20000)	n/a	aluminium	n/a	pit	yes	seasonal
19. Naimona'nyi	n/a	16	n/a	n/a	n/a	n/a	annual
20. Naradu	n/a	46	bamboo	n/a	pit	yes	monthly
21. Neh Nar	SOI (1:10000)	50	wooden	n/a	pit	yes	monthly
22. Rulung	SOI (1:20000)	22	wooden	n/a	pit	yes	sub-monthly
23. Shaune Garang	SOI (1:20000)	20	aluminium	n/a	pit	yes	sub-monthly
24. Shishram	SOI (1:20000)	n/a	aluminium	n/a	pit	yes	seasonal

\* accumulation; <sup>a</sup>galvanized iron pipes; n/a = not available.

1 **Table S6:** Glaciological annual mass balance data for the HK region. The positive mass balances are given in green color.

Glacier	CG	GL	AX	CB	DR	DG	KW	MR	PK	RS	TB	CN	YL	CS	HT	GR	GG	KH	NY	ND	NN	RL	SG	SR
Year																								
1970																								
1971																								
1972																								
1973																								
1974																								
1975																0.48								
1976																0.26					-0.24			
1977																-0.83	-0.68				-0.46			
1978																-0.89	-0.6				-0.86			
1979			-0.53													-0.36	-0.25				-0.54			
1980	-0.38															-0.7	-0.49				-0.45	-0.06		
1981	-0.39															-1.02	-0.97				-0.48	-0.15		
1982	-0.30										-0.32					0.57	0.2				-0.24		-0.30	
1983	-0.29										0.22					0.06	0.51				-0.01		0.02	
1984	-0.16										-0.08						-0.76	-0.27			-0.63		-0.85	-0.29
1985	-0.24					-0.78					-0.06						-0.42						-0.68	
1986	-0.07					-0.95					-0.06												-0.23	
1987						-1.04					-0.07												-0.80	
1988						-1.29					-0.61												-0.63	
1989						-0.98																	0.34	
1990						-1.24																	-0.27	
1991																							-0.83	
1992							-0.25																	
1993					-0.22		-0.64																	
1994					-0.23																			
1995					-0.31																			
1996			-0.53																					
1997			-0.49																					
1998			-1.38		-0.34																			
1999			-0.52		-0.46					-0.60														
2000					-0.38																			
2001															-1.66					-0.44				
2002															-1.22					-0.35				
2003																					-0.40			
2004		-1.23		-0.74										-1.43	-1.62									
2005				-0.79										-1.24	-1.86									
2006				-0.82										0.13	-0.65									
2007				-0.75										-1.43	-1.39				-0.66					
2008				-0.67				0.39						-1.00	-2.61				-0.66					
2009				-0.67			-1.09	-0.10						-0.95	-1.34				-0.72					
2010				-0.65			-0.30	-0.48	-0.92					0.12	-0.75				-0.47					
														0.32					-0.28					

2011								0.46	-0.11			-0.95		0.06	-1.46									
2012								-0.67	-1.12			-1.73	-0.89	-0.46	-1.19					-1.1				
2013		-1.81						0.42	-0.07			-0.92		-0.77						-1.15				
2014		-1.11						-0.20	-1.23			-1.33		-0.08						-0.85				
2015								-0.02	-0.70			-1.28								-0.79				
Mean MB	-0.26	-1.38	-0.69	-0.73	-0.32	-1.04	-0.57	-0.03	-0.69	-0.60	-0.14	-1.24	-0.89	-0.56	-1.43	-0.27	-0.38	-0.27	-0.56	-0.72	-0.43	-0.11	-0.42	-0.29

**Table S7:** Classification of the glaciological mass balance series.

Glacier	A	B	C	D	E	F	G	H	I	J	K	L	M	N	O	P	Score*	Category**
1. Changmekhangpu	0	0	0	0.5	n/a	1	1	0	0	0	0	0.5	0	0	0	0	0.20	Dubious
2. Gangju La	1	1	1	1	n/a	1	1	1	1	n/a	0.5	0	0.5	0	0.5	1	0.75	Excellent
3. AX010	0	1	0	1	n/a	1	1	1	1	0	0.5	0	0	0	0	0	0.43	Fair
4. Chorabari	0	0	0.5	0.5	1	1	1	0	0	0	0	0.5	0	0	0	0	0.28	Dubious
5. Dokriani	0	0	0	0	0	1	1	1	1	1	0	0.5	0	0	0	0.5	0.38	Fair
6. Dunagiri	0	0	0	1	0	n/a	1	0	0	0	0	1	0	0.5	0	0.5	0.27	Dubious
7. Kangwure	0	0	0	1	n/a	n/a	0	1	1	0	0	0	0	0	0	0	0.21	Dubious
8. Mera	0	1	1	0.5	1	1	1	1	1	1	0	0	0	0	0	0.5	0.56	Good
9. Pokalde	0	1	1	1	1	1	1	1	1	1	0.5	0.5	0.5	0.5	0	0.5	0.72	Excellent
10. Rikha Samba	0	1	0	0	n/a	n/a	1	1	1	n/a	n/a	n/a	n/a	n/a	n/a	n/a	0.57	Good
11. Tipra Bank	0	0	0	0.5	0	n/a	1	0.5	1	0.5	0	0	0	0.5	0.5	0	0.30	Fair
12. West Changri Nup	1	1	1	1	1	1	1	1	1	0	0	0	0	0	0	0.5	0.59	Good
13. Yala	0	0	1	0	1	1	1	1	1	n/a	n/a	n/a	n/a	n/a	n/a	n/a	0.67	Excellent
14. Chhota Shigri	1	1	1	0	1	1	1	1	1	1	0.5	0	0.5	0	0	0	0.63	Excellent
15. Hamtah	0	0	0	n/a	0	n/a	0	0	0	0	0	0	0	0	0	0	0.00	Dubious
16. Gara	0	0	0	0.5	0	1	1	0.5	1	1	0	0	0	0.5	0.5	0.5	0.41	Fair
17. Gor Garang	0	0	0	1	0	n/a	1	0	1	1	0	0.5	0	0.5	0.5	0.5	0.40	Fair
18. Kolahoi	0	0	0	n/a	0	n/a	1	1	0	n/a	n/a	n/a	n/a	n/a	n/a	n/a	0.29	Dubious
19. Naimona'nyi	0	0	0	0	n/a	n/a	0	1	1	1	0	0.5	0	0.5	0.5	0	0.32	Fair
20. Naradu	0	0	0	1	1	n/a	1	0	1	0.5	0	0	0	0.5	0.5	0	0.37	Fair
21. Neh Nar	0	0	0	1	1	n/a	1	1	1	0	0	0.5	0	0.5	0.5	0.5	0.47	Good
22. Rulung	0	0	0	1	1	n/a	1	1	1	n/a	n/a	n/a	n/a	n/a	n/a	n/a	0.63	Excellent
23. Shaune Garang	0	0	0	0	0	n/a	1	0.5	1	1	0	0	0	0.5	0.5	0.5	0.33	Fair
24. Shishram	0	0	0	n/a	0	n/a	1	1	1	n/a	n/a	n/a	n/a	n/a	n/a	n/a	0.43	Fair

\* Final score is computed by dividing the sum of all intermediate scores (A-P) with the number of available parameters for each mass balance series. \*\* Excellent = score > 0.60; Good = 0.45 < score < 0.60; Fair = 0.30 < score < 0.45; Dubious = score < 0.30; n/a = not available.

**A.** Geodetic verification of glaciological mass balance: yes = 1; no = 0.

**B.** Uncertainty analysis: yes = 1; no = 0.

**C.** Map quality: high = 1; medium = 0.5; low (or unknown) = 0.

**D.** Stake density: high (>10 stakes/km<sup>2</sup>) = 1; medium (5-10 stakes/km<sup>2</sup>) = 0.5; low (<5 stakes/km<sup>2</sup>) = 0.

**E.** Stake material: bamboo/wood = 1; metal = 0.

**F.** Accumulation measurements: yes = 1; no = 0.

**G.** Snow/ice density measurements: yes = 1; no = 0.

**H.** Debris cover: high (>50%) = 0, medium (10-50%) = 0.5; low (<10%) = 1.

**I.** Avalanche-fed: high = 0; low = 1.

**J.** Mass balance-ELA relationship: strong ( $r^2 > 0.7$ ) = 1; moderate ( $0.3 < r^2 < 0.7$ ) = 0.5; weak ( $r^2 < 0.3$ ) = 0.

**K.** Mass Balance-annual temperature relationship: strong ( $r^2 > 0.7$ ) = 1; moderate ( $0.3 < r^2 < 0.7$ ) = 0.5; weak ( $r^2 < 0.3$ ) = 0.

**L.** Mass Balance-winter temperature relationship: strong ( $r^2 > 0.7$ ) = 1; moderate ( $0.3 < r^2 < 0.7$ ) = 0.5; weak ( $r^2 < 0.3$ ) = 0.

**M.** Mass Balance-summer temperature relationship: strong ( $r^2 > 0.7$ ) = 1; moderate ( $0.3 < r^2 < 0.7$ ) = 0.5; weak ( $r^2 < 0.3$ ) = 0.

**N.** Mass Balance-annual precipitation relationship: strong ( $r^2 > 0.7$ ) = 1; moderate ( $0.3 < r^2 < 0.7$ ) = 0.5; weak ( $r^2 < 0.3$ ) = 0.

**O.** Mass Balance-winter precipitation relationship: strong ( $r^2 > 0.7$ ) = 1; moderate ( $0.3 < r^2 < 0.7$ ) = 0.5; weak ( $r^2 < 0.3$ ) = 0.

**P.** Mass Balance-summer precipitation relationship: strong ( $r^2 > 0.7$ ) = 1; moderate ( $0.3 < r^2 < 0.7$ ) = 0.5; weak ( $r^2 < 0.3$ ) = 0.



**Table S8:** Geodetic mass balance data for the HK region.

Region/Glacier	Area (km <sup>2</sup> )	Period	Mass balance (m w.e. yr <sup>-1</sup> )	Year of observation (periods)	Reference
<b>Eastern Himalaya</b>					
Bhutan (BT1)	1384	1999-2010	-0.22 ± 0.12	11 (1)	Gardelle and others (2013)
East Nepal and Bhutan (ENB)	9550	2003-2009	-0.30 ± 0.09	6 (1)	Kääb and others (2012)
Bhutan (BT2)	6632	2003-2009	-0.66 ± 0.32	6 (1)	Neckel and others (2014)
Nepal-Bhutan border (NB)	365	1974-2006	-0.17 ± 0.05	32 (1)	Maurer and others (2016)
Gangju La (GL)	0.3	2004-2014	-0.69	10 (4)	Tshering and Fujita (2016)
<b>Central Himalaya</b>					
Mt. Everest region (ER1)	62	1970-2007	-0.32 ± 0.08	37 (2)	Bolch and others (2011)
Khumbu region (KR1)	17	1970-2007	-0.27 ± 0.08	37 (4)	Bolch and others (2011)
Khumbu region (KR2)	183	1992-2008	-0.40 ± 0.25	16 (2)	Nuimura and others (2012)
Khumbu region (KR3)	74	2000-2011	-0.41 ± 0.21	11 (1)	Gardelle and others (2013)
Mt. Everest region (ER2)	1461	2000-2011	-0.26 ± 0.13	11 (1)	Gardelle and others (2013)
Mt. Everest region (ER3)	–	2000-2015	-0.52 ± 0.22	15 (1)	King and others (2017)
West Nepal (WN1)	908	1999-2011	-0.32 ± 0.13	12 (1)	Gardelle and others (2013)
West Nepal (WN2)	2371	2003-2009	-0.37 ± 0.25	6 (1)	Neckel and others (2014)
Langtang Himal (LH1)	155	1974-1999	-0.32 ± 0.18	25 (1)	Pellicciotti and others (2015)
Langtang Himal (LH2)	87.2	1974-2006	-0.21 ± 0.08	32 (1)	Ragettli and others (2016)
		2006-2015	-0.38 ± 0.17	9 (1)	
AX010 (AX)	0.4	1978-2008	-0.75 ± 0.09	30 (4)	Fujita and Nuimura (2011)
Yala (YL)	1.9	1983-2009	-0.58 ± 0.08	26 (2)	Fujita and Nuimura (2011)
Rikha Samba (RS)	4.6	1974-2010	-0.46 ± 0.07	36 (2)	Fujita and Nuimura (2011)
Rongbuk Catchment (RC)	155.6	1974-2006	-0.40 ± 0.27	32 (2)	Ye and others (2015)
Kangwure (KW)	2.0	1975-2008	-0.20 ± 0.08	33 (1)	Ma and others (2010)
Dokriani (DR)	7.0	1962-1995	-0.30	33 (1)	Dobhal and others (2008)
HP, UK and west Nepal (HPUKWN)	14550	2003-2009	-0.32 ± 0.06	6 (1)	Kääb and others (2012)
Gangotri (GT)	211	1968-2014	-0.19 ± 0.12	46 (2)	Bhattacharya and others (2016)
<b>Western Himalaya</b>					
Lahaul & Spiti (LS1)	915	1999-2004	-0.70 to -0.85	5 (1)	Berthier and others (2007)
Lahaul & Spiti (LS2)	2110	1999-2011	-0.45 ± 0.13	12 (1)	Gardelle and others (2013)
Lahaul & Spiti (LS3)	1796	2000-2012	-0.52 ± 0.32	12 (1)	Vijay and Braun (2016)
Chhota Shigri (CS1)	15.5	1988-2010	-0.17 ± 0.09	22 (1)	Vincent and others (2013)
Chhota Shigri (CS1)	15.5	1999-2010	-0.44 ± 0.16	11 (1)	Vincent and others (2013)

Chhota Shigri (CS3)	15.5	2005-2014	$-0.39 \pm 0.24$	9 (1)	Azam and others (2016)
Hamtah (HT)	3.2	1999–2011	$-0.45 \pm 0.16$	12 (1)	Vincent and others (2013)
Jammu and Kashmir (JK)	4900	2003-2009	$-0.55 \pm 0.08$	6 (1)	Kääb and others (2012)
<b>Karakoram</b>					
Siachen (SC)	936	1999-2007	$-0.03 \pm 0.21$	8 (1)	Agarwal and others (2016)
Hunza Basin, central Karakoram (HB)	2868	~1973-2009	$-0.06 \pm 0.08$	36 (2)	Bolch and others (2017)
Karakoram (KK1)	21750	2003-2009	$-0.03 \pm 0.04$	6 (1)	Kääb and others (2012)
Karakoram (KK2)	12366	1973-2000	$-0.09 \pm 0.03$	27 (1)	Neckel and others (2014)
East Karakoram (EK)	5328	1999-2010	$+0.11 \pm 0.14$	11 (1)	Gardelle and others (2013)
West Karakoram (WK)	5434	1999-2008	$+0.09 \pm 0.18$	9 (1)	Gardelle and others (2013)
Central Karakoram (CK)	5615	1999-2008	$+0.11 \pm 0.22$	9 (1)	Gardelle and others (2012)
<b>Regional Means</b>					
HKKH	60100	2003-2008	$-0.21 \pm 0.05$	5 (1)	Kääb and others (2012)
PKH	21900	1999-2008/11	$-0.14 \pm 0.08$	~10 (1)	Gardelle and others (2013)
HMA	118200	2003-2009	$-0.20 \pm 0.10$	6 (1)	Gardner and others (2013)

HP = Himachal Pradesh; UK = Uttarakhand; HKKH = Hindu Kush-Karakoram-Himalaya; PKH = Pamir-Karakoram-Himalaya;

**Table S9:** Mass balance modelling studies in the HK region.

Glacier name (region/country)	Location	Area (km <sup>2</sup> )	MB Period	Mass balance (m w.e. yr <sup>-1</sup> )	Model	Reference
<b>Central Himalaya</b>						
1. Kangwure (KW), Xixiabangma, China	28°27'N 85°45'E	1.9	1994-2008	-0.50*	SM	Yao and others (2012)
2. Langtang (LT), Langtang region, Nepal	28°16'N 85°43'E	53.5	1986-1997	-0.11*	TI	Tangborn and Rana (2000)
3. Mera (MR) Khumbu region, Nepal	27°70'N 86°90'E	5.1	1962-2007	-0.25±0.03	TI	Shea and others (2015)
<b>Western Himalaya</b>						
4. Chhota Shigri (CS1), Lahaul-Spiti, India	32°28'N 77°52'E	15.5	1969-2012	-0.30±0.36	TI	Azam and others (2014a)
5. Chhota Shigri (CS2), Lahaul-Spiti, India	32°28'N 77°52'E	15.5	2000-2013	-0.68±0.10	AM	Brun and others (2015)
<b>Karakoram</b>						
6. Siachen (SC), Nubra Valley, India	35°35'N 77°15'E	987	1986-1991	-0.51*	HY	Bhutiyan (1999)
7. Siachen (SC), Nubra Valley, India	35°35'N 77°15'E	1220	1986-1991	+0.22 to -0.23*	HY	Zaman and Liu (2015)

\*uncertainty not given or the mass balance values come from non-peer reviewed source. SM= statistical method;  
 TI= Temperature index method; AM= Albedo model; HY= Hydrology method

**Table S10:** Modelled annual mass balance data for the HK region. The details are provided in Table S9.

Year	KW	LT	MR	CS1	CS2	SC
1962			-0.34			
1963			-0.44			
1964			-0.49			
1965			-0.30			
1966			-0.19			
1967			-0.60			
1968			-0.38			
1969			-0.35			
1970			-1.15	-1.26		
1971			-1.45	-0.37		
1972			-0.13	0.43		
1973			-0.23	-0.94		
1974			0.00	-0.90		
1975			-0.18	0.44		
1976			-0.50	0.93		
1977			-0.23	-0.04		
1978			-0.12	0.12		
1979			-0.09	-0.44		
1980			-0.14	-0.96		
1981			-0.36	-0.67		
1982			-0.42	0.02		
1983			-0.59	0.32		
1984			-0.41	-1.66		
1985			0.11	-0.84		
1986			-0.02	0.01		
1987		0.24	-0.14	-0.07		-0.49
1988		0.12	-0.09	0.24		-0.57
1989		-0.40	0.05	0.38		0.36
1990		0.39	-0.01	-0.09		-0.79
1991		-0.06	-0.03	-0.70		-1.08
1992		-0.37	-0.05	0.12		
1993		0.08	0.05	-0.06		
1994	-0.48	-0.70	-0.19	-0.40		
1995	-0.46	-0.48	-0.32	-0.12		
1996	-0.31	0.30	-0.22	0.12		
1997	-0.25	0.36	-0.04	0.13		
1998	-0.51		-0.13	0.39		
1999	-0.40		-0.24	0.03		
2000	-0.23		0.08	-0.19	-0.82	
2001	-0.69		0.01	-1.01	-1.09	
2002	-0.50		-0.21	-0.59	-0.94	
2003	-0.57		-0.17	-1.02	-1.08	
2004	-0.48		-0.20	-0.64	-0.93	
2005	-0.73		-0.02	0.55	-0.52	
2006	-1.02		-0.36	-0.77	-0.98	
2007	-0.39		-0.37	-0.92	-0.70	
2008	-0.49			-0.55	-0.98	
2009				-1.29	-0.30	
2010				0.24	0.20	
2011				0.13	0.33	
2012				-1.00	-0.70	
2013				-0.60	-0.79	
2014						
Mean	-0.50	-0.05	-0.25	-0.31	-0.66	-0.51

**Table S11:** Comparison of surface energy balance components in different regions in High Mountain Asia. R, H, LE and  $F_{\text{surface}}$  are the net radiation, sensible heat, latent heat and net energy flux available at glacier surface. For sake of comparison, we assign a negative contribution (in %) to negative heat fluxes and vice versa in order to have the resulting heat flux budget at glacier surface equal to 100%. All Fluxes are in  $\text{W m}^{-2}$ , values in brackets are the % contribution of each energy flux. Other fluxes are the conductive heat flux and heat flux from precipitation.

Glacier	Altitude (m a.s.l.)	Region (monsoon dominated, Y or N)	Period	R ( $\text{W m}^{-2}$ )	H ( $\text{W m}^{-2}$ )	LE ( $\text{W m}^{-2}$ )	Other ( $\text{W m}^{-2}$ )	$F_{\text{surface}}$ ( $\text{W m}^{-2}$ )	Ref.
AX010	4960 (P <sup>a</sup> )	central Himalaya (Y)	25 May-25 Sep 1978	64 (85)	8 (10)	4 (5)	n/a	74 (100)	Kayastha and Ohata (1999)
AX010	5080 (P)	central Himalaya (Y)	25 May-25 Sep 1978	55 (83)	8 (12)	3 (5)	n/a	63 (100)	Kayastha and Ohata (1999)
Baltoro	3490-8610 (G <sup>b</sup> )	Karakoram (N)	25 June-31 Aug 2004	102 (138)	10 (13)	-14 (19)	-24 (32)	74 (100)	Collier and others (2013)
Chhtota Shigri	4670 (P)	western Himalaya (Y)	8 July-5 Sep 2013	188 (82)	31 (13)	11 (5)	n/a	230 (100)	Azam and others (2014b)
Chongce ice cap	5850 (P)	west Kunlun mountains (N)	Jul-Aug 1987	36 (258)	17 (125)	-39 (283)	n/a	14 (100)	Takahashi and others (1989)
Guxiang No. 3	4400 (P)	Nyainqentanglha Range (Y)	Jul-Aug 1965	148 (65)	63 (27)	19 (8)	n/a	229 (100)	Wang and others (1982)
Keqicar	4265 (P)	suthwest Tianshan (N)	16 June-7 Sep 2005 <sup>c</sup>	63 (274)	14 (61)	-54 (235)	n/a	23 (100)	Li and other (2011)
Laohugou No. 12	5040 (P)	western Qilian (N)	June-Sep 2009	27 (150)	10 (57)	-12 (65)	-8 (42)	18 (100)	Sun and others (2012)
Laohugou No. 12	4550 (P)	western Qilian (N)	1 June-30 Sep 2011	81 (108)	7 (9)	-13 (17)	n/a	75 (100)	Sun and others (2014)
Parlung No. 4	4800 (P)	southeast TP <sup>d</sup> (Y)	21 May-8 Sep 2009	150 (86)	28 (16)	-1 (1)	-1 (1)	176 (100)	Yang and others (2011)
Parlung No. 4	5202 (P)	southeast TP (Y)	May-Sep 2011	84 (140)	12 (20)	-11 (18)	-12 (20)	73 (100)	Zhu and others (2015)
Purogangri ice cap	5350-6370 (G)	north central TP (Y)	Oct 2001-Sep 2011	58 (290)	11 (55)	-35 (175)	-14 (70)	20 (100)	Huintjes and others (2015)
Qiyi	4473 (P)	Qilian Mountain (N)	Jul-Oct 2007	63 (113)	14 (25)	-6 (11)	-16 (28)	55 (100)	Jiang and others (2010)
Urumqi glacier 1	3910 (P)	TainShan Mountain (N)	Jul-Aug 1986-1990	73 (90)	13 (16)	-5 (6)	n/a	81 (100)	Kang and Ohmura (1994)
Xiao Dongkemadi	5600 (P)	Tanggula Mountain (N)	Sep 1989-Sep 1992	44 (196)	44 (196)	-64 (286)	-1 (5)	23 (100)	Zhang and others (1996)
Xixibangma	5700 (P)	south central TP (N)	23 Aug-11 Sep 1991	28 (200)	5 (33)	-19 (133)	n/a	14 (100)	Aizen and others (2002)
Zhadang	5515-6090 (G)	central TP (N)	April 2009-Sep 2011	5 (39)	18 (131)	-11 (80)	1 (9)	14 (100)	Mölg and others (2012)
Zhadang	5660 (P)	central TP (N)	1 May-30 Sep 2010	62 (103)	10 (17)	-8 (13)	-4 (7)	60 (100)	Zhang and others (2013)
Zhadang	5660 (P)	central TP (N)	1 May-15 Sep 2011	27 (117)	8 (35)	-10 (43)	-2 (9)	23 (100)	Zhang and others (2013)
Zhadang	5655 (P)	central TP (N)	May-Sep 2011	39 (156)	8 (32)	-11 (44)	-11 (44)	25 (100)	Zhu and others (2015)

<sup>a</sup>G = glacier-wide scale, <sup>b</sup>P = point scale, <sup>c</sup> = with a gap of 1 July to 7 August, <sup>d</sup>TP = Tibetan Plateau, n/a = not available.

## References

- Agarwal V, Bolch T, Syed TH, Pieczonka T, Strozzi T, Nagaich R (2017) Area and mass changes of Siachen Glacier (East Karakoram). *J. Glaciol.* **63**(237), 148–163
- Ageta Y, Naito N, Iwata S and Yabuki H (2003) Glacier distribution in the Himalayas and glacier shrinkage from 1963 to 1993 in the Bhutan Himalayas. *Bull. Glaciol. Res.* **20**, 29–40
- Ageta Y, Ohata T, Tanaka Y, Ikegami K and Higuchi K (1980) Mass balance of glacier AX010 in Shorong Himal, east Nepal during the summer monsoon season. *J. Jpn. Soc. Snow Ice* **41**(Special), 34–41
- Aizen VB, Aizen EM and Nikitin SA (2002) Glacier regime on the northern slope of the Himalaya (Xixibangma glaciers). *Quat. Int.* **97**, 27–39
- Auden JB (1937) Snout of the Gangotri Glacier, Tehri Garhwal. *Rec Geol Surv India* **72**(2), 135–140
- Bahuguna IM, Kulkarni AV and Nayak S (2004) DEM from IRS-1C PAN stereo coverages over Himalayan glaciated region—accuracy and its utility. *Int. J. Remote Sens.* **25**(19), 4029–4041
- Bajracharya SR, Maharjan SB, Shrestha F, Bajracharya OR, Baidya SK (2014) *Glacier status in Nepal and decadal change from 1980 to 2010 based on Landsat data*. Research Report 2014/2, Kathmandu, International Centre for Integrated Mountain Development (ICIMOD)
- Bajracharya SR and Shrestha B (2011) *The status of glaciers in the Hindu Kush-Himalayan region*. International Centre for Integrated Mountain Development (ICIMOD)
- Bajracharya SR, Maharjan SB and Shrestha F (2014) The status and decadal change of glaciers in Bhutan from the 1980s to 2010 based on satellite data. *Ann. Glaciol.* **55**(66), 159–166
- Bajracharya SR, Maharjan SB, Shrestha F (2011) ‘Glaciers shrinking in Nepal Himalaya.’ In Blanco, J; Kheradmand, H (eds) *Climate change: Geophysical foundations and ecological effects*, (InTech, Rijeka, Croatia). 445–458
- Bali R, Agarwal KK, Ali SN and Srivastava P (2011) Is the recessional pattern of Himalayan glaciers suggestive of anthropogenically induced global warming? *Arab. J. Geosci.* **4**(7–8), 1087–1093
- Bali R, Ali SN, Agarwal KK, Rastogi SK, Krishna K and Srivastava P (2013) Chronology of late Quaternary glaciation in the Pindar valley, Alaknanda basin, Central Himalaya (India). *J. Asian Earth Sci.* **66**, 224–233
- Banerjee A and Shankar R (2014) Estimating the avalanche contribution to the mass balance of debris covered glaciers. *Cryosphere Discuss.* **8**(1), 641–657
- Baral P and 9 others (2014) Preliminary results of mass-balance observations of Yala Glacier and analysis of temperature and precipitation gradients in Langtang Valley, Nepal. *Ann. Glaciol.* **55**(66), 9–14
- Basantes-Serrano R and 7 others (2016) Slight mass loss revealed by reanalyzing glacier mass-balance observations on Glacier Antisana 15 $\alpha$  (inner tropics) during the 1995–2012 period. *J. Glaciol.* **62**(231), 124–136



- Basnett S, Kulkarni AV and Bolch T (2013) The influence of debris cover and glacial lakes on the recession of glaciers in Sikkim Himalaya, India. *J. Glaciol.* **59**(218), 1035–1046
- Belò M, Mayer C, Smiraglia C and Tamburini A (2008) The recent evolution of Liligo glacier, Karakoram, Pakistan, and its present quiescent phase. *Ann. Glaciol.* **48**(1), 171–176
- Berthier E, Arnaud Y, Kumar R, Ahmad S, Wagnon P and Chevallier P (2007) Remote sensing estimates of glacier mass balances in the Himachal Pradesh (Western Himalaya, India). *Remote Sens. Environ.* **108**(3), 327–338
- Bhambri R and Bolch T (2009) Glacier mapping: a review with special reference to the Indian Himalayas. *Prog. Phys. Geogr.* **33**(5), 672–704
- Bhambri R, Bolch T, Chaujar RK and Kulshreshtha SC (2011) Glacier changes in the Garhwal Himalaya, India, from 1968 to 2006 based on remote sensing. *J. Glaciol.* **57**(203), 543–556
- Bhutiyani MR (1999) Mass-balance studies on Siachen glacier in the Nubra valley, Karakoram Himalaya, India. *J. Glaciol.* **45**(149), 112–118
- Bolch T, Pieczonka T and Benn DI (2011) Multi-decadal mass loss of glaciers in the Everest area (Nepal Himalaya) derived from stereo imagery. *Cryosphere* **5**(2), 349–358
- Brun F and 8 others (2015) Seasonal changes in surface albedo of Himalayan glaciers from MODIS data and links with the annual mass balance. *Cryosphere* **9**(1), 341–355
- Chaujar RK (1989) Geomorphological studies of Chhota Shigri Glacier with special reference to mapping of its landforms, Technical report No 3 on Multi-Disciplinary glacier expedition to Chhota Shigri, 1988, Department of Science and Technology. 3, 131–139
- Che T, Xiao L and Liou Y-A (2014) Changes in glaciers and glacial lakes and the identification of dangerous glacial lakes in the Pumqu River Basin, Xizang (Tibet). *Adv. Meteorol.* Article ID 903709, 1–8
- Chen X, Cui P, Li Y, Yang Z and Qi Y (2007) Changes in glacial lakes and glaciers of post-1986 in the Poiqu River basin, Nyalam, Xizang (Tibet). *Geomorphology* **88**(3), 298–311
- Chitranshi A, Sangewar CV, Srivastava D, Puri VMK, Dutta SS (2003) Recession pattern of Meru Bamak Glacier, Bhagirathi Basin, Uttaranchal. Abstracts, workshop on Gangotri Glacier. 11–12
- Cotter GD (1906) Notes on certain glaciers in Kumaon. *Rec Geol Surv India* **35**(4), 148–157
- Dee DP and 9 others (2011) The ERA-Interim reanalysis: Configuration and performance of the data assimilation system. *Q. J. R. Meteorol. Soc.* **137**(656), 553–597
- Dobhal DP and Mehta M (2010) Surface morphology, elevation changes and terminus retreat of Dokriani Glacier, Garhwal Himalaya: implication for climate change. *Himal. Geol.* **31**(1), 71–78
- Dobhal DP, Gergan JT and Thayyen RJ (2004) Recession and morphogeometrical changes of Dokriani glacier (1962–1995) Garhwal Himalaya, India. *Curr. Sci.* **86**(5), 692–696
- Dobhal DP, Gergan JT and Thayyen RJ (2008) Mass balance studies of the Dokriani Glacier from 1992 to 2000, Garhwal Himalaya, India. *Bull Glaciol Res* **25**, 9–17

Dobhal DP, Mehta M and Srivastava D (2013) Influence of debris cover on terminus retreat and mass changes of Chorabari Glacier, Garhwal region, central Himalaya, India. *J. Glaciol.* **59**(217), 961–971

Dutta S, Ramanathan AL and Linda A (2012) Glacier fluctuation using satellite data in Beas basin, 1972–2006, Himachal Pradesh, India. *J. Earth Syst. Sci.* **121**(5), 1105–1112

Dyrgerov MB and Meier MF (2005) Glaciers and the Changing Earth System: A 2004 Snapshot. *Institute of Arctic and Alpine Research*, Occasional Paper **58**

Frauenfelder R and Kääb A (2009) Glacier mapping from multitemporal optical remote sensing data within the Brahmaputra river basin. *Proceedings of the 33rd International Symposium on Remote Sensing of Environment*. 4–8

Fujita K and Nuimura T (2011) Spatially heterogeneous wastage of Himalayan glaciers. *Proc. Natl. Acad. Sci.* **108**(34), 14011–14014

Fujita K, Kadota T, Rana B, Kayastha RB and Ageta Y (2001a) Shrinkage of Glacier AX010 in Shorong region, Nepal Himalayas in the 1990s. *Bull. Glaciol. Res.* **18**, 51–54

Fujita K, Nakazawa F and Rana B (2001b) Glaciological observations on Rikha Samba Glacier in Hidden Valley, Nepal Himalayas, 1998 and 1999. *Bull. Glaciol. Res.* **18**, 31–35

Fujita K, Takeuchi N and Seko K (1998) Glaciological observations of Yala Glacier in Langtang Valley, Nepal Himalayas, 1994 and. *Bull. Glacier Res.* **16**, 75–8

Ganjoo RK (2010) Are secular movements in the glaciers of Ladakh Mountains, Ladakh (J & K State, India) a response to climate change? International Symposium Benefiting from Earth Observation, ICIMOD, Kathmandu, Oct. 4-6

Gärtner-Roer I, Naegeli K, Huss M, Knecht T, Machguth H and Zemp M (2014) A database of worldwide glacier thickness observations. *Glob. Planet. Change* **122**, 330–344

Gautam CK and Mukherjee BP (1992) Synthesis of glaciological studies on Tipra Bank Glacier Bhyundar Ganga Basin, district Chamoli, Uttar Pradesh (F.S. 1980-1988) Geological Survey of India, Northern Region, Lucknow

Ghosh S and Pandey AC (2013) Estimating the variation in glacier area over the last 4 decade and recent mass balance fluctuations over the Pensilungpa Glacier, J&K, India. *Glob. Perspect. Geogr.* **1**(4), 58–65

Godwin-Austen HH (1864) On the glaciers of the Mustakh Range. *J. R. Geogr. Soc. Lond.* **34**, 19–56

Govindha Raj KB (2011) Recession and reconstruction of Milam Glacier, Kumaon Himalaya, observed with satellite imagery. *Current Sci.*, **100**, 1420-1425

Govindha Raj KB, Remya SN and Kumar KV (2013) Remote sensing-based hazard assessment of glacial lakes in Sikkim Himalaya. *Curr. Sci.*, **104**, 359-364

GSI (Geological Survey of India) (1977) Report of the interdepartmental expedition to Gara Glacier 1975, Northern Region Calcutta. 16–19

GSI (Geological Survey of India) (1991) Annual general report, Part 8. Volume 124

GSI (Geological Survey of India) (1992) Annual general report. Part 8. Volume 125

GSI (Geological Survey of India) (1995) Annual general report, Part 8. Volume 129

- GSI (Geological Survey of India) (1997) Annual general report, Part 8. Volume 131
- GSI (Geological Survey of India) (1999) Annual general report. Part 8. Volume 133
- GSI (Geological Survey of India) (2000) Annual general report. Part 8. Volume 134
- GSI (Geological Survey of India) (2002) Annual general report, Part 8. Volume 136
- GSI (Geological Survey of India) (2003) Annual general report, Part 8. Volume 137
- GSI (Geological Survey of India) (2004) Annual general report, Part 8. Volume 138
- GSI (Geological Survey of India) (2011) Annual general report, Part 8. Volume 144
- GSI (Geological Survey of India) (2001) Glaciology of Indian Himalaya. Special Publication no 63
- Hewitt K (2011) Glacier change, concentration, and elevation effects in the Karakoram Himalaya, Upper Indus Basin. *Mt. Res. Dev.* **31**(3), 188–200
- Huss M, Hock R, Bauder A and Funk M (2010) 100-year mass changes in the Swiss Alps linked to the Atlantic Multidecadal Oscillation. *Geophys. Res. Lett.* **37**(10), 1–5
- Jangpangi BS, Vohra CP (1959) Reports on the Glaciological Study of the Milam, Poting and Shankalpa (Ralam) Glaciers, Pithoragarh district, Unpublished report, Geological Survey of India
- Jiang X, Wang N-L, Yang S-P, He J-Q and Song G-J (2010) The surface energy balance on the Qiyi Glacier in Qilian Mountains during the ablation period. *J. Glaciol. Geocryol.* **32**(4), 686–695
- Jin R, Li X, Che T, Wu L and Mool P (2005) Glacier area changes in the Pumqu river basin, Tibetan Plateau, between the 1970s and 2001. *J. Glaciol.* **51**(175), 607–610
- Kamp U, Byrne M and Bolch T (2011) Glacier fluctuations between 1975 and 2008 in the Greater Himalaya Range of Zaskar, southern Ladakh. *J. Mt. Sci.* **8**(3), 374–389
- Kang E and Ohmura AA (1994) A parameterized energy balance model of glacier melting on the Tianshan Mountain. *Acta Geogr. Sin.* **49**, 467–476 [in Chinese].
- Kanth TA, Shah AA and Hassan Z (2011) Geomorphologic character & receding trend of Kolahoi Glacier in Kashmir Himalaya. *Recent Res. Sci. Technol.* **3**, 68–73
- Kaul MN (1986) Mass balance of Liddar glaciers. *Trans. Inst. Indian Geogr.* **8**, 95–111
- Kayastha RB, Ohata T and Ageta Y (1999) Application of a mass-balance model to a Himalayan glacier. *J. Glaciol.* **45**(151), 559–567
- King O, Quincey DJ, Carrivick JL and Rowan AV (2017) Spatial variability in mass loss of glaciers in the Everest region, central Himalayas, between 2000 and 2015. *Cryosphere* **11**(1), 407–426
- Koul MN and Ganjoo RK (2010) Impact of inter-and intra-annual variation in weather parameters on mass balance and equilibrium line altitude of Naradu Glacier (Himachal Pradesh), NW Himalaya, India. *Clim. Change* **99**(1), 119–139
- Kulkarni AV and Bahuguna IM (2002) Correspondence. Glacial retreat in the Baspa basin, Himalaya, monitored with satellite stereo data. *J. Glaciol.* **48**, 171–172

- Kulkarni AV and 6 others (2007) Glacial retreat in Himalaya using Indian Remote Sensing satellite data. *Curr. Sci.*, **92**, 69–74
- Kulkarni AV, Dhar S, Rathore BP and Kalia R (2006) Recession of samudra tapu glacier, chandra river basin, Himachal Pradesh. *J. Indian Soc. Remote Sens.* **34**(1), 39–46
- Kulkarni AV, Rathore BP, Mahajan S and Mathur P (2005) Alarming retreat of Parbati glacier, Beas basin, Himachal Pradesh. *Curr. Sci.*, **88**, 1844–1849
- Kulkarni AV, Rathore BP, Singh SK and Bahuguna IM (2011) Understanding changes in the Himalayan cryosphere using remote sensing techniques. *Int. J. Remote Sens.* **32**(3), 601–615
- Kumar R and others (2014) Mass and Energy Balance study of Naradu Glacier, Himachal Himalaya. National Conference of Himalayan Glaciology. Shimla, India. 24
- Lama L, Kayastha RB, Maharjan SB, Bajracharya SR, Chand MB and Mool PK (2015) Glacier area and volume changes of Hidden Valley, Mustang, Nepal from ~ 1980s to 2010 based on remote sensing. *Proc. Int. Assoc. Hydrol. Sci.* **368**, 57–62
- Li J, Liu S, Zhang Y and Shangguan D (2010) Surface energy balance of Keqicar Glacier, Tianshan Mountains, China, during ablation period. *Sci. Cold Arid Reg.* **3**, 197–205
- Liu S and 7 others (2006) Glacier retreat as a result of climate warming and increased precipitation in the Tarim river basin, northwest China. *Ann. Glaciol.* **43**(1), 91–96
- Liu S, Xie Z, Song G, Ma L and Ageta Y (1996) Mass balance of Kangwure (flat-top) Glacier on the north side of Mt. Xixiabangma, China. *Bull. Gla. Res.* **14**, 37–43
- Longstaff TG (1910) Dr. Longstaff's Himalayan Expedition, 1909. *Geogr. J.* **35**(1), 64–65
- Ma L, Tian L, Pu J and Wang P (2010) Recent area and ice volume change of Kangwure Glacier in the middle of Himalayas. *Chin. Sci. Bull.* **55**(20), 2088–2096
- Mason K (1938) Progress of Himalayan Surveys. *Him. J.*, **11**, 170
- Maurer JM, Rupper SB and Schaefer JM (2016) Quantifying ice loss in the eastern Himalayas since 1974 using declassified spy satellite imagery. *Cryosphere* **10**(5), 2203–2215
- Mehta M, Dobhal DP and Bisht MPS (2011) Change of Tipra glacier in the Garhwal Himalaya, India, between 1962 and 2008. *Prog. Phys. Geogr.* **35**(6), 721–738
- Mehta M, Dobhal DP, Pratap B, Verma A, Kumar A and Srivastava D (2013) Glacier changes in Upper Tons River basin, Garhwal Himalaya, Uttarakhand, India. *Z. Für Geomorphol.* **57**(2), 225–244
- Minora U and 9 others (2013) 2001–2010 glacier changes in the Central Karakoram National Park: a contribution to evaluate the magnitude and rate of the "Karakoram anomaly". *Cryosphere Discuss.* **7**(3), 2891–2941
- Mishra R, Kumar A and Singh D (2014) Long term monitoring of mass balance of Hamtah Glacier, Lahaul and Spiti district, Himachal Pradesh. *Geolo Surv India* **147**(8), 230–231
- Mölg T, Maussion F, Yang W and Scherer D (2012) The footprint of Asian monsoon dynamics in the mass and energy balance of a Tibetan glacier. *Cryosphere*, **6**, 1445–1461
- Mukhtar MA, Prakash O (2013) Glacio-geomorphological studies in the pro-glacial region of Gepang Gath Glacier, Lahaul and Spiti district, Himachal Pradesh on expedition basis 2012–13, Geological survey of India

- Nainwal HC, Banerjee A, Shankar R, Semwal P and Sharma T (2016) Shrinkage of Satopanth and Bhagirath Kharak Glaciers, India, from 1936 to 2013. *Ann. Glaciol.* **57**(71), 131–139
- Naithani AK, Nainwal HC, Sati KK and Prasad C (2001) Geomorphological evidences of retreat of the Gangotri glacier and its characteristics. *Curr. Sci.*, **80**, 87–94
- Negi HS, Thakur NK and Ganju A (2012) Monitoring of Gangotri glacier using remote sensing and ground observations. *J. Earth Syst. Sci.* **121**(4), 855–866
- Nuimura T and 9 others (2015) The GAMDAM glacier inventory: a quality-controlled inventory of Asian glaciers. *Cryosphere* **9**, 849–864
- Oberoi LK, Siddiqui MA and Srivastava D (2001) Recession pattern of Miyar glacier, Lahaul and Spiti district, Himachal Pradesh. Geological Survey of India, Special Publication **65**, 57–60
- Odell NE (1963) The Kolahoi northern glacier, Kashmir. *J. Glaciol.* **4**(35), 633–635
- Ostrem G and Stanley AD (1969) *Glacier mass balance measurements: a manual for field and office work* (Ottawa, Ontario)
- Pandey P and Venkataraman G (2013) Changes in the glaciers of Chandra–Bhaga basin, Himachal Himalaya, India, between 1980 and 2010 measured using remote sensing. *Int. J. Remote Sens.* **34**(15), 5584–5597
- Pandey P, Venkataraman G and Shukla SP (2011) Study of retreat of Hamtah glacier, Indian Himalaya, using remote sensing technique. *Geoscience and Remote Sensing Symposium (IGARSS), 2011 IEEE International*. IEEE, 3194–3197
- Pratap B, Dobhal DP, Bhambri R, Mehta M and Tewari VC (2016) Four decades of glacier mass balance observations in the Indian Himalaya. *Reg. Environ. Change* **16**(3), 643–658
- Purdon WH (1861) On the trigonometrical survey and physical configuration of the Valley of Kashmir. *J. R. Geogr. Soc. Lond.* **31**, 14–30
- Rabatel A and 7 others (2012) Can the snowline be used as an indicator of the equilibrium line and mass balance for glaciers in the outer tropics? *J. Glaciol.* **58**(212), 1027–1036
- Rai PK, Nathawat MS and Mohan K (2013) Glacier retreat in Doda Valley, Zaskar Basin, Jammu & Kashmir, India. *Univers. J. Geosci.* **1**(3), 139–149
- Raina VK (2009) Himalayan glaciers: a state-of-art review of glacial studies, glacial retreat and climate change. *Himal. Glaciers State-Art Rev. Glacial Stud. Glacial Retreat Clim. Change*
- Raina VK, Kaul MK and Singh S (1977) Mass-balance studies of Gara Glacier. *J. Glaciol.* **18**(80), 415–423
- Ren J, Jing Z, Pu J and Qin X (2006) Glacier variations and climate change in the central Himalaya over the past few decades. *Ann. Glaciol.* **43**(1), 218–222
- Sangewar CV and Sangewar MA (2007) Siddiqui, Thematic compilation of mass balance data on glaciers of Satluj Catchment in Himachal Himalaya (Field Season: 2006-07) Geological Survey of India, Northern Region, Lucknow

Sangewar CV (2012) Remote sensing applications to study Indian glaciers. *Geocarto Int.* **27**(3), 197–206

Sangewar CV and Kulkarni AV (2011) Observational studies of the recent past. *Rep. Study Group Himal. Glaciers Prep. Off. Princ. Sci. Advis. Gov. India* PSA/2011/2, 25-76

Schmidt S and Nüsser M (2009) Fluctuations of Raikot Glacier during the past 70 years: a case study from the Nanga Parbat massif, northern Pakistan. *J. Glaciol.* **55**(194), 949–959

Schmidt S and Nüsser M (2012) Changes of High Altitude Glaciers from 1969 to 2010 in the Trans-Himalayan Kang Yatze Massif, Ladakh, Northwest India. *Arctic, Antarctic, and Alpine Research*, **44**, 107–121

Shrestha ML and Shrestha AB (2004) Recent trends and potential climate change impacts on glacier retreat/glacier lakes in Nepal and potential adaptation. *Presentation by ML Shrestha, Director of the Department of Hydrology and Meteorology of Nepal, at the OECD Global Forum on Sustainable Development, Paris.* 11–12

Shrivastava D, Sangewar C V, Kaul M K, Jamwal K S (2001) Mass balance of Rulung Glacier- a Trans-Himalayan glacier, Indus basin, Ladakh. *Proc. Symp. Snow, Ice and Glacier*, March 1999, Geol. Surv. India, Special Publication, **53**, 41–46

Shukla A, Ali I, Hasan N, Romshoo SA (2017) Dimensional changes in the Kolahoi glacier from 1857 to 2014. *Environ. Monit. Assess.* **189**, 1-18

Shukla SP, Siddiqui MA, Hampaiash P and Swaroop S (2001) Secular movement studies of selected glaciers of Yamuna and Ghagra Basins. *Dhradun Tehri Uttarakashi Pithoragarh Dist. Geol. Surv. India Rec.* **133**, 161–165

Singh S, Kumar R, Bhardwaj A, Sam L, Shekhar M, Singh A, Kumar R and Gupta A (2016) Changing climate and glacio-hydrology in Indian Himalayan Region: a review. *Wiley Interdiscip. Rev. Clim. Change* **7**(3), 393–410

Srivastava D and Mukkerji S (2001) *Glaciology of Indian Himalaya: a bilingual contribution in 150th year of Geological Survey of India.* Geological Survey of India

Srivastava D, Gupta KR and Mukherjee S (2004) Geological Survey of India Special Publication **80**, 33–38

Sun W and 9 others (2014) Ablation modeling and surface energy budget in the ablation zone of Laohugou glacier No. 12, western Qilian mountains, China. *Ann. Glaciol.* **55**(66), 111–120

Sun W and 7 others (2012) The surface energy budget in the accumulation zone of the Laohugou Glacier No. 12 in the western Qilian Mountains, China, in summer 2009. *Arct. Antarct. Alp. Res.* **44**(3), 296–305

Survey of India (2005) National map policy. <http://www.surveyofindia.gov.in/tenders/nationalmappolicy/nationalmappolicy.pdf>

Swaroop S, Siddiqui MA, Asthana R, Chaturvedi A (1995) Report on glaciological studies on Triloknath Glacier, district Lahaul and Spiti, Himachal Pradesh (Field Season 1994-95), Geological Survey of India

Takahashi S, Ohata T and Yingqin X (1989) Characteristics of heat and water fluxes on glacier and ground surfaces in the West Kunlun Mountains. *Bull. Glac. Res.* **7**, 89–98

Tangborn W and Rana B (2000) Mass balance and runoff of the partially debris-covered Langtang Glacier, Nepal. *IAHS Publ.* 264 (Symposium at Seattle 2000 – Debris-Covered Glaciers), 99–108

Tewari AP (1966) Recent changes in the position of the snout of the Pindari Glacier (Kumaon Himalaya), Almora District, Uttar Pradesh, India. Geological Survey of India, Chandigarh, India

Tshering P and Fujita K (2016) First in situ record of decadal glacier mass balance (2003–2014) from the Bhutan Himalaya. *Ann. Glaciol.* **57**(71), 289–294

Vijay S and Brown M (2016) Elevation Change Rates of Glaciers in the Lahaul-Spiti (Western Himalaya, India) during 2000–2012 and 2012–2013. *Remote Sens.* **8**, 2-16

Vincent C, Le Meur E, Six D and Funk M (2005) Solving the paradox of the end of the Little Ice Age in the Alps. *Geophys. Res. Lett.* **32**, 1–4

Vohra CP (1980) Some problems of glacier inventory in the Himalayas. In Proceedings of the Riederalp Workshop, September 1978, IAHS-AISH Publication 126, 67–74

Vohra CP (1981) Himalayan glaciers. *Himalaya Asp. Change*, 138–151

Wagnon P and 9 others (2007) Four years of mass balance on Chhota Shigri Glacier, Himachal Pradesh, India, a new benchmark glacier in the western Himalaya. *J. Glaciol.* **53**(183), 603–611

Wang Z, Deng Y, Zeng X (1982) Water-heat conditions for maritime glaciers developing in Guxiang, Tibetan Region. In Memoirs of Lanzhou Institute of Glaciology and Geocryology, CAS, No. 3. Science Press, Beijing, 82–90 [in Chinese].

WWF (2009) Witnessing change: glaciers in Indian Himalayas. New Delhi, India: WWF India, 14–16

Yamada T and 7 others (1992) Fluctuations of the glaciers from the 1970s to 1989 in the Khumbu, Shorong and Langtang regions, Nepal Himalayas. *Bull. Glacier Res.* **10**, 11–19

Yang W and 6 others (2011) Summertime surface energy budget and ablation modeling in the ablation zone of a maritime Tibetan glacier. *J. Geophys. Res. Atmospheres*, **116**(D14), 1–11

Yao T and 9 others (2012) Different glacier status with atmospheric circulations in Tibetan Plateau and surroundings. *Nat. Clim. Change*, **2**, 663–667

Ye Q and 8 others (2015) Glacier mass changes in Rongbuk catchment on Mt. Qomolangma from 1974 to 2006 based on topographic maps and ALOS PRISM data. *J. Hydrol.* **530**, 273–280

Ye Q, Yao T and Naruse R (2008) Glacier and lake variations in the Mapam Yumco basin, western Himalaya of the Tibetan Plateau, from 1974 to 2003 using remote-sensing and GIS technologies. *J. Glaciol.* **54**(188), 933–935

Ye Q, Yao T, Kang S, Chen F and Wang J (2006) Glacier variations in the Naimona'nyi region, western Himalaya, in the last three decades. *Ann. Glaciol.* **43**(1), 385–389

Ye Q, Zhong Z, Kang S, Stein A, Wei Q and Liu J (2009) Monitoring glacier and supra-glacier lakes from space in Mt. Qomolangma region of the Himalayas on the Tibetan Plateau in China. *J. Mt. Sci.* **6**(3), 211–220



Zaman Q and Liu J (2015) Mass balance of Siachen Glacier, Nubra valley, Karakoram Himalaya: facts or flaws?, *J. Glaciol.* **61**, 1012–1014

Zemp M and 9 others (2013) Reanalysing glacier mass balance measurement series. *The Cryosphere* **7**(4), 1227–1245

Zhang G and 9 others (2013) Energy and mass balance of Zhadang glacier surface, central Tibetan Plateau. *J. Glaciol.* **59**(213), 137–148

Zhang Y, Tandong Y, Jianchen P, Ohata T, Yabuki H, Fujita K (1996) Energy budget at ELA on Dongkemadi Glacier in the Tonggula Mts. Tibetan Plateau. *J. Glaciol. Geocryol.* **18**(1), 10–19